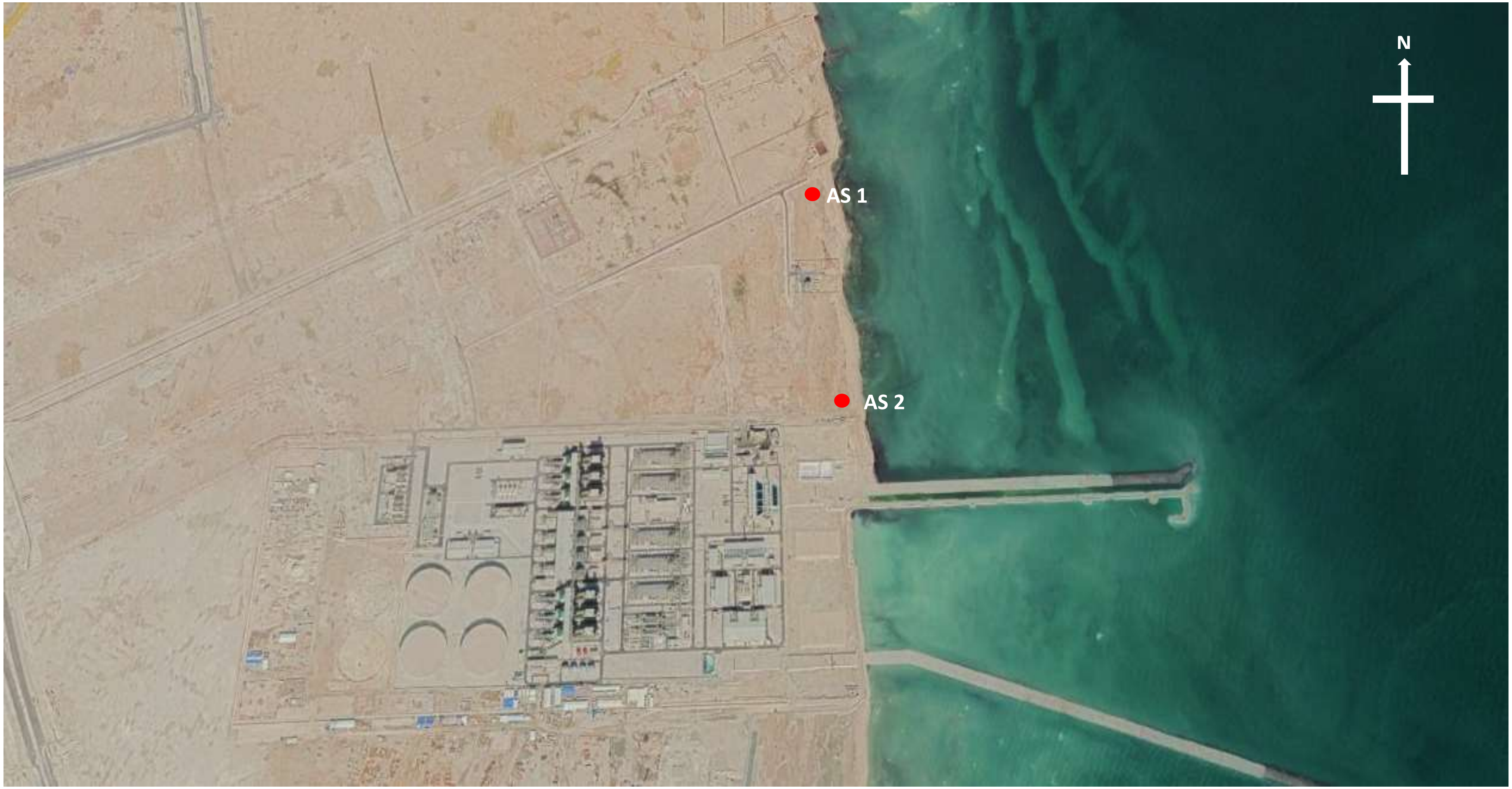

LEGEND

● AS – Ambient Air Quality Monitoring Station

APPENDIX B - CALIBRATION CERTIFICATES

Element Doha LLC
Street 46, Building 30, Salwa Industrial Area,
PO Box 23650, Doha, State of Qatar
P: +974 4460 3202
F: +974 4460 3246
info.qatar@element.com
element.com

اليمنت الدوحة ذ م م
المنطقة الصناعية في سلوى، شارع رقم ٤٦ مبنى رقم ٣٠،
صندوق بريد ٢٣٦٥٠، الدوحة، قطر
هاتف: ٣٢٠٢ ٤٤٦٠ ٩٧٤ +
فاكس: ٣٢٤٦ ٤٤٦٠ ٩٧٤ +
info.qatar@element.com
element.com

CALIBRATION CERTIFICATE (EX-M-OP-AM-MD-906-F1 Ambient PM)

CERTIFICATE NUMBER: EX-M-OP-AM-MD-906-F1-04/17/01
(Format: EX-M-OP-AM-MD-906-F1-MM/YY/0?)

Date: 05/10/2018   Valid to: 05/10/2019

Test Equipment:

Reference Equipment:

Test PM analyser:		Reference PM10 analyser:		Reference PM2.5 analyser:	
Model :	AQMESH	Manufacturer:	Turnkey Instruments	Manufacturer:	Turnkey Instruments
		Type:	Air Monitors	Type:	Osiris
Serial No:	1832150	Serial No:	TNT 1297	Serial No:	TNT 1297

Parameter	**PM2.5**	**PM10**
Time period	**24 hr average**	**24 hr average**
Reference µg/m³	10.1	34.7
Test µg/m³	9.68	33.4
Deviation (%)	-4.2	-3.7
Tolerance (5%)	5	5
Pass / Fail	Pass	Pass

Calibrated by: Oliver Olang'   Signed:

Date of Calibration: 05/10/2018

Is a Certificate and Sticker Check required by a senior member of staff? NO

[Check Element Competency Matrix to see if a counter signature check is required]

Element Doha LLC
Street 46, Building 30, Salwa Industrial Area,
PO Box 23650, Doha, State of Qatar
P: +974 4460 3202
F: +974 4460 3246
info.qatar@element.com
element.com

اليمنت الدوحة ذ م م
المنطقة الصناعية في سلوى، شارع رقم ٤٦ مبنى رقم ٣٠،
صندوق بريد ٢٣٦٥٠، الدوحة، قطر
هاتف: ٣٢٠٢ ٤٤٦٠ ٩٧٤ +
فاكس: ٣٢٤٦ ٤٤٦٠ ٩٧٤ +
info.qatar@element.com
element.com

CALIBRATION CERTIFICATE (FCAL-20 TVOCS)

CERTIFICATE NUMBER: EX-CC-QE002-1 (Format: EX-CC-20.1 0715)

Date: 23/02/2019 (dd/mm/yy)

Valid to: 23/02/2020

Test Equipment:

Test meter:

Model : IQ610

Serial No: May-38

Reference Point 1:

Reference Gas:

Manufacturer: Isobutene

Concentration: 10 ppb

Reference Point 2:

Reference Gas:

Manufacturer: Isobutene

Concentration: 8000 ppb

Value	10 ppb	8000 ppb
Start volume (L)	228.0	207.00
End volume (L)	238.4	226.80
Test Item (ppb)	10.00	8000.00
Target (ppb)	10.00	8007.00
Deviation (%)	0.0	0.1
Tolerance (5%)	0.50	400.35
Pass / Fail	**Pass**	**Pass**

Calibrated by: Oliver Olang

Signed:

Date of Calibration: 23/02/2019

Is a Certificate and Sticker Check required by a senior member of staff? NO

APPENDIX C – PHOTOGRAPHIC REPORT

<table>
<tr><td></td><td rowspan="2">AS 1</td></tr>
<tr><td></td></tr>
</table>

	AS 2
	

APPENDIX D – RAW DATA

RAW DATA

PARTICULATES AND GASES

AS 1

Time Beginning	Time Ending	PM_{10} µg/m³	NO_2 µg/m³	SO_2 µg/m³	CO µg/m³	O_3 µg/m³	TEMP. °C	HUM. %RH	AIRPRES mbar	WD °	WIND m/s
28/06/2019 12:15	28/06/2019 12:30	123.6	103.235	2.124	421.052	113.162	33.1	69	994.8	60.222	3.345
28/06/2019 12:30	28/06/2019 12:45	126.48	102.562	1.211	455.541	119.186	34.2	70	994.3	82.431	4.792
28/06/2019 12:45	28/06/2019 13:00	111.67	94.869	1.921	452.79	111.266	34.9	68.9	994.8	59.305	3.864
29/06/2019 12:30	29/06/2019 12:45	109.2	107.215	1.316	361.627	106.608	39.5	49.1	996.2	127.908	2.81
29/06/2019 12:45	29/06/2019 13:00	107.24	104.735	2.053	360.783	112.146	39.9	49.2	995.4	126.172	3.024
29/06/2019 13:00	29/06/2019 13:15	110.59	108.985	0.684	347.702	113.682	40.1	47.7	995.4	126.413	3.14
30/06/2019 12:30	30/06/2019 12:45	119.16	133.658	1.026	492.166	103.918	38.9	57.9	995.6	78.482	3.302
30/06/2019 12:45	30/06/2019 13:00	126.11	141.504	1.053	489.935	92.238	38.9	58.6	995.6	89.782	2.974
01/07/2019 12:30	01/07/2019 12:45	110.5	165.946	2.526	467.243	132.976	38.5	56	997.1	280.109	2.713
01/07/2019 12:45	01/07/2019 13:00	117.39	131.004	1.368	470.416	112.346	38.7	56.3	996.6	349.756	2.725
02/07/2019 12:00	02/07/2019 12:15	116.3	107.235	2.316	539.57	139.542	36.7	59.6	994.4	90.936	2.503
02/07/2019 12:15	02/07/2019 12:30	115.23	102.677	1.763	468.174	132.866	37.3	58.2	994.6	108.109	1.463
02/07/2019 12:30	02/07/2019 12:45	116.23	106.369	1.211	407.77	130.538	37.6	51.1	995	148.702	1.084
03/07/2019 12:30	03/07/2019 12:45	116.42	105.235	1.895	371.341	106.326	36	66	996.7	67.342	3.509
03/07/2019 12:45	03/07/2019 13:00	116.11	129.023	1.816	372.644	103.652	35.6	67.1	996.5	73.965	3.77
03/07/2019 13:00	03/07/2019 13:15	118.19	117.465	1.763	370.226	112.426	35.4	67.9	996.1	75.357	3.551
04/07/2019 12:15	04/07/2019 12:30	115.07	148.831	1.316	310.045	106.764	36.7	59.4	997.4	80.153	4.247
04/07/2019 12:30	04/07/2019 12:45	125.02	141.042	1.368	319.037	119.15	36.7	60	997.3	77.861	3.841

AS 2

Time Beginning	Time Ending	PM_{10} µg/m³	NO_2 µg/m³	SO_2 µg/m³	CO µg/m³	O_3 µg/m³	TEMP. °C	HUM. %RH	AIRPRES mbar	WD °	WIND m/s
28/06/2019 13:15	28/06/2019 13:30	114.59	172.562	1.105	464.923	115.116	34.7	52.8	995.8	111.768	3.195
28/06/2019 13:30	28/06/2019 13:45	119.62	180.119	1.158	480.814	126.068	36.1	54.6	995.7	106.163	3.565
28/06/2019 13:45	28/06/2019 14:00	115.13	163.138	1.053	405.365	117.356	37	52.7	995.5	115.962	3.411
29/06/2019 13:30	29/06/2019 13:45	119.02	156.581	1.316	412.299	107.022	39.8	52.3	994.8	120.502	3.129
29/06/2019 13:45	29/06/2019 14:00	117.28	166.023	1.921	456.988	109.72	39.7	52.8	994.8	126.205	2.754
29/06/2019 14:00	29/06/2019 14:15	118.34	165.523	1.526	421.948	109.69	39.8	53.8	994.5	125.214	2.64
30/06/2019 13:45	30/06/2019 14:00	117.3	135.408	1.342	482.09	78.936	39.2	54.4	996	61.092	3.014
30/06/2019 14:00	30/06/2019 14:15	115.23	141.754	1.947	449.045	84.06	39.1	56.1	995.8	63.953	3.005
01/07/2019 13:15	01/07/2019 13:30	116.03	135.215	1.421	365.021	168.146	39	53.8	996	346.56	3.33
01/07/2019 13:30	01/07/2019 13:45	114.6	144.177	1.026	366.024	163.454	39	54.3	995.9	343.227	3.113
01/07/2019 13:45	01/07/2019 14:00	112.66	146.35	1.245	365.997	155.828	39	54.5	995.8	338.414	3.213
02/07/2019 13:00	02/07/2019 13:15	113.31	136.812	1.263	349.962	145.53	36.9	60.9	994.6	99.251	3.108
02/07/2019 13:15	02/07/2019 13:30	117.47	139.254	1.712	498.68	139.664	36.9	61.9	994.2	84.044	3.186
02/07/2019 13:30	02/07/2019 13:45	117.95	133.735	1.684	468.422	139.146	36.8	63.3	994.2	100.114	4.015
03/07/2019 13:40	03/07/2019 13:55	112.07	132.965	1.737	351.331	138.46	35.4	68.4	995.8	66.089	3.074
03/07/2019 13:55	03/07/2019 14:10	114.58	139.138	1.132	353.159	149.116	35.3	69	995.9	51.276	2.963
03/07/2019 14:10	03/07/2019 14:25	117.76	148.023	1.421	341.41	137.32	35.3	68.5	995.9	53.034	3.23
04/07/2019 13:00	04/07/2019 13:15	116.23	125.352	1.079	287.513	106.764	37	56.7	997.4	71.625	3.399
04/07/2019 13:15	04/07/2019 13:30	114.45	132.431	1.234	334.521	124.98	37.2	56.5	997.3	93.329	2.695
04/07/2019 13:30	04/07/2019 13:45	117.79	145.985	1.474	333.928	123.844	37.3	56.3	997.5	90.122	1.9

AS 1 TVOCs

DATE /TIME	TVOC ppb	TEMP º C	HUMIDITY % RH
28/06/2019 13:15	298	34.7	52.8
28/06/2019 13:16	252	36.1	54.6
28/06/2019 13:17	211	37	52.7
28/06/2019 13:18	199	37.1	54.3
28/06/2019 13:19	199	37.1	57.5
28/06/2019 13:20	186	37.3	56.6
28/06/2019 13:21	178	37.4	57.1
28/06/2019 13:22	179	37.3	58.3
28/06/2019 13:23	170	37.1	58
28/06/2019 13:24	169	37.2	57.1
28/06/2019 13:25	175	37.4	56.9
28/06/2019 13:26	178	37.1	57.2
28/06/2019 13:27	167	37.5	56.4
28/06/2019 13:28	162	37.6	55.9
28/06/2019 13:29	167	37.6	58.6
28/06/2019 13:30	171	37.6	56.5
28/06/2019 13:31	166	37.5	57.6
28/06/2019 13:32	159	37.8	55.6
28/06/2019 13:33	159	37.7	54.7
28/06/2019 13:34	162	37.5	56.9
28/06/2019 13:35	168	37.3	58.8
28/06/2019 13:36	169	37.8	55.9
28/06/2019 13:37	165	37.8	53.6
28/06/2019 13:38	168	38.3	55.1
28/06/2019 13:39	166	38.4	56.4
28/06/2019 13:40	164	38.2	54.9
28/06/2019 13:41	161	38.4	52.1
28/06/2019 13:42	165	38.6	51.4
28/06/2019 13:43	172	38.8	53.4
28/06/2019 13:44	170	38.7	56.2
28/06/2019 13:45	169	38.8	56.2
29/06/2019 13:30	227	36.3	55.4
29/06/2019 13:31	226	36.3	55.4
29/06/2019 13:32	226	36.8	55.4
29/06/2019 13:33	226	36.7	55.5
29/06/2019 13:34	228	35.9	55.5
29/06/2019 13:35	222	36	55.6
29/06/2019 13:36	229	35.9	55.6
29/06/2019 13:37	229	36.1	55.8
29/06/2019 13:38	230	36.8	58.2
29/06/2019 13:39	236	36.8	60.6

29/06/2019 13:40	231	36.6	61.3
29/06/2019 13:41	221	36.8	61.6
29/06/2019 13:42	215	36.7	61.9
29/06/2019 13:43	217	36.5	62.1
29/06/2019 13:44	246	36.5	62.1
29/06/2019 13:45	246	36.7	62.2
29/06/2019 13:46	245	36.5	61.6
29/06/2019 13:47	246	36.6	60
29/06/2019 13:48	252	36.6	58.8
29/06/2019 13:49	264	36.5	57.6
29/06/2019 13:50	273	36.7	56.7
29/06/2019 13:51	274	36.4	56.1
29/06/2019 13:52	274	36.5	55.7
29/06/2019 13:53	276	36.7	55.6
29/06/2019 13:54	242	36.4	58.5
29/06/2019 13:55	205	36.3	61.8
29/06/2019 13:56	201	36.6	63.5
29/06/2019 13:57	299	36.5	64.7
29/06/2019 13:58	299	36.6	65.2
29/06/2019 13:59	298	36.7	65.4
29/06/2019 14:00	297	36.7	65.6
30/06/2019 13:49	268	41.1	48.7
30/06/2019 13:50	265	40.9	48.2
30/06/2019 13:51	268	41	49.8
30/06/2019 13:52	265	41.2	50
30/06/2019 13:53	260	41.2	49.3
30/06/2019 13:54	259	41.1	49.4
30/06/2019 13:55	257	40.8	49
30/06/2019 13:56	257	40.6	49.2
30/06/2019 13:57	255	40.7	49.5
30/06/2019 13:58	256	41	50.4
30/06/2019 13:59	254	41.1	50.9
30/06/2019 14:00	254	41.5	51.4
30/06/2019 14:01	253	41.8	51.3
30/06/2019 14:02	253	41.6	50.8
30/06/2019 14:03	251	41.3	50
30/06/2019 14:04	250	38.2	49.4
30/06/2019 14:05	253	38.7	50.4
30/06/2019 14:06	252	38.8	50.8
30/06/2019 14:07	295	39.7	54.1
30/06/2019 14:08	283	40.9	62.6
30/06/2019 14:09	259	40.7	62

01/07/2019 13:15	227	40.5	56.5
01/07/2019 13:16	228	40.8	56.9
01/07/2019 13:17	230	40.5	57.5
01/07/2019 13:18	231	40.7	57.7
01/07/2019 13:19	231	41	57.5
01/07/2019 13:20	229	40.8	56.6
01/07/2019 13:21	232	40.3	57.1
01/07/2019 13:22	237	40.2	58.3
01/07/2019 13:23	234	40.5	58
01/07/2019 13:24	228	40.8	57.1
01/07/2019 13:25	226	41	56.9
01/07/2019 13:26	228	41	57.2
01/07/2019 13:27	227	41.2	56.4
01/07/2019 13:28	226	41.2	55.9
01/07/2019 13:29	227	41.1	56
01/07/2019 13:30	224	41.2	55.3
01/07/2019 13:31	221	41.1	54.8
01/07/2019 13:32	224	41	56.3
01/07/2019 13:33	227	40.9	57.3
01/07/2019 13:34	226	40.9	57.6
01/07/2019 13:35	226	40.6	57.8
01/07/2019 13:36	226	40.8	58.2
01/07/2019 13:37	228	41	58.8
01/07/2019 13:38	222	41	57.8
01/07/2019 13:39	229	41.3	59.3
01/07/2019 13:40	229	41.3	59.2
01/07/2019 13:41	230	41.3	59.6
01/07/2019 13:42	236	41.6	60.9
01/07/2019 13:43	231	40.4	59.8
01/07/2019 13:44	221	39.9	56.7
01/07/2019 13:45	215	37.7	54.4
02/07/2019 13:00	263	38	64.5
02/07/2019 13:01	233	37.6	65.5
02/07/2019 13:02	213	37.6	62.1
02/07/2019 13:03	221	37.7	65.7
02/07/2019 13:04	220	37.9	67.9
02/07/2019 13:05	219	38.1	69.1
02/07/2019 13:06	219	38.3	69.8
02/07/2019 13:07	223	38.7	70.8
02/07/2019 13:08	221	38.5	69.5
02/07/2019 13:09	216	37.9	67.2
02/07/2019 13:10	217	37.9	66.6

02/07/2019 13:11	218	37.5	66.4
02/07/2019 13:12	222	37.3	68.1
02/07/2019 13:13	226	37.3	69.6
02/07/2019 13:14	220	37.3	67.8
02/07/2019 13:15	220	37.5	69.1
02/07/2019 13:16	224	37.6	71.3
02/07/2019 13:17	231	37.6	72.7
02/07/2019 13:18	237	37.6	73.4
02/07/2019 13:19	226	38	70.6
02/07/2019 13:20	216	38.1	69.2
02/07/2019 13:21	221	37.7	69.7
02/07/2019 13:22	227	37.8	69.9
02/07/2019 13:23	226	37.6	69.3
02/07/2019 13:24	226	37.3	69.5
02/07/2019 13:25	229	37.2	70.4
02/07/2019 13:26	224	37.4	69.9
02/07/2019 13:27	221	36	70
02/07/2019 13:28	227	35.9	71.6
02/07/2019 13:29	234	35.9	72.9
02/07/2019 13:30	228	35.9	72.3
03/07/2019 13:40	248	36.1	83.2
03/07/2019 13:41	229	36.8	80.2
03/07/2019 13:42	214	36.8	77.9
03/07/2019 13:43	207	36.6	76.6
03/07/2019 13:44	206	36.8	75.1
03/07/2019 13:45	199	36.7	72.2
03/07/2019 13:46	191	36.5	70.8
03/07/2019 13:47	192	36.5	70.7
03/07/2019 13:48	194	36.7	70.9
03/07/2019 13:49	193	36.5	71.3
03/07/2019 13:50	194	36.6	72.2
03/07/2019 13:51	196	36.6	73.3
03/07/2019 13:52	200	36.5	74.4
03/07/2019 13:53	200	36.7	74
03/07/2019 13:54	194	36.4	72.1
03/07/2019 13:55	195	36.5	72.4
03/07/2019 13:56	201	36.7	73.6
03/07/2019 13:57	198	36.4	73.6
03/07/2019 13:58	206	36.3	75.4
03/07/2019 13:59	208	36.6	75.4
03/07/2019 14:00	198	36.5	74.2
03/07/2019 14:01	194	36.1	73.8
03/07/2019 14:02	199	36.5	74.7

03/07/2019 14:03	202	36.4	75.9
03/07/2019 14:04	194	36.2	74.5
03/07/2019 14:05	207	36.3	75.9
03/07/2019 14:06	210	36.3	76.8
03/07/2019 14:07	203	37.3	76.4
03/07/2019 14:08	203	37.7	76.4
03/07/2019 14:09	205	38.1	76.1
03/07/2019 14:10	204	38.9	76.2
04/07/2019 13:00	298	38.3	67.1
04/07/2019 13:01	252	38.3	68.4
04/07/2019 13:02	211	38.6	61.3
04/07/2019 13:03	199	38.9	60.5
04/07/2019 13:04	199	38.8	62
04/07/2019 13:05	186	38.8	58.6
04/07/2019 13:06	178	39	56.5
04/07/2019 13:07	179	38.9	57.6
04/07/2019 13:08	170	38.7	55.6
04/07/2019 13:09	169	38.8	54.7
04/07/2019 13:10	175	39	56.9
04/07/2019 13:11	178	39	58.8
04/07/2019 13:12	167	39.2	55.9
04/07/2019 13:13	162	39.4	53.6
04/07/2019 13:14	167	39.6	55.1
04/07/2019 13:15	171	39.4	56.4
04/07/2019 13:16	166	39.1	54.9
04/07/2019 13:17	159	39	52.1
04/07/2019 13:18	159	39.2	51.4
04/07/2019 13:19	162	39	53.4
04/07/2019 13:20	168	39	56.2
04/07/2019 13:21	169	39.1	56.2
04/07/2019 13:22	165	38.8	55.4
04/07/2019 13:23	168	38.7	56.9
04/07/2019 13:24	166	39	55.7
04/07/2019 13:25	164	39.3	55.6
04/07/2019 13:26	161	39.2	55.1
04/07/2019 13:27	165	38.9	55.7
04/07/2019 13:28	172	38.6	57.7
04/07/2019 13:29	170	38.9	57.7
04/07/2019 13:30	169	38.8	58.2

AS 2 TVOCs

DATE /TIME	TVOC ppb	TEMP ⁰ C	HUMIDITY % RH
28/06/2019 12:15	193	33.1	69
28/06/2019 12:16	196	34.2	70
28/06/2019 12:17	204	34.9	68.9
28/06/2019 12:18	206	35.9	67.4
28/06/2019 12:19	200	36.8	67.5
28/06/2019 12:20	184	37.7	67.3
28/06/2019 12:21	185	37.7	67.3
28/06/2019 12:22	196	37.7	67.1
28/06/2019 12:23	199	38.1	66.8
28/06/2019 12:24	198	38.5	66.4
28/06/2019 12:25	199	38.5	65.6
28/06/2019 12:26	201	38.6	66.4
28/06/2019 12:27	197	38.7	64.5
28/06/2019 12:28	186	38.8	66.3
28/06/2019 12:29	185	38.4	64.3
28/06/2019 12:30	193	37.6	63.2
28/06/2019 12:31	206	38.3	63.7
28/06/2019 12:32	213	38.2	63.1
28/06/2019 12:33	212	38.4	64.5
28/06/2019 12:34	216	37.9	62.9
28/06/2019 12:35	212	37.9	63.2
28/06/2019 12:36	209	38.3	63.8
28/06/2019 12:37	213	38.5	63.4
28/06/2019 12:38	198	37.5	62.3
28/06/2019 12:39	197	37.8	64.7
28/06/2019 12:40	187	37.8	62.5
28/06/2019 12:41	204	38.5	63.1
28/06/2019 12:42	206	38.7	62.1
28/06/2019 12:43	197	38.9	64.3
28/06/2019 12:44	198	37.5	61.9
28/06/2019 12:45	187	37.9	62.7
29/06/2019 12:30	208	39.3	55.6
29/06/2019 12:31	206	39.7	55.6
29/06/2019 12:32	203	39.4	55.7
29/06/2019 12:33	199	39.3	55.8
29/06/2019 12:34	196	39.7	55.7
29/06/2019 12:35	193	40.2	55.7
29/06/2019 12:36	189	39.9	55.6
29/06/2019 12:37	188	39.9	55.5
29/06/2019 12:38	185	39.8	55.3
29/06/2019 12:39	183	40	55.5

29/06/2019 12:40	181	40.2	55.3
29/06/2019 12:41	179	40.4	54.8
29/06/2019 12:42	177	40.5	54.9
29/06/2019 12:43	175	39.9	55.1
29/06/2019 12:44	173	39.7	55.3
29/06/2019 12:45	171	39.5	55.5
29/06/2019 12:46	171	39.4	55.5
29/06/2019 12:47	169	39.5	55.4
29/06/2019 12:48	168	39.6	55.5
29/06/2019 12:49	166	39.5	55.6
29/06/2019 12:50	166	39.6	55.5
29/06/2019 12:51	165	39.8	55.5
29/06/2019 12:52	164	39.6	55.6
29/06/2019 12:53	163	39.5	55.7
29/06/2019 12:54	162	38.5	55.6
29/06/2019 12:55	161	38.2	55.5
29/06/2019 12:56	193	38.2	55.5
29/06/2019 12:57	196	38.6	55.5
29/06/2019 12:58	204	38.7	55.6
29/06/2019 12:59	206	38.8	55.6
29/06/2019 13:00	200	38.3	55.6
30/06/2019 12:30	185	38.9	60.4
30/06/2019 12:31	257	39	59.6
30/06/2019 12:32	260	39	60.3
30/06/2019 12:33	254	39.1	58.5
30/06/2019 12:34	243	39.1	56.5
30/06/2019 12:35	249	39.3	57.2
30/06/2019 12:36	244	39.4	55.8
30/06/2019 12:37	246	39.4	56.3
30/06/2019 12:38	241	39.3	55.2
30/06/2019 12:39	224	39.5	51
30/06/2019 12:40	225	39.9	49.8
30/06/2019 12:41	229	40.1	49.9
30/06/2019 12:42	238	39.9	51.6
30/06/2019 12:43	243	39.7	53.3
30/06/2019 12:44	242	39.5	53.4
30/06/2019 12:45	241	39.4	53.6
01/07/2019 12:00	266	40.4	55.2
01/07/2019 12:01	268	39.9	57.1
01/07/2019 12:02	270	39.6	58.2
01/07/2019 12:03	267	39.4	58.9
01/07/2019 12:04	267	39.6	59.9

01/07/2019 12:05	267	39.4	60.9
01/07/2019 12:06	266	39.4	61.8
01/07/2019 12:07	266	39.4	61.9
01/07/2019 12:08	264	39.3	62
01/07/2019 12:09	267	39.7	62.6
01/07/2019 12:10	263	39.3	62.4
01/07/2019 12:11	264	39.3	63.3
01/07/2019 12:12	266	39.7	64.2
01/07/2019 12:13	259	39.4	63.2
01/07/2019 12:14	255	39.3	62.5
01/07/2019 12:15	257	39.7	62.5
01/07/2019 12:16	253	40.2	61.6
01/07/2019 12:17	250	39.9	61.2
01/07/2019 12:18	249	39.9	61.3
01/07/2019 12:19	245	39.8	60.5
01/07/2019 12:20	246	40	60.3
01/07/2019 12:21	246	40.2	60.4
01/07/2019 12:22	247	40.4	60.6
01/07/2019 12:23	240	40.5	59.4
01/07/2019 12:24	233	40.6	57.8
01/07/2019 12:25	233	40.4	57.5
01/07/2019 12:26	231	40.3	57
01/07/2019 12:27	236	40.7	58.4
01/07/2019 12:28	229	40.7	56.8
01/07/2019 12:29	227	40.5	56.6
01/07/2019 12:30	231	40.9	57.4
02/07/2019 12:30	225	33.2	71
02/07/2019 12:31	218	35.6	73.6
02/07/2019 12:32	223	37.5	73.8
02/07/2019 12:33	231	38.2	70.9
02/07/2019 12:34	229	38.6	67.9
02/07/2019 12:35	228	38.8	66.8
02/07/2019 12:36	228	39.2	66.3
02/07/2019 12:37	228	39.3	65.8
02/07/2019 12:38	214	39.5	64.1
02/07/2019 12:39	190	39.9	60.3
02/07/2019 12:40	189	40.2	59.6
02/07/2019 12:41	194	39.4	61.1
02/07/2019 12:42	193	38.6	63
02/07/2019 12:43	196	38.5	64.5
02/07/2019 12:44	204	38.6	66.2
02/07/2019 12:45	206	38.6	67
02/07/2019 12:46	200	38.4	66.2

02/07/2019 12:47	184	38.6	61.6
02/07/2019 12:48	185	38.6	61
02/07/2019 12:49	196	38.1	65
02/07/2019 12:50	199	37.9	66.6
02/07/2019 12:51	198	37.9	66.8
02/07/2019 12:52	199	37.8	67.3
02/07/2019 12:53	201	37.7	68.3
02/07/2019 12:54	197	37.8	67.3
02/07/2019 12:55	186	38.2	63.3
02/07/2019 12:56	185	38.5	62.3
02/07/2019 12:57	193	38.1	65.7
02/07/2019 12:58	186	38.5	63.6
02/07/2019 12:59	185	38.5	64.3
02/07/2019 13:00	193	38.6	65.4
03/07/2019 12:33	296	35.8	79
03/07/2019 12:34	276	36.9	77.2
03/07/2019 12:35	251	37.4	70.9
03/07/2019 12:36	232	37.7	67.5
03/07/2019 12:37	216	37.5	65.7
03/07/2019 12:38	212	37.8	65.7
03/07/2019 12:39	209	38.5	65.7
03/07/2019 12:40	203	38.3	64.8
03/07/2019 12:41	196	37.9	63.8
03/07/2019 12:42	197	38	64.1
03/07/2019 12:43	197	38.1	64
03/07/2019 12:44	195	38.2	63.5
03/07/2019 12:45	190	37.9	62.9
03/07/2019 12:46	189	37.9	63.5
03/07/2019 12:47	187	38	64.1
03/07/2019 12:48	186	38.3	64.5
03/07/2019 12:49	184	38.1	64
03/07/2019 12:50	184	38.5	63.3
03/07/2019 12:51	182	38.2	62.9
03/07/2019 12:52	183	38.2	63.9
03/07/2019 12:53	182	38.6	63.7
03/07/2019 12:54	185	38.7	63.8
03/07/2019 12:55	185	38.8	63.1
03/07/2019 12:56	180	38.3	62.6
03/07/2019 12:57	179	38.1	62.7
03/07/2019 12:58	178	38.1	63.5
03/07/2019 12:59	176	37.9	62.9
03/07/2019 13:00	181	38.2	63.5
03/07/2019 13:01	173	38.2	64.1

03/07/2019 13:02	175	38.6	64.5
03/07/2019 13:03	174	38.7	64
04/07/2019 12:27	182	37.7	56.7
04/07/2019 12:28	183	39.3	58.4
04/07/2019 12:29	171	40	52.7
04/07/2019 12:30	166	40.1	51.2
04/07/2019 12:31	163	40.1	49.6
04/07/2019 12:32	161	39.7	48.1
04/07/2019 12:33	162	39.6	48
04/07/2019 12:34	163	39.3	49
04/07/2019 12:35	164	39.8	48.9
04/07/2019 12:36	164	39.7	48.6
04/07/2019 12:37	166	39.8	50.2
04/07/2019 12:38	167	39.7	51.7
04/07/2019 12:39	166	39.8	51.4
04/07/2019 12:40	164	40.1	49
04/07/2019 12:41	165	40.1	48.4
04/07/2019 12:42	167	39.9	50.2
04/07/2019 12:43	166	39.9	47.9
04/07/2019 12:44	167	39.7	48.5
04/07/2019 12:45	168	39.7	50.1
04/07/2019 12:46	167	39.8	48.7
04/07/2019 12:47	167	39.8	45.9
04/07/2019 12:48	168	39.4	47.5
04/07/2019 12:49	168	39.4	48
04/07/2019 12:50	168	39.7	45.1
04/07/2019 12:51	168	39.7	46.2
04/07/2019 12:52	169	39.7	47.7
04/07/2019 12:53	169	39.7	47.7
04/07/2019 12:54	169	39.7	46
04/07/2019 12:55	170	39.4	46.8
04/07/2019 12:56	164	39.1	48.6
04/07/2019 12:57	175	39.3	48.4

Appendix H – Hydrodynamic Modelling Studies

HR Wallingford
Working with water

Umm Al Houl Power, Qatar

Recirculation & thermal dispersion studies

DKR5430-RT001-R02-00

September 2015

Document information

Document permissions	Confidential - client
Project number	DKR5430
Project name	Umm Al Houl Power, Qatar
Report title	Recirculation & thermal dispersion studies
Report number	RT001
Release number	R02-00
Report date	September 2015
Client	Samsung C&T
Client representative	Mr Hyoung Jin
Project manager	Manuela Escarameia
Project director	Ian Willoughby

Document history

Date	Release	Prepared	Approved	Authorised	Notes
03 Sep 2015	02-00	AJN	TEJ	IRW	
03 Jul 2015	01-00	AJN	TEJ	GBS	Issued for review [IFR]

Document authorisation

Prepared	Approved	Authorised

Contents

Figures

Tables

1. Introduction

1.1. Background

A consortium led by Mitsubishi Corporation including Samsung C&T as EPC contractor has been awarded the construction and operation of a new Independent Water and Power Project (IWPP) known as Umm Al Houl Power (UHP), previously called Facility ‘D’, north of Mesaieed on the east coast of Qatar – Figure 1.1.

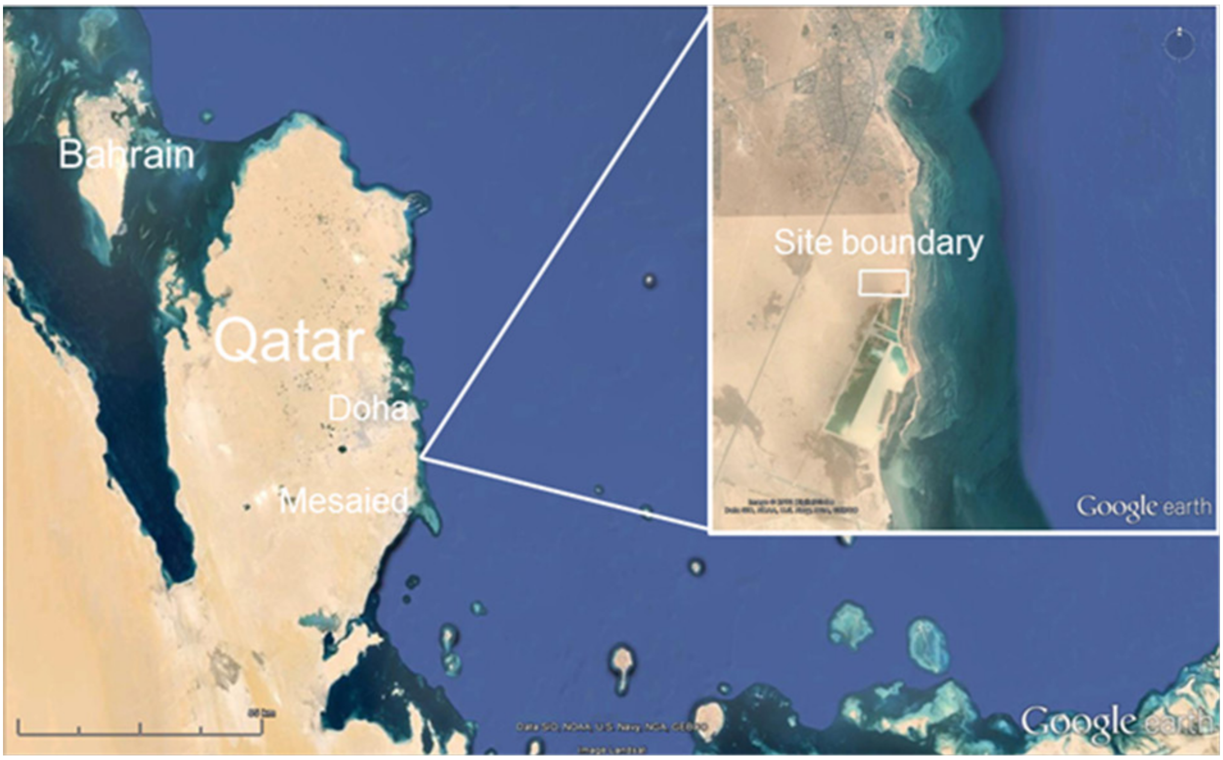

Figure 1.1: Site location

HR Wallingford is providing a range of studies to support the detailed design process and the Environmental & Social Impact Assessment (ESIA):

- Task 1 – Recirculation & thermal dispersion studies, inc thermal dispersion EISA chapter;
- Task 2 – Hydraulic design assessment for seawater intake & outfall structures;
  - Task 2a - Wave study;
  - Task 2b – Hydraulics of intake, outfall and pumping station, inc. transient analysis;
  - Task 2c – Scour protection for intake & outfall (conceptual design);
- Task 3 – Physical model study of pumping station;
- Task 4 – Sediment ingress & dispersion assessments;
- Task 5 – Metocean & bathymetric survey.

This report relates to Task 1 Recirculation & thermal dispersion studies and describes the calibration of the hydrodynamic model, and the investigation of the recirculation and dispersion of the thermal/saline plume from the UHP under two operating conditions for the preferred configuration of the intake and outfall. Additional analysis to support the EIA conducted by Mott MacDonald is presented in Appendix C.

1.2. Report conventions

The horizontal coordinate system used throughout this report is Qatar National Grid (QNG). The vertical coordinate system is Qatar National Height Datum (QNHD) which is equivalent to mean sea level (MSL). Units are metres (m) in both dimensions.

2. Data received

Table 2.1 lists the data received that are relevant to Task 1.

Table 2.1: Relevant data received

Ref	From	Date received dd/mm/yyyy	Name	Filename	Contents
1	From surveyors MTEC	22/06/2015	Metocean Survey Al Whakrah Qatar Final Report Rev00; Data sets	307_Whakrah_Final_Report_Metocean_R01.pdf	ADCP velocity and wave data
2	From surveyors MTEC	14/05/2015	Bathymetric chart, Rev 00 12/05/2015	307_Al_Whakrah_bathymetric_chart_5k_r0.dwg	Bathymetric chart with 0.5m contours
3	From surveyors MTEC	21/05/2015	Bathymetric Survey; Al Wakrah, Qatar Final Report	307 Bathymetric survey_final_report_r0.doc	Bathymetric survey
4	Samsung C&T	22/06/15	UHP Seawater flow rate	UHP_Seawater Flow Rate Design Data 150616.xlsx	Intake and outfall flow rates, temperature and salinity increases
5	Samsung C&T	22/06/15	Intake head Structure	1005~1006 Intake Head Structure Sectional Details rev01.dwg	Drawings of intake head structure
6	Samsung C&T	22/06/15	Intake and discharge overall layout	1001_Intake Discharge Overall Layout_rev02.dwg	Overall layout of intake and outfalls
7	Samsung C&T	22/06/15	Intake pipeline Plan	UHP-SCT-C00-UPZ-D-1002.dwg	Plan of intake pipeline

Ref	From	Date received dd/mm/yyyy	Name	Filename	Contents
8	Samsung C&T	22/06/15	Intake pipeline section	UHP-SCT-C00-UPZ-D-1021.dwg	Sections through intake pipelines
9	Samsung C&T	22/06/15	Intake pipeline Profile	UHP-SCT-C00-UPZ-D-1022-1023.dwg	Longitudinal profile along intake pipelines , showing protection.
10	Samsung C&T	22/06/15	Discharge pipeline sections	1010~1011 Discharge Pipeline Sectional Details(1).dwg	Sections through discharge pipelines
11	Samsung C&T	22/06/15	Diffuser	1012 Discharge Pipeline Sectional Details(3).dwg	Details of outfall diffuser
12	Samsung C&T	22/06/15	Discharge pipeline profile	1013-1014 Discharge Pipeline profile.dwg	Longitudinal profile along discharge pipelines , showing protection.

3. Survey data

3.1. Overview

MTEC was commissioned by HR Wallingford to collect bathymetric and metocean data in the vicinity of the site (Ref.1 in Table 2.1) Detailed bathymetry data were collected in April 2015 covering an area approximately 12 km^2 in size. Currents and water levels were recorded with an ADCP and an Aquadopp from 22 April to 9 May 2015. The ADCP was located approximately 2.5 km offshore at the -5 m QNHD contour, and the Aquadopp was located approximately 4 km offshore at the -10 m QNHD contour. A weather station was also installed at Al Wakrah from 21 April to 20 May 2015. The locations of the bathymetric survey and metocean survey instruments are shown in Figure 3.1.

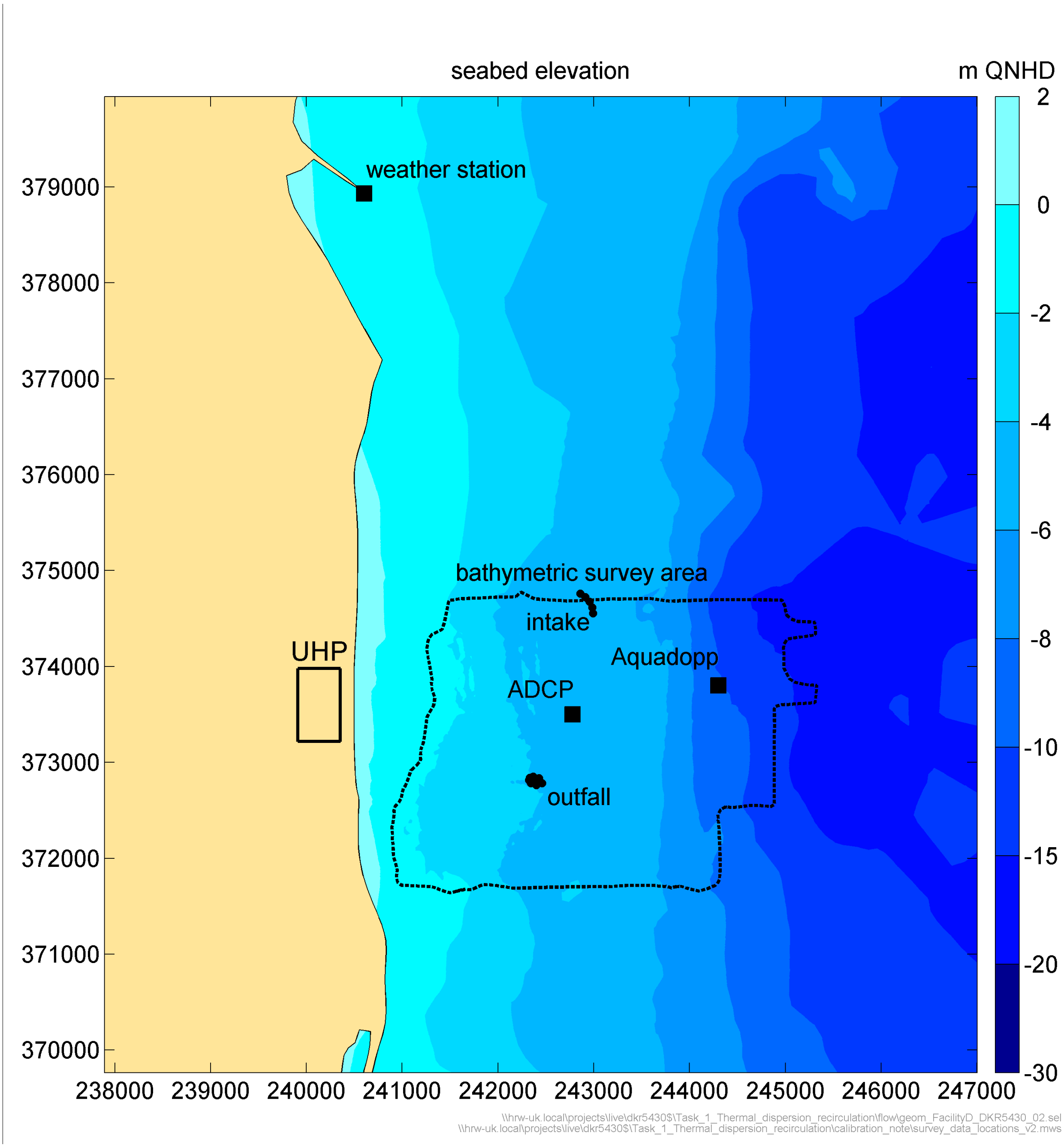

Figure 3.1: Locations of bathymetric survey and metocean survey instruments (horizontal coordinate system is Qatar National Grid (QNG))

3.2. Wind data

The weather station installed at Al Wakrah recorded the wind speed and direction at one minute intervals at an elevation of 10m above sea level. The data were averaged over a 10 minute period to remove short period gusts and noise. The wind speed and direction are shown in Figure 3.2.

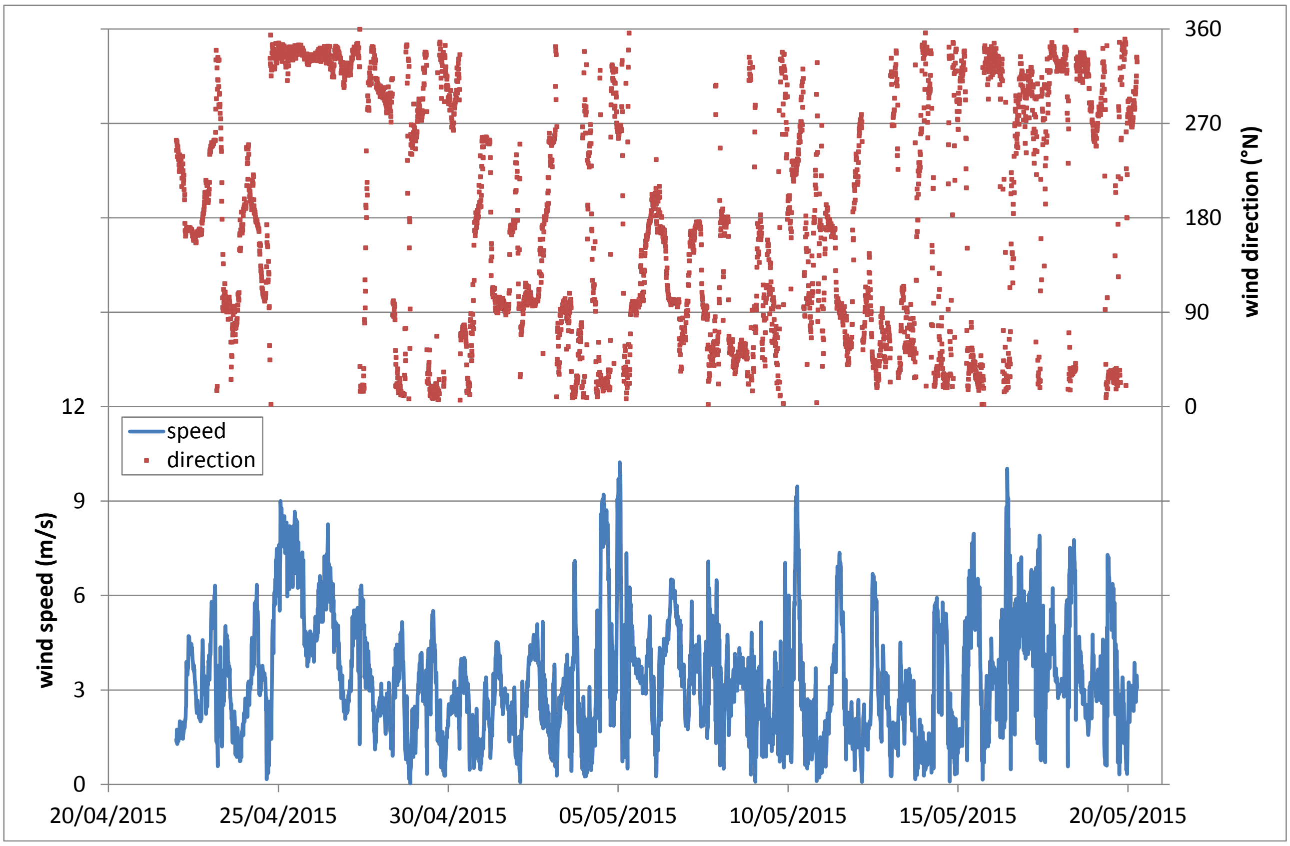

Figure 3.2: 10 minute average wind speed and direction, 10m elevation, Al Wakrah, 21 April to 20 May 2015

The wind speeds for this period are generally weak, around 3 m/s, with a few short higher speed events of around 9 to 10 m/s. There are daily peaks in wind speed which could be indicative of land/sea breezes generated by differential atmospheric cooling of the land and sea. The direction is generally varying though there is a period of persistent winds from north west on 25 April that may be indicative of shamal winds.

The wind distribution for the survey period is shown in Figure 3.3. Winds are most commonly from north west and from east, which matches the long term trends in wind distribution recorded at Doha International Airport (Figure 3.4). However winds from north east and south occurred more frequently during the survey period than are found annually. Winds from close to north appear to be absent from survey data, which is unusual given the location of the instrument.

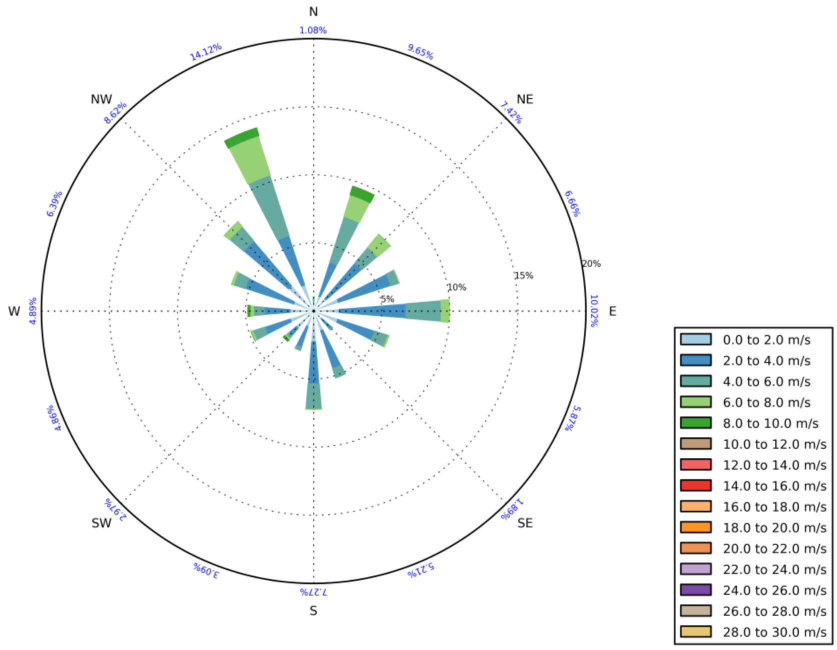

Figure 3.3: Wind distribution at Al Wakrah, 21 April to 20 May 2015

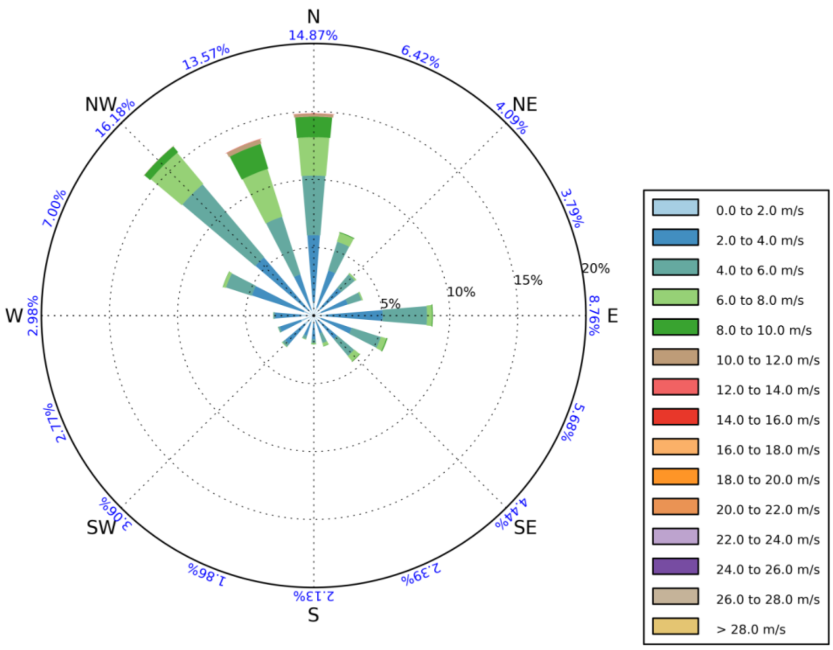

Figure 3.4: Wind distribution at Doha International Airport for 2009-2013

3.3. Tidal elevation data

The tidal elevations at the ADCP and Aquadopp are shown in Figure 3.5 and Figure 3.6 respectively. Tides at the two sites are similar and there is a clear spring-neap cycle with neap tides around 1 May 2015 and spring tides around 8 May 2015. The tides are of a mixed type with both diurnal (one high or low water per day) and semi-diurnal features (two high or low waters per day).

There is evidence of a non-tidal event between 25 April 2015 and 28 April 2015 that caused a reduction in the tidal range. This is likely to have been caused by meteorological effects (the period is coincident with the period of persistent winds from the north west).

Between 30 April 2015 and 9 May 2015 the difference between the daily highest high water and lowest low water, referred to as the high tidal range, is around 1.1 m on average. This agrees reasonably well with the Admiralty tide tables (UK Hydrographic Office, 2014) which state the mean high tidal range at Al Wakrah is 1.0 m. This indicates that this period is reasonably representative of tides at the site.

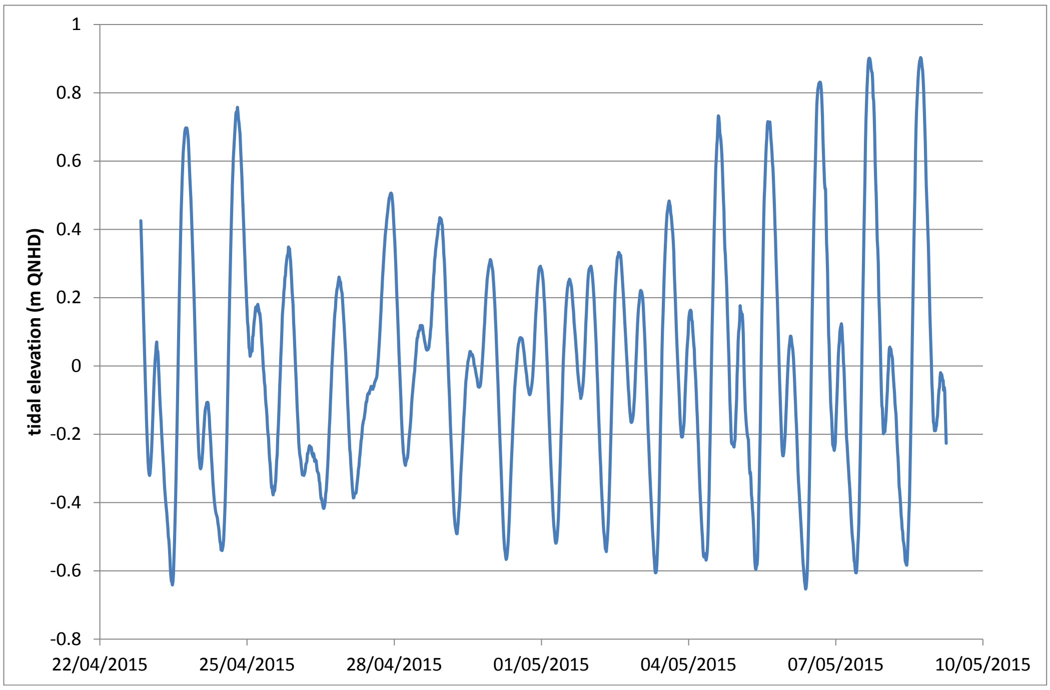

Figure 3.5: Tidal elevation at the ADCP location

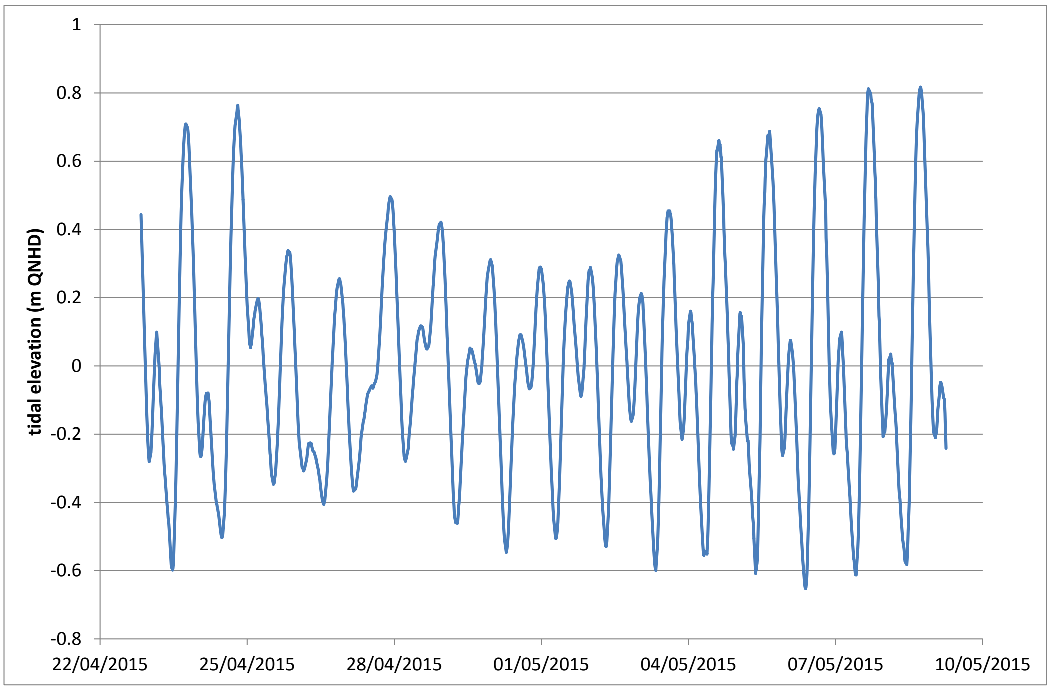

Figure 3.6: Tidal elevation at the Aquadopp location

3.4. Current data

Current speed and direction were recorded near the -5 m QNHD contour with an ADCP. The instrument recorded the currents through the water column at 20 depths referred to as “bins”. The depth-averaged current speed and direction were calculated by averaging over all bins and are shown in Figure 3.7. The current speeds are weak, generally less than 0.3 m/s, and are predominantly north-going and south-going. For the event between 25 April and 28 April the current is almost constantly south-going. This indicates that the currents at this time are not dominated by standard tidal variation.

The Aquadopp was located near the -10 m QNHD contour and recorded currents across 40 bins. The depth-averaged current speed and direction were calculated by averaging over all bins and are shown in Figure 3.8. The currents are faster than at the ADCP, with speeds of up to 0.5 m/s. This increase is larger than expected given the instruments are only around 1.5 km apart and there are no obvious features to accelerate the flow other than distance from the shoreline. The current directions are similar to the ADCP and predominantly alternate between north-going and south-going.

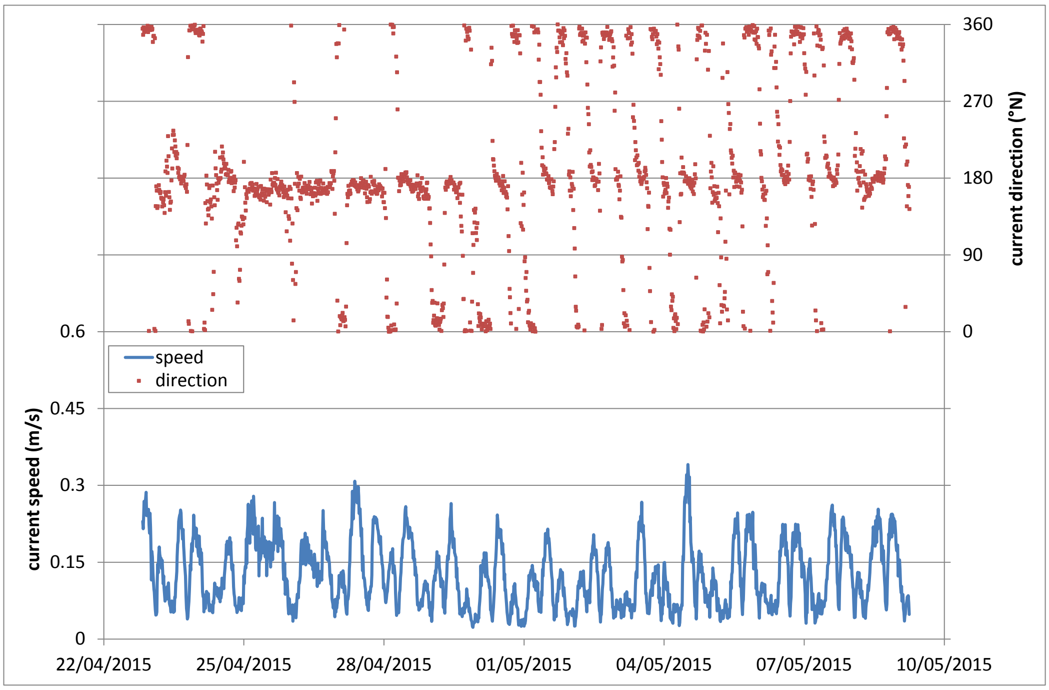

Figure 3.7: Depth-averaged current speed and direction at the ADCP location

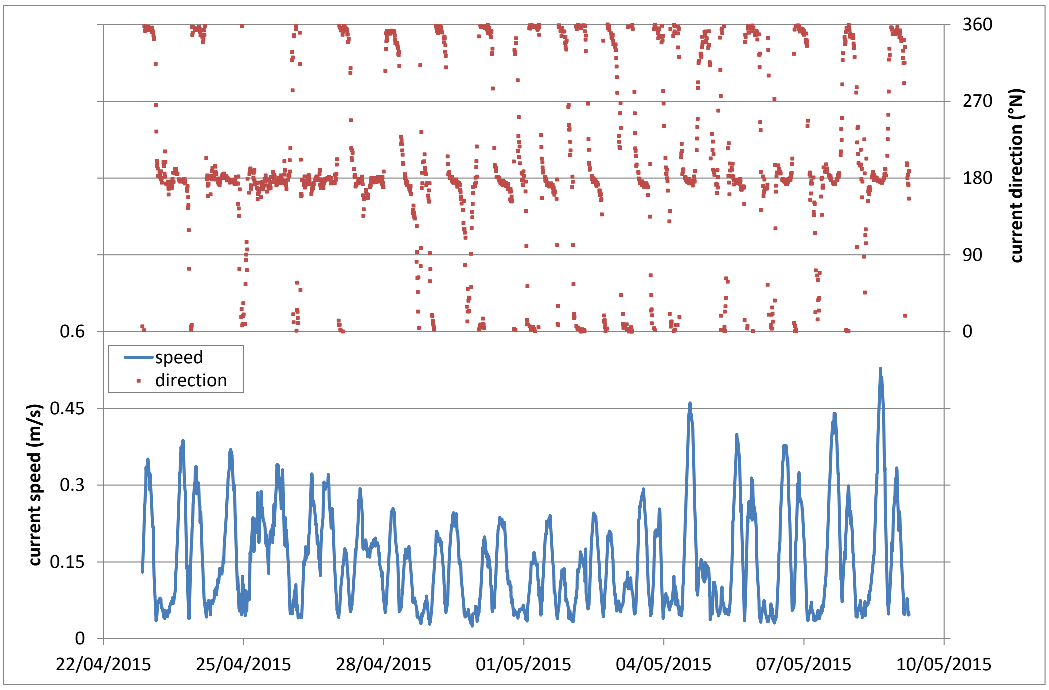

Figure 3.8: Depth-averaged current speed and direction at the Aquadopp location

4. Model configuration

4.1. TELEMAC system

Hydrodynamics at the site have been examined using the TELEMAC finite element modelling system. The TELEMAC system was originally developed by EDF LNHE and is now under the directorship of a consortium of organisations; HR Wallingford is a key participant in the consortium. TELEMAC represents the area of interest using a completely flexible mesh of triangular elements. As the mesh is unstructured it can be refined to represent coastlines and other important structures accurately within the resolution of the elements. HR Wallingford has wide experience of simulating currents in the coastal waters of Qatar, and elsewhere in the Middle East, using the TELEMAC system.

TELEMAC-3D, the three dimensional module of the TELEMAC system, was used to allow the simulation of the vertical transport and structure of the effluent plumes during the recirculation assessment. This solves the equations of motion and transport in multiple layers, including the important effects of buoyant spreading, inhibition of vertical mixing associated with sharp density gradients, and shear of wind-driven currents. Important atmospheric processes, including cooling of surface plumes to the atmosphere, are also represented. These processes are essential to obtain a good representation of thermal/saline plume dispersion. TELEMAC-3D has been used by HR Wallingford in more than 100 thermal and saline dispersion studies worldwide, including many in Qatar's coastal waters, and in particular during the bidding stage of the Facility 'D' project (HR Wallingford, 2014).

4.2. Mesh and bathymetry

Our TELEMAC-3D model of the coastal waters near the site was developed in the previous bid-stage study (HR Wallingford, 2014). The model covers an area approximately 30 km alongshore by 10 km offshore. The coastline is based on data from international hydrographic offices supplied through the C-Map database. For the present study the model has been updated to include the reclamations to the south of the site currently under construction as part of the Doha New Port Project. The model mesh was enhanced in the region of the potential location of the intake and outfall as shown in Figure 4.1. The mesh resolution is 20 m in the vicinity of the site, rising gradually to 1 km at the sea boundaries.

The bathymetry of the model developed during the bid-stage was based on information from:

- international hydrographic offices supplied through the C-Map database;
- with the addition of data at the IWPP site provided by QEWC;
- some additional near shore data provided by COWI.

This model bathymetry was then was updated to include survey data collected by MTEC in April 2015. This updated model bathymetry is presented in Figure 4.2.

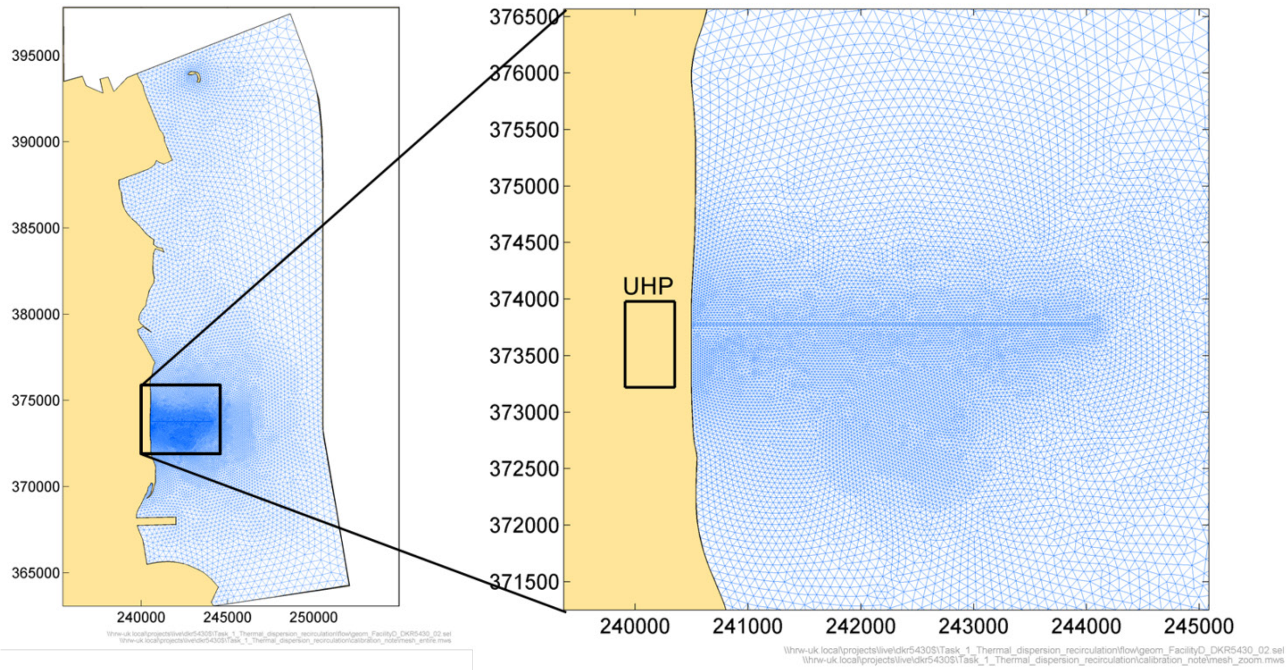

Figure 4.1: Model mesh – full extent and in the vicinity of the site

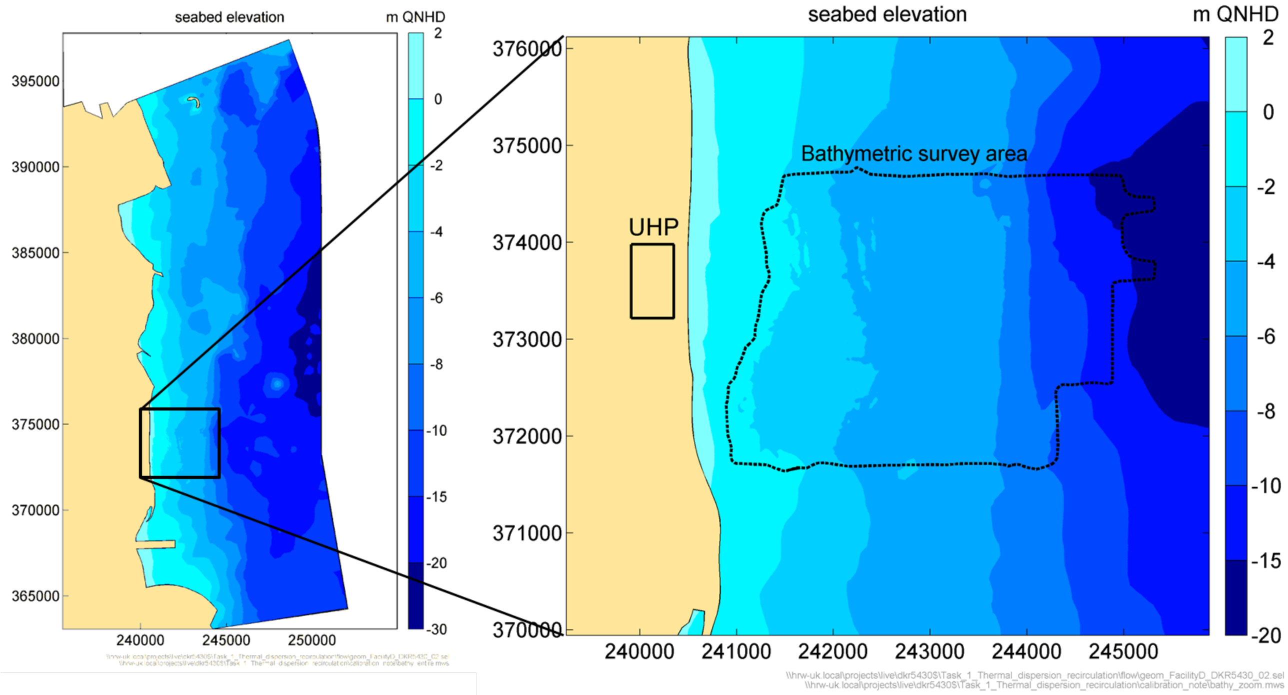

Figure 4.2: Model bathymetry – full extent and in the vicinity of the site

4.3. Boundary conditions

HR Wallingford's existing regional model of the Gulf was used to provide boundary conditions to the local model. As shown in Figure 4.3, it covers the Gulf, the Straits of Hormuz and the Gulf of Oman, and extends out into the Arabian Sea. Bathymetry is taken from data available from international hydrographic offices, supplemented by local surveys. Currents and water levels are driven by astronomical tides at the eastern boundary. Predicted water levels have been calibrated against tidal elevation data at 36 locations distributed across the model area.

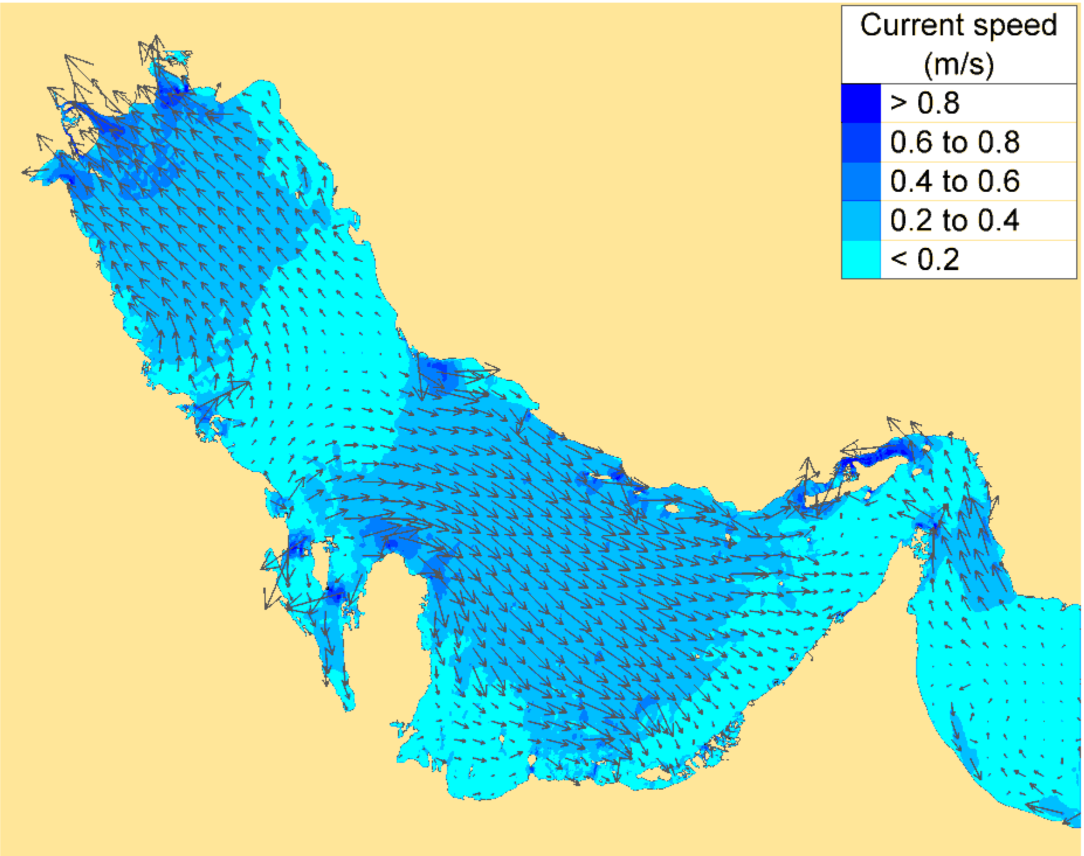

Figure 4.3: Example simulated currents in the Gulf regional model

Tidal elevations were extracted from the Gulf model for the period 22 April to 9 May 2015 to correspond to the same period as the current meter data. These elevations were then used to drive the detailed local model. This procedure is commonly known as nesting, and is a well-established procedure for simulating currents across regions of different scale.

4.4. Winds

Observed winds were applied within the model using the winds recorded at the weather station at Al Wakrah (Figure 3.2). The wind was applied uniformly in space across the entire model.

5. Hydrodynamic modelling results

The hydrodynamic model was run for the period from 22 April to 9 May 2015 to allow comparison with the current meter data. The model was calibrated by modifying the boundary conditions to generate the appropriate tidal elevations at the current meters. The model is compared with the data for the period from 30 April to 9 May 2015 as during this period the tides are dominated by astronomical processes.

The tidal elevation predicted by the model and recorded by the ADCP and Aquadopp are shown in Figure 5.1 and Figure 5.2 respectively. Generally there is good agreement between the model and the data, with differences of at most 0.1 m.

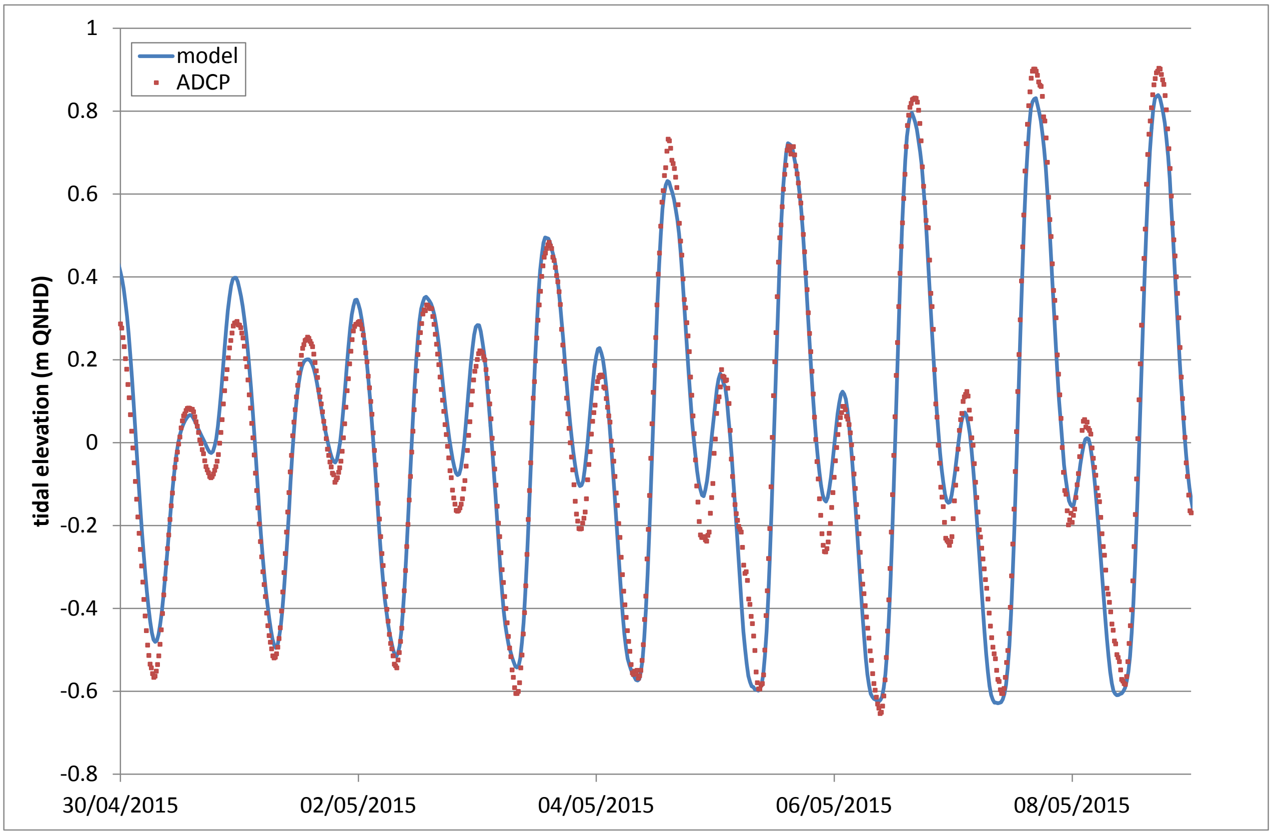

Figure 5.1: Comparison of tidal elevations at the ADCP location

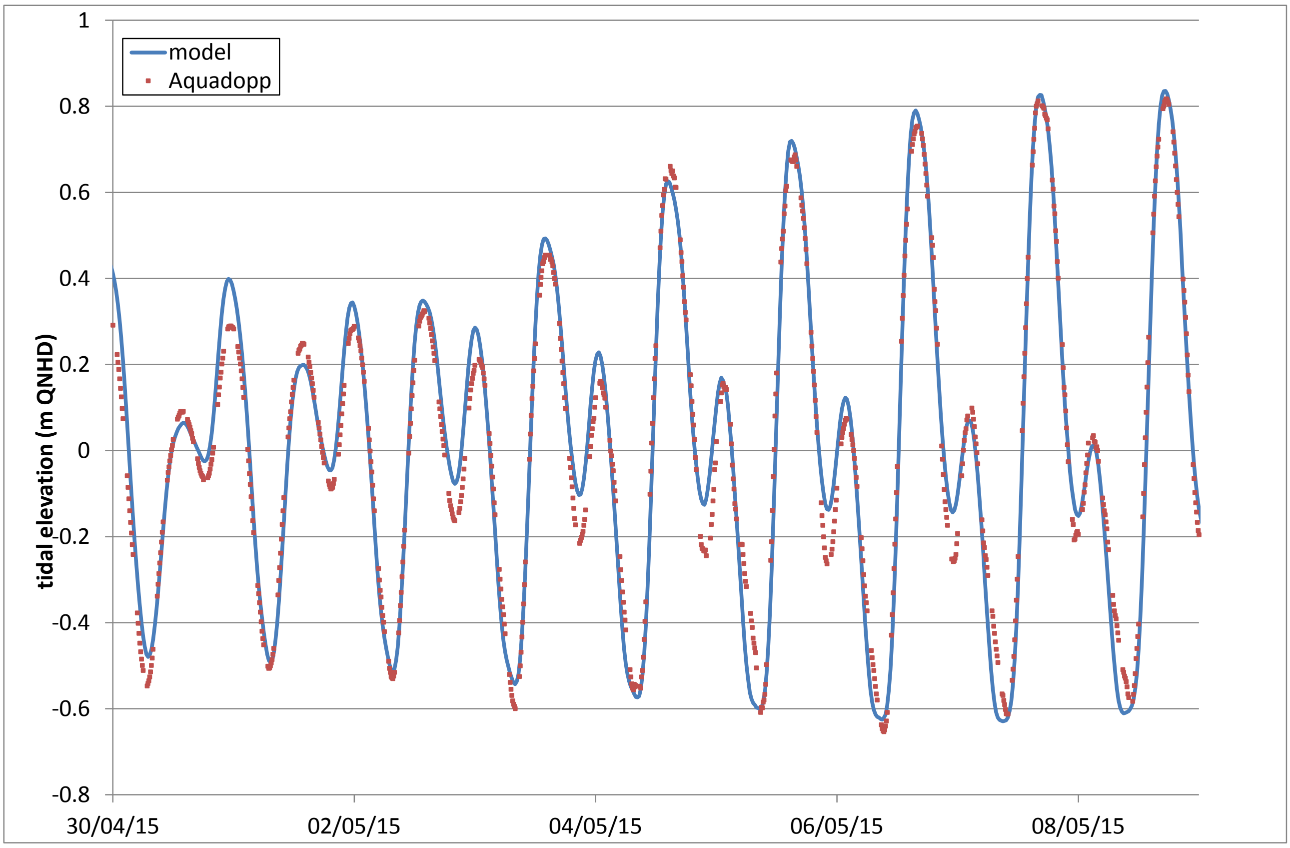

Figure 5.2: Comparison of tidal elevations at the Aquadopp location

Simulated current vectors at the site are shown in Figure 5.3 at times of peak flood and peak ebb during the spring tide on 8 May 2015. The tide floods to the south and ebbs to the north, and current speeds generally increase with distance offshore.

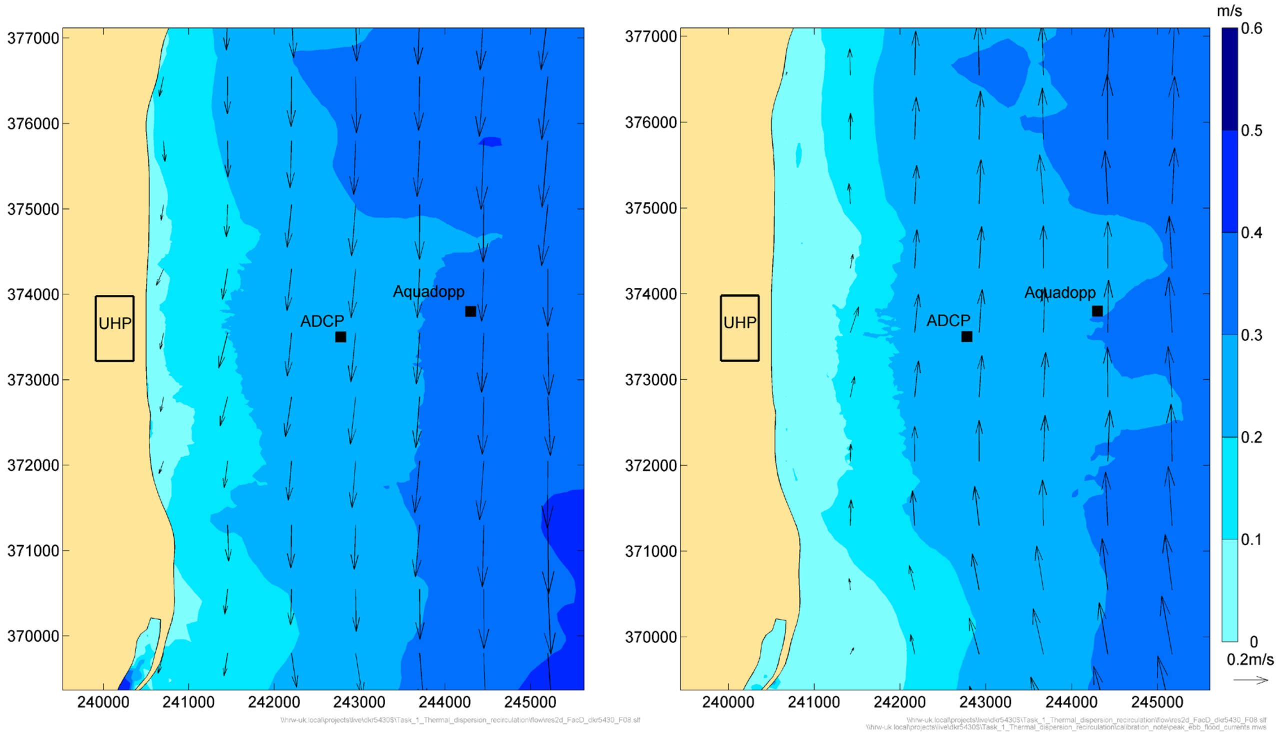

Figure 5.3: Simulated peak flood (left) and peak ebb (right) currents on 8 May 2015

Figure 5.4 shows the comparison between the depth-averaged current speeds recorded at the ADCP location and predicted by the model for the period 30 April to 9 May 2015. There is reasonable agreement with differences in peak speed of at most 0.07 m/s. The depth-averaged current directions at the ADCP location are shown in Figure 5.5 for the same period and indicate reasonable agreement with the direction alternating between north-going and south-going as the tide ebbs and floods.

Figure 5.6 shows the comparison between the depth-averaged current speeds recorded at the Aquadopp location and predicted by the model for the period 30 April to 9 May 2015. There is some agreement with peak speeds generally predicted by the model to be within 0.1 m/s of the recorded peak speeds. There are two events where the peak speed is recorded as being around 0.2 m/s faster than in the model. The agreement is not as good as at the ADCP location however the plume is more likely to occupy the area in the vicinity of the ADCP location as it is significantly closer to the outfall (see Figure 3.1). Therefore this level of agreement at the Aquadopp location is deemed reasonable for the dispersion and recirculation study.

A comparison of the depth-averaged current directions at the Aquadopp location are shown in Figure 5.7. Generally there is reasonable agreement between the model and the measurements with the current directions approximately north-going and south-going.

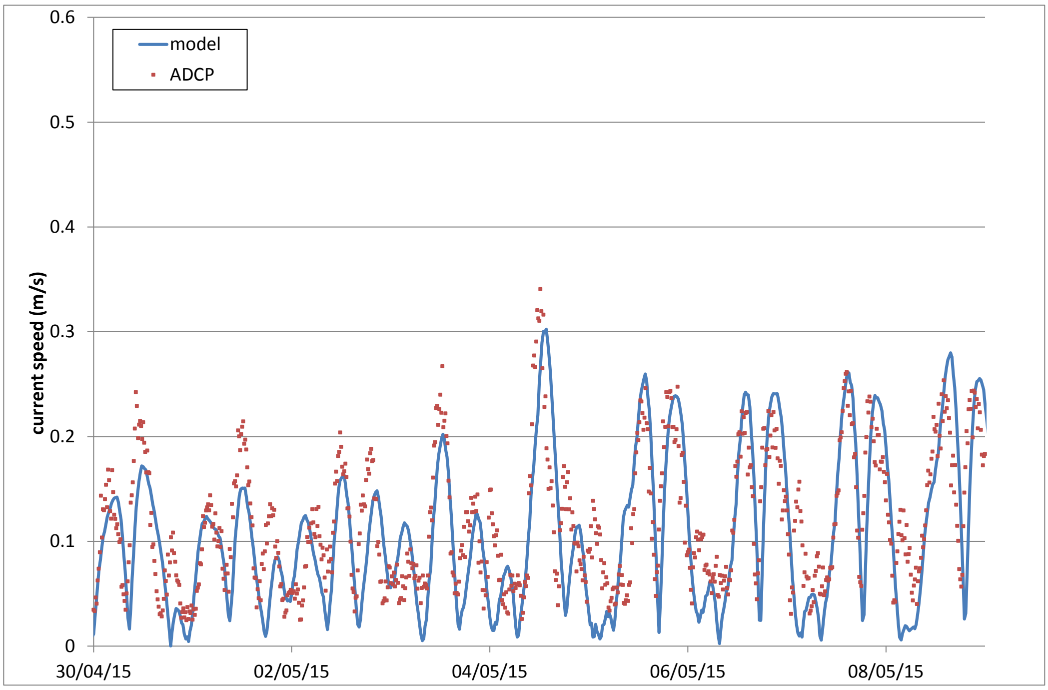

Figure 5.4: Comparison of depth-averaged current speeds at the ADCP location

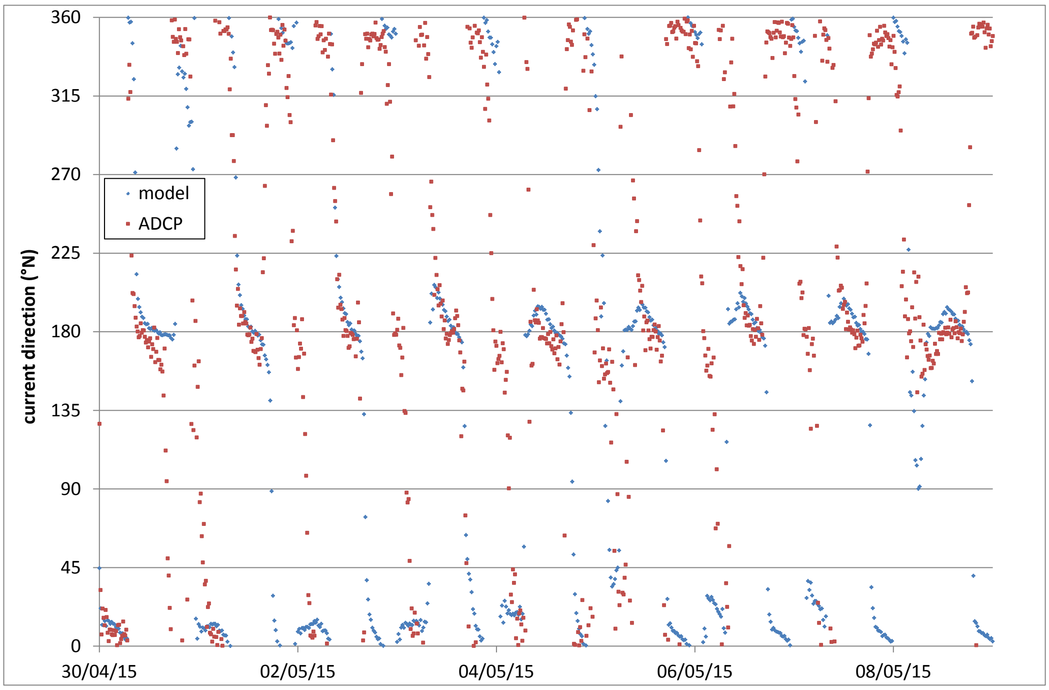

Figure 5.5: Comparison of depth-averaged current direction at the ADCP location

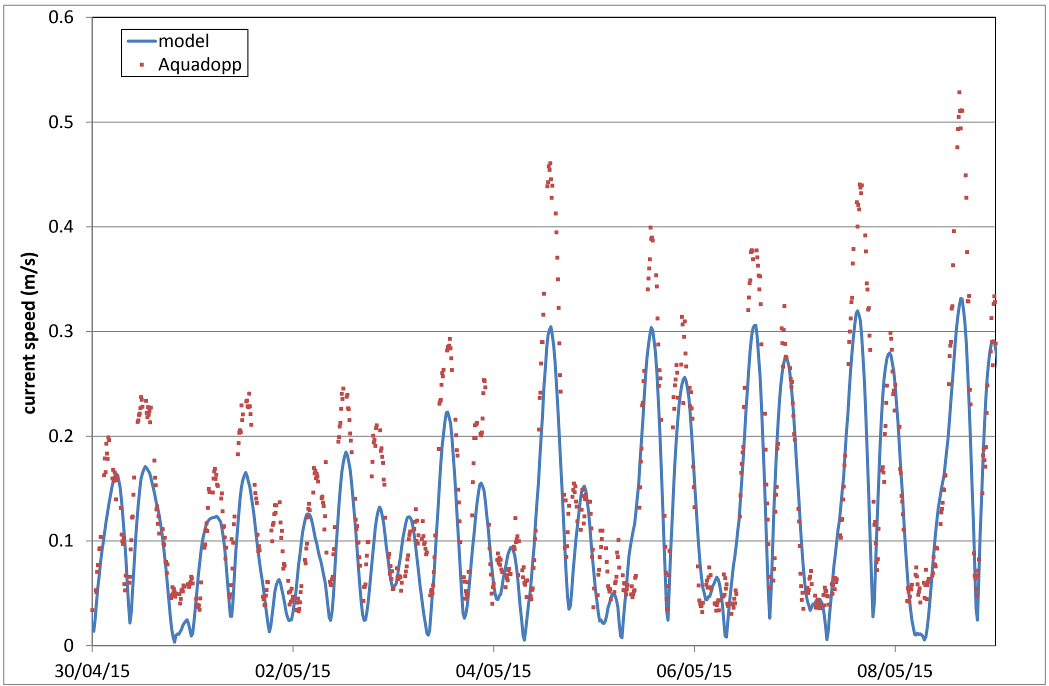

Figure 5.6: Comparison of depth-averaged current speeds at the Aquadopp location

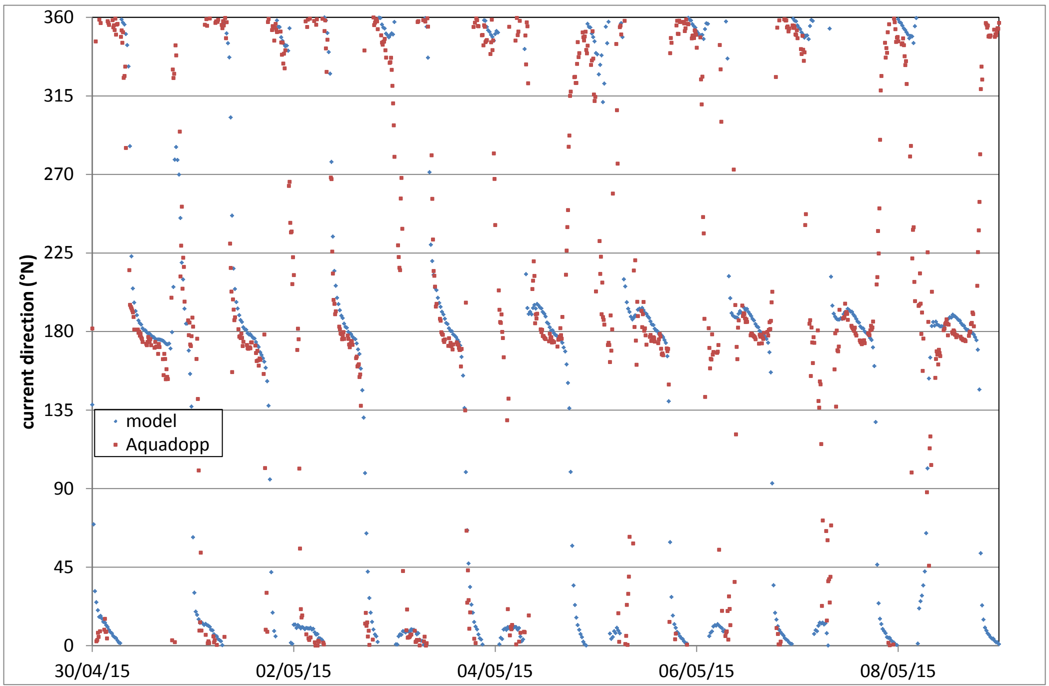

Figure 5.7: Comparison of depth-averaged current direction at the Aquadopp location

A statistical comparison of the tidal range and peak current speed at the ADCP location from the model and the data is shown in Table 5.1. The predicted average and maximum tidal range are within 0.05 m of the measured values and the root mean square error is small (0.08 m). The average and maximum of the peak ebb and flood current speeds are within 0.05 m/s of the measured values, and the root mean square error is 0.04 m/s. The same statistical comparison is presented for the Aquadopp location in Table 5.2. The predicted and measured tidal range again show good agreement with a root mean square error of 0.07 m. The root mean square error between the predicted and measured peak speed is 0.08 m/s indicating reasonable agreement. Therefore the model and data agree reasonably well at the ADCP and Aquadopp locations with acceptable levels of error.

Table 5.1: Comparison of predicted and measured tidal range and peak current speed at the ADCP location

	Tidal range (m)		Peak current speed (m/s)	
	Average	Maximum	Average	Maximum
Model	0.71	1.46	0.17	0.30
ADCP data	0.76	1.51	0.18	0.34
Root mean square error	0.08		0.04	

Table 5.2: Comparison of predicted and measured tidal range and peak current speed at the Aquadopp location

	Tidal range (m)		Peak current speed (m/s)	
	Average	Maximum	Average	Maximum
Model	0.70	1.46	0.19	0.33
Aquadopp data	0.73	1.42	0.23	0.53
Root mean square error	0.07		0.08	

6. Recirculation and dispersion assessment

6.1. Layout

The proposed locations of the intake and outfall (see Appendix A) are shown in Figure 6.1. The intake will be located offshore at the end of a 2500 m long pipeline, where the bed level is approximately -5.5 m QNHD. The pipeline with be covered by partially submerged rock armouring with the crest of the rock armouring generally at the level of the natural bathymetry except around the bend in the pipeline where it is close to mean higher high-water (MHHW) elevation (Figure 6.2).

A submerged outfall will be located at the end of a 2000 m long pipeline, with a diffuser located at a sea bed elevation of approximately -4.0 to -4.5 m QNHD. The pipeline with be covered by partially submerged rock armouring with the crest of the rock armouring approximately 1 to 2 m above the natural sea bed elevation for around 1300 m of its length (Figure 6.3).

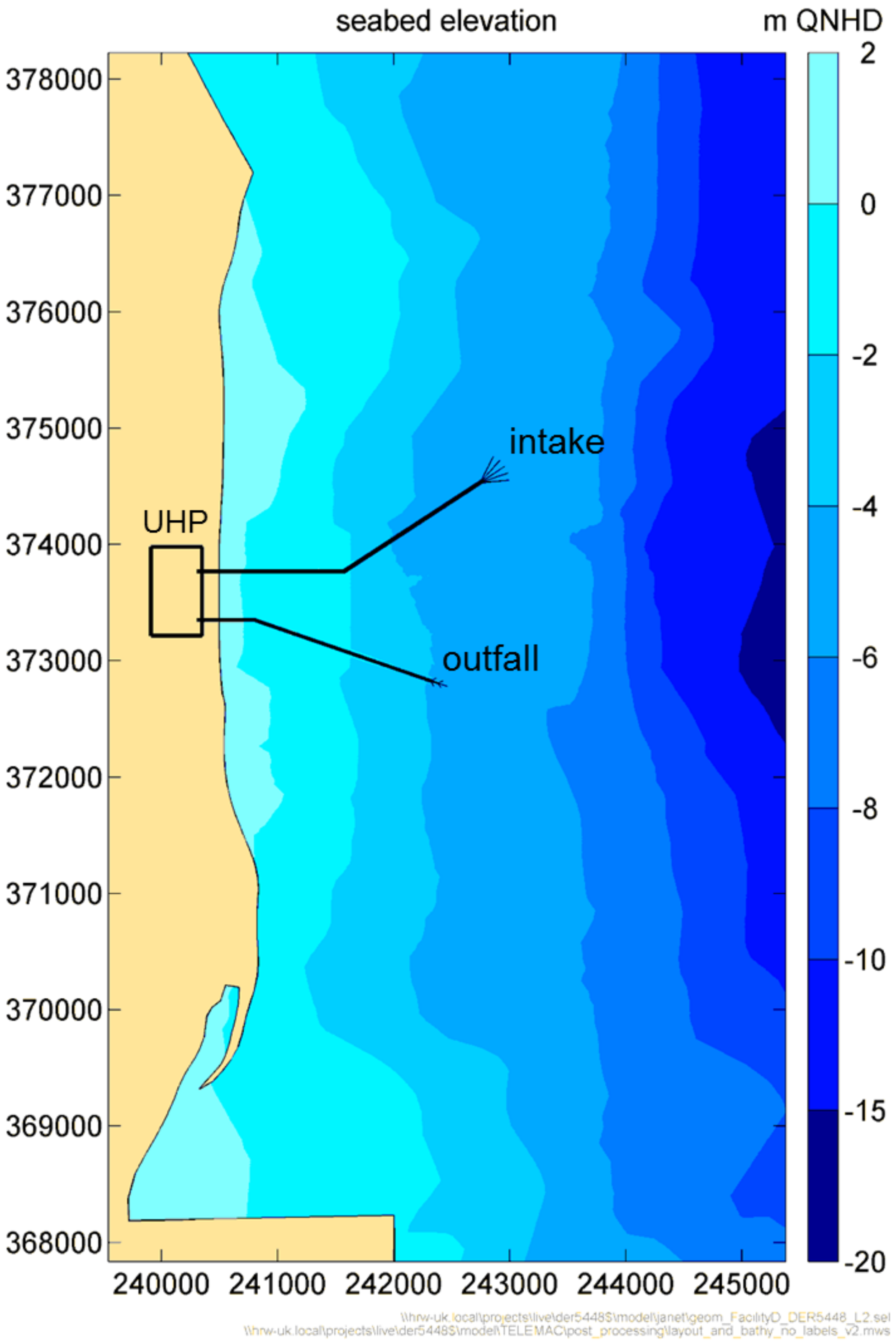

Figure 6.1: Intake and outfall locations

Source: Samsung C&T

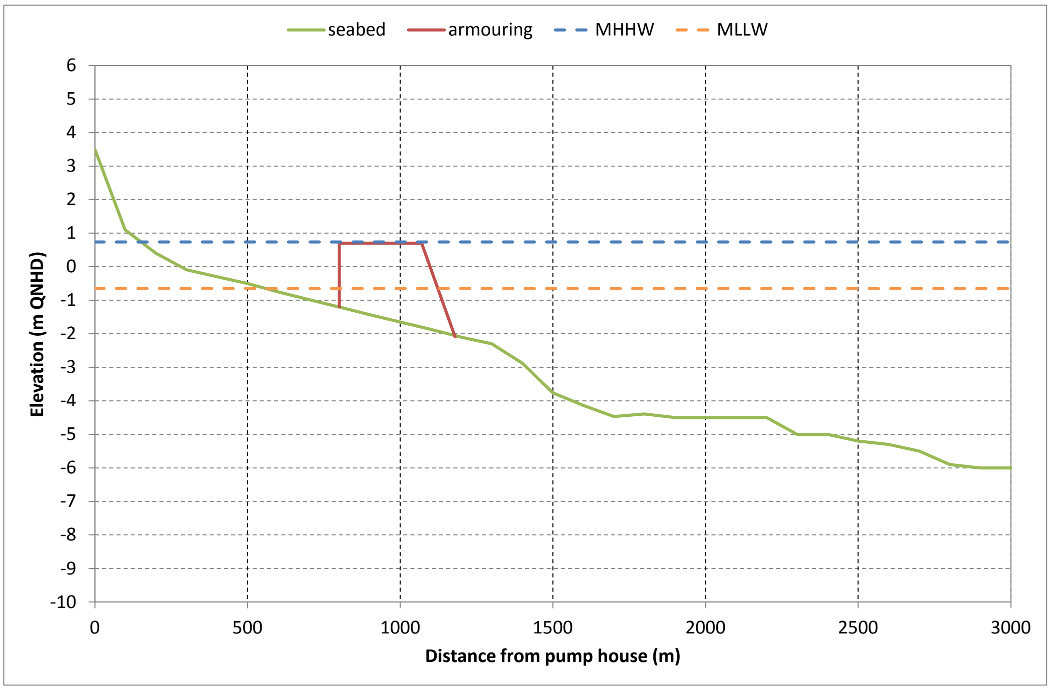

Figure 6.2: Profile of intake armouring

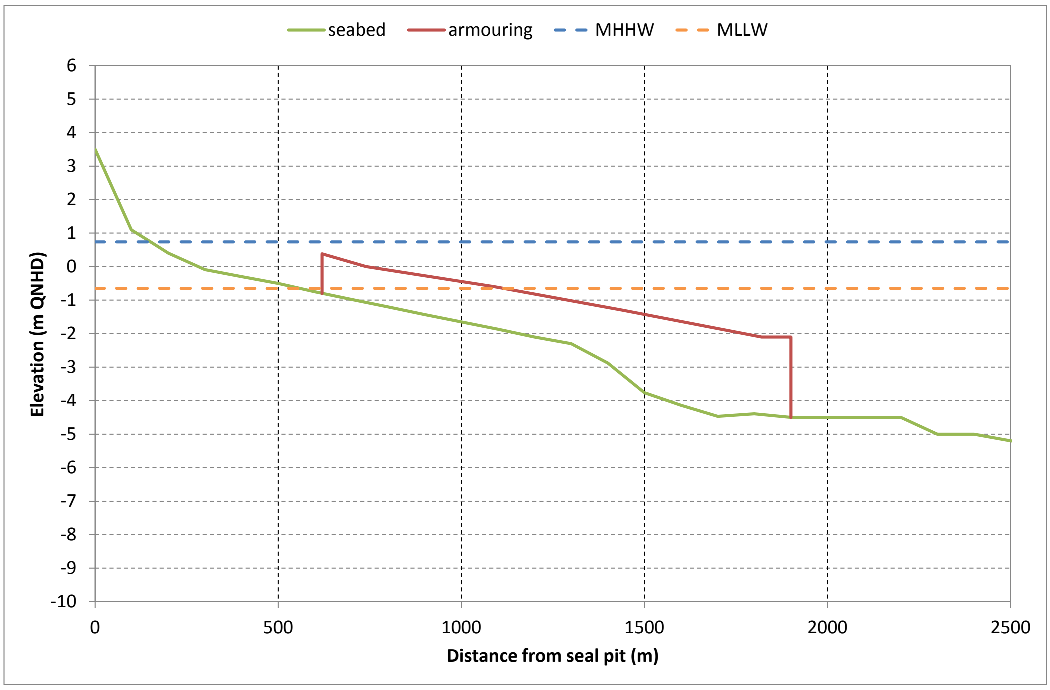

Figure 6.3: Profile of outfall armouring

6.2. Discharge parameters

Two operating phases were considered for the IWPP: a standard operational phase when cooling water will be required for the full power plant and all the desalination plants are in operation, and an early operational phase when only the Reverse Osmosis (RO) plant will be in operation and when auxiliary cooling for a gas turbine generator will be required.

The IWPP intake and discharge parameters are given in Table 6.1 for the standard operational phase and Table 6.2 for the early operation phase of the facility. The same parameters were used for both summer and winter simulations.

Table 6.1: IWPP intake and discharge parameters (standard operation)

	Intake	Discharge		
	Flow rate (m^3/h)	Flow rate (m^3/h)	Temperature rise (°C)	Salinity rise (ppt)
Cooling water plant	159,200	159,200	7	0
Auxiliary cooling for the Gas Turbine Generator	6,200	6,200	7	0
Multi-Stage Flash (MSF) desalination plant	96,000	81,961	10	7.73
Reverse osmosis (RO) desalination plant	28,600	15,826	1.5	37.3
Total	**290,000**	**263,187**	**7.60**	**4.65**

Source: Samsung C&T 16/6/2015

Table 6.2: IWPP intake and discharge parameters (early phase)

	Intake	Discharge		
	Flow rate (m^3/h)	Flow rate (m^3/h)	Temperature rise (°C)	Salinity rise (ppt)
Auxiliary cooling for the Gas Turbine Generator	6,200	5,290	7	0
Reverse osmosis (RO) desalination plant	28,600	15,826	1.5	37.3
Total	**34,031**	**21,393**	**2.88**	**27.98**

Source: Samsung C&T 16/6/2015

The ambient conditions used are shown in Table 6.3. The summer temperature and salinity data are based on advised design conditions. Winter sea temperature is the same value as was used in HR Wallingford's previous study at the site and for recent similar studies for Ras Abu Fontas plant (10 km north of the site). The sea salinity is assumed to be the same throughout the year.

Table 6.3: Ambient sea conditions

	Summer	Winter
Sea temperature (°C)	35	20
Sea salinity (ppt)	45.9	45.9

6.3. Seawater and discharge densities

The behaviour of the plume on discharge will depend on its density relative to that of the ambient seawater. Based on the data presented in Table 6.1 to Table 6.3, the density of the seawater and the discharges for both operational phases during summer and winter conditions are shown in Table 6.4.

Table 6.4: Seawater and discharge densities

	Density (kg/m^3)		
	Seawater	IWPP discharge (standard operation)	IWPP discharge (early phase)
Summer conditions	1027.7	1028.2	1047.6
Winter conditions	1032.8	1033.9	1053.2

Source: *Densities calculated using the state equation in El-Dessouky and Ettouny (2002)*

During standard operation the IWPP discharge is both warmer and more saline than the ambient seawater. The increased temperature will tend to reduce the discharge density, and the increased salinity will tend to increase the density. The resulting discharge is of similar density to the ambient seawater in summer and marginally more dense in winter. Because of this, the discharge plume will be close to neutrally buoyant, and may mix through the whole water column, causing higher temperatures and salinities at both the sea bed and the sea surface, in both seasons.

For the early operational phase of the plant, the discharge is marginally higher in temperature and significantly more saline than the ambient seawater. The discharge is therefore more dense than the ambient seawater in both summer and winter, and negatively buoyant. The effluent plume will tend to sink towards the sea bed, and is expected to increase salinities and temperatures there, with relatively little impact at the sea surface.

6.4. Environmental regulations

For once-though cooling water systems, the Qatari Supreme Council for the Environment (SCE) (now Ministry of Environment, MoE) standards (QSCE (2003)) specify that the maximum allowable temperature difference is 3°C. This is defined as the temperature difference between the outfall and ‘the integrated vertical front of the agreed mixing zone’. The extent of this mixing zone should be determined using a ‘verified 3-dimensional hydrodynamic dispersion model and a site specific ecological study’. Therefore, the extent of the mixing zone as a distance from the outfall is not specified in the standards. Note that this temperature regulation poses no restriction to the discharge during the early phase of the plant as the excess temperature is expected to be below 3°C.

No standard is specified for excess salinity. For other projects in Qatar, we have been asked by the regulator to present model results to show the predicted extent of the area where the excess salinity due to the discharge is greater than 10% of the background ambient salinity. We have adopted this threshold level for this study – at the UHP site this corresponds to an increase in salinity of 4.6 ppt. This criterion will be satisfied during the standard operation phase as the effluent is discharged at an excess salinity of 4.6 ppt.

6.5. Model configuration

The TELEMAC-3D model described in Chapter 4 was updated to incorporate the IWPP outfall and intake structures. The model mesh was enhanced in the vicinity of the proposed structures as shown in Figure 6.5 to resolve the discharge plume. The mesh resolution near the IWPP outfall and intake locations was set to 20 m. The model bathymetry was updated to reflect the intake and outfall armouring and is shown in Figure 6.6.

For the standard operation case vertical variations were represented using seven equally spaced quasi-horizontal ‘planes’. The first plane is located at the sea bed and the seventh plane is located at the sea surface, and the plane spacing is 1/6 of the water depth. Near the outfall and intake the distance between neighbouring planes is around 0.6 m and 0.9 m respectively.

The effluent for the early phase case is more dense than the ambient water and the plume is expected to stay close to the sea bed. The mesh vertical resolution was increased near the sea bed to represent this. Ten horizontal planes were used with seven planes equally spaced in the lower half of the water column and three planes equally spaced in the upper half of the water column. At the outfall location the plane spacing is around 0.15 m at the sea bed and around 0.55 m at the sea surface.

The boundary conditions developed in Chapter 4 for the calibration of the hydrodynamic model were used in all simulations. These conditions include a spring-neap cycle with the smallest neap tides between days 8 and 12 and the largest spring tides between day 14 and the end of the simulation (see Figure 6.4).

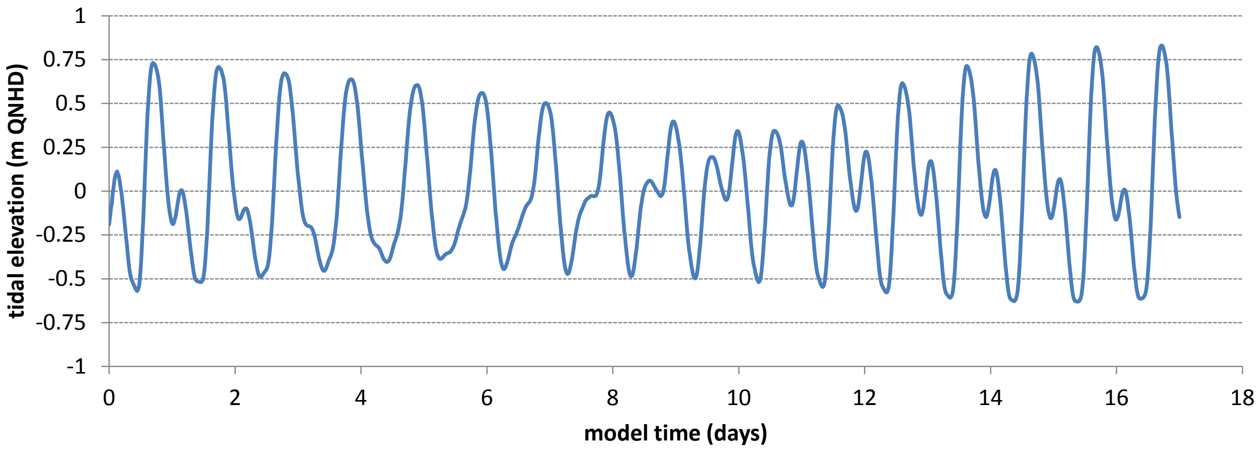

Figure 6.4: Tidal elevation at the intake

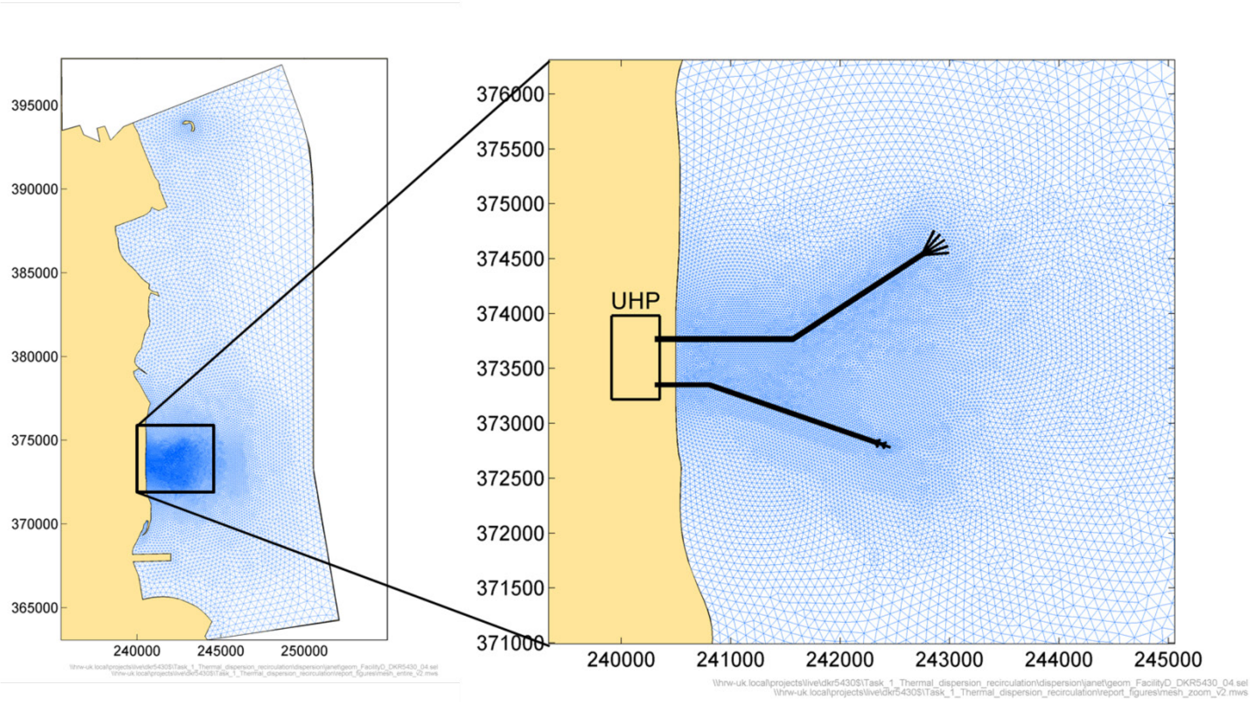

Figure 6.5: Model mesh (updated) – full extent and in the vicinity of the site

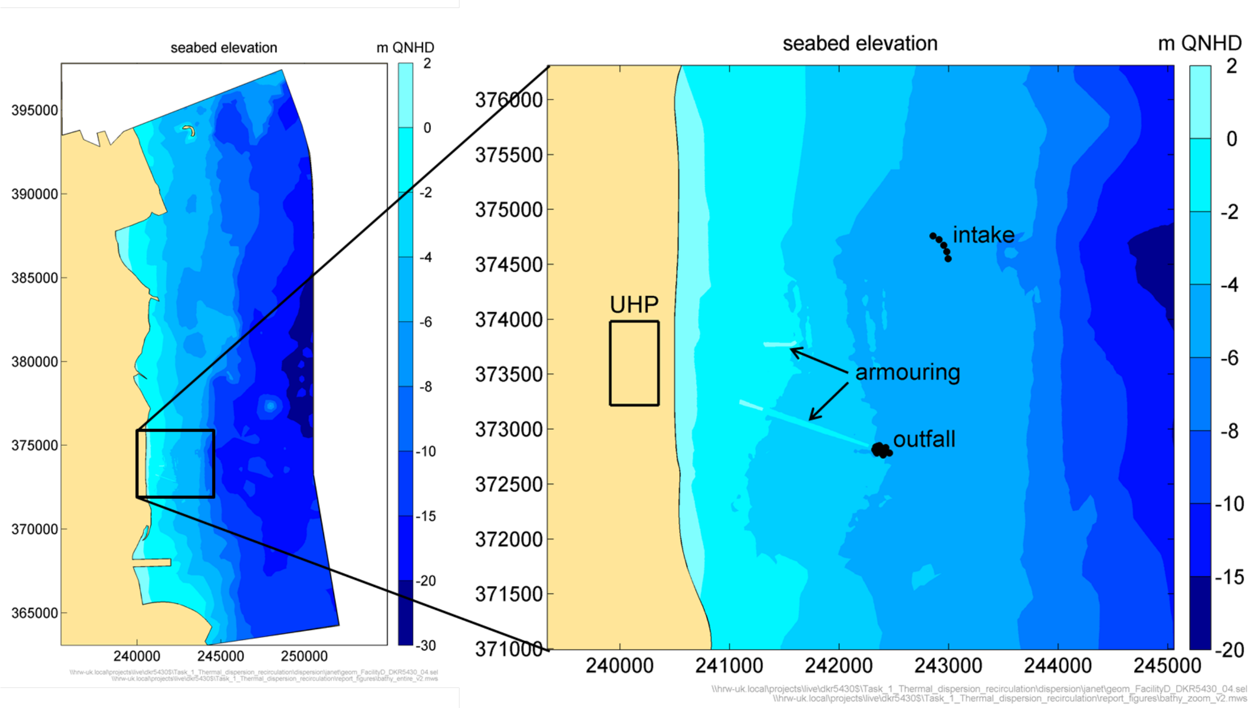

Figure 6.6: Model bathymetry (updated) – full extent and in the vicinity of the site

6.6. Intake and outfall representation

The outfall and intake were represented at the locations shown in Figure 6.1 with the parameters from Table 6.1 and Table 6.2. For the standard operation phase, the intake was represented at the sea bed with five computational nodes, one for each of the five intake pipelines. The outfall diffuser was represented at the sea bed with fifteen computational nodes. Based on the proposed outfall diffuser design, it was anticipated that there would be little initial dilution. Therefore no initial dilution was included in the model.

For the early operation phase, it is understood that one intake pipeline and one outfall pipeline will be operational. The intake was represented at the sea bed with one computational node at the offshore end of the most southerly intake pipeline. The outfall was represented at the sea bed with three computational nodes at the offshore end of the most northerly outfall pipeline. These were selected to represent the smallest distance between the outfall and intake and, therefore, the worst case combination in terms of recirculation.

6.7. Environmental conditions

Some of the simulations were conducted with observed winds using the data recorded at the weather station at Al Wakrah (Figure 3.2). The wind was applied uniformly in space across the entire model, as for the hydrodynamic model calibration.

The wind distribution at Doha International Airport (approximately 20 km north of the site) for the period 2009 to 2013 (see Figure 3.4) was also analysed to ascertain the range of potential wind conditions over a longer period. The most commonly occurring winds are from the north-west and a wind from this direction at 6 m/s was adopted to represent a constant wind condition.

Periods of little or no wind (speeds less than 2 m/s) occur around 10% of the time and are often most adverse in terms of environmental compliance of the discharge mixing zone. Simulations with no wind (also referred to as 'calm') were conducted to represent this condition.

Summer and winter ambient sea conditions were simulated using the parameters in Table 6.3. Combining the ambient sea conditions and the wind conditions, a total of six environmental conditions was simulated for each operational phase:

- Summer sea temperature with observed wind;
- Summer sea temperature under calm conditions;
- Summer sea temperature with a constant 6 m/s wind from north-west;
- Winter sea temperature with observed wind;
- Winter sea temperature under calm conditions;
- Winter sea temperature with a constant 6 m/s wind from north-west.

6.8. Results

The dispersion of the IWPP saline and heated water was simulated under the six environmental conditions described in Section 6.7 for the standard operational phase and the early phase of the plant (a total of twelve simulations). The simulations were run for 17 days to include a full spring-neap tidal cycle (15 days) plus an initial two days to allow the model to stabilize.

6.8.1. Standard operation phase

The predicted maximum and average sea surface and sea bed excess temperatures were calculated over the 15 day period. These are shown as contour plots in Figure 6.7 to Figure 6.12 for the standard operation phase. The 3°C temperature contour is at the boundary between the yellow and blue areas. The mean 3°C mixing zones are at most 2 km across, and the maximum 3°C mixing zones extend around 4 to 9 km alongshore and 1 to 3 km offshore. The increase in salinity is predicted to be less than 10% of the ambient salinity everywhere in the model throughout the simulations. As this means that the excess salinity is never predicted to exceed the environmental threshold, contour plots of the excess salinity for the standard operation phase are not shown in the main body of the report, but are included in Appendix B for completeness.

For summer conditions the excess temperatures and excess salinities show similar patterns at the sea surface and the sea bed because the discharge is almost neutrally buoyant. The increase in density between the ambient and the discharge is marginally larger in winter and therefore the plume is larger at the bed than at the surface during these simulations. The north-west wind generally reduces the plume extent northwards and offshore. The footprint of excess temperature is larger under calm conditions due to reduced atmospheric cooling.

The MoE regulations state that the size of the 3°C mixing zone should be determined from the 'integrated vertical front'. This is understood to be the depth-averaged excess temperature. Mixing zone areas calculated for the six simulated environmental conditions are shown in Table 6.5. The areas were calculated from time-averaging the depth-averaged excess temperature over 15 days and are found to be around 0.05 km^2 to 0.13 km^2 .

Table 6.5: Areas over which the time-averaged and depth-averaged excess temperature exceeds 3°C under standard operation

	Area (m^2)	Area (km^2)
Summer, observed wind	81710	0.08
Summer, calm	129960	0.13
Summer, north-west wind	68723	0.07
Winter, observed wind	54260	0.05
Winter, calm	84415	0.08
Winter, north-west wind	47188	0.05

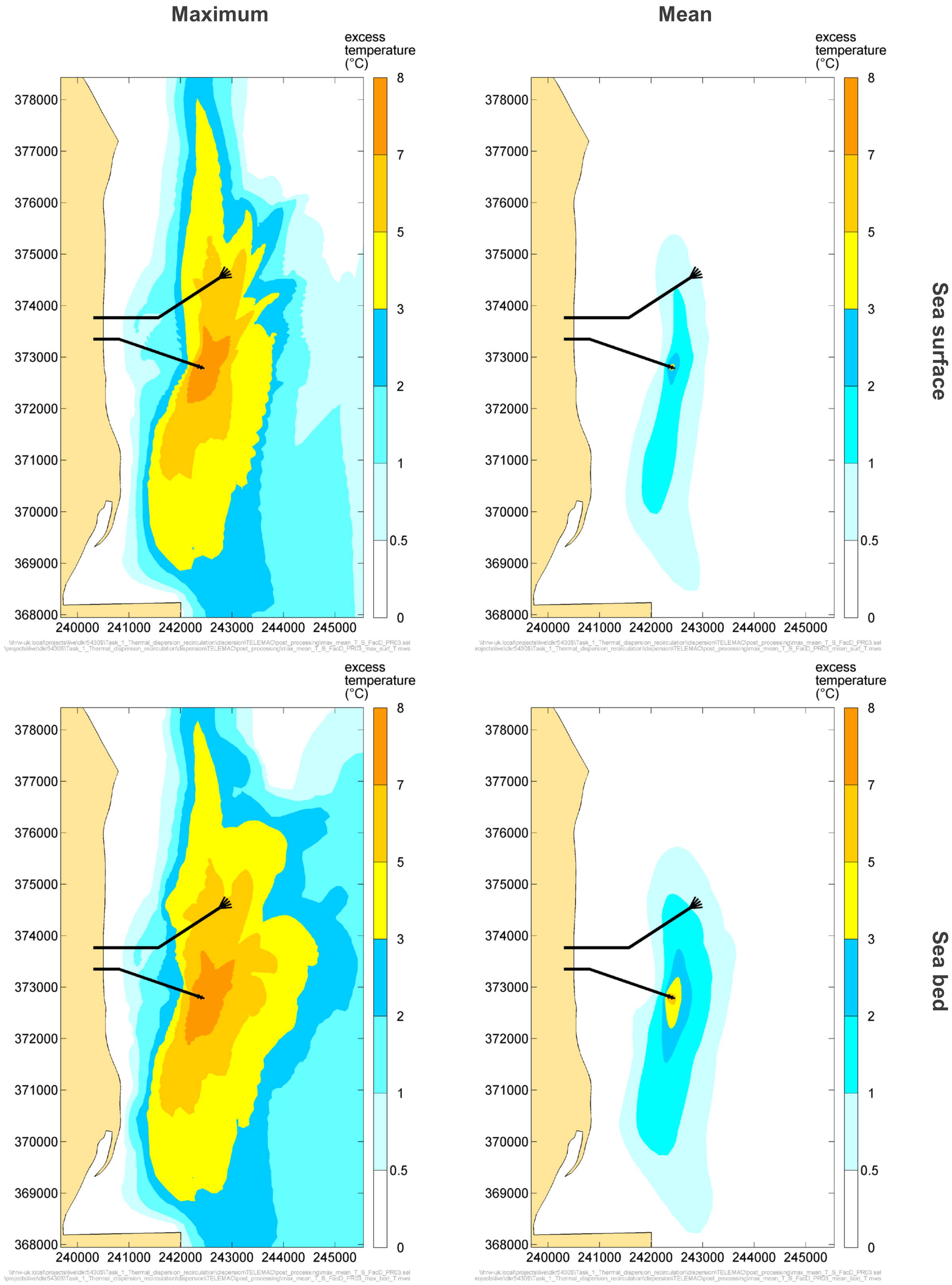

Figure 6.7: Maximum and mean sea surface and sea bed excess temperature, summer, observed wind, standard operation

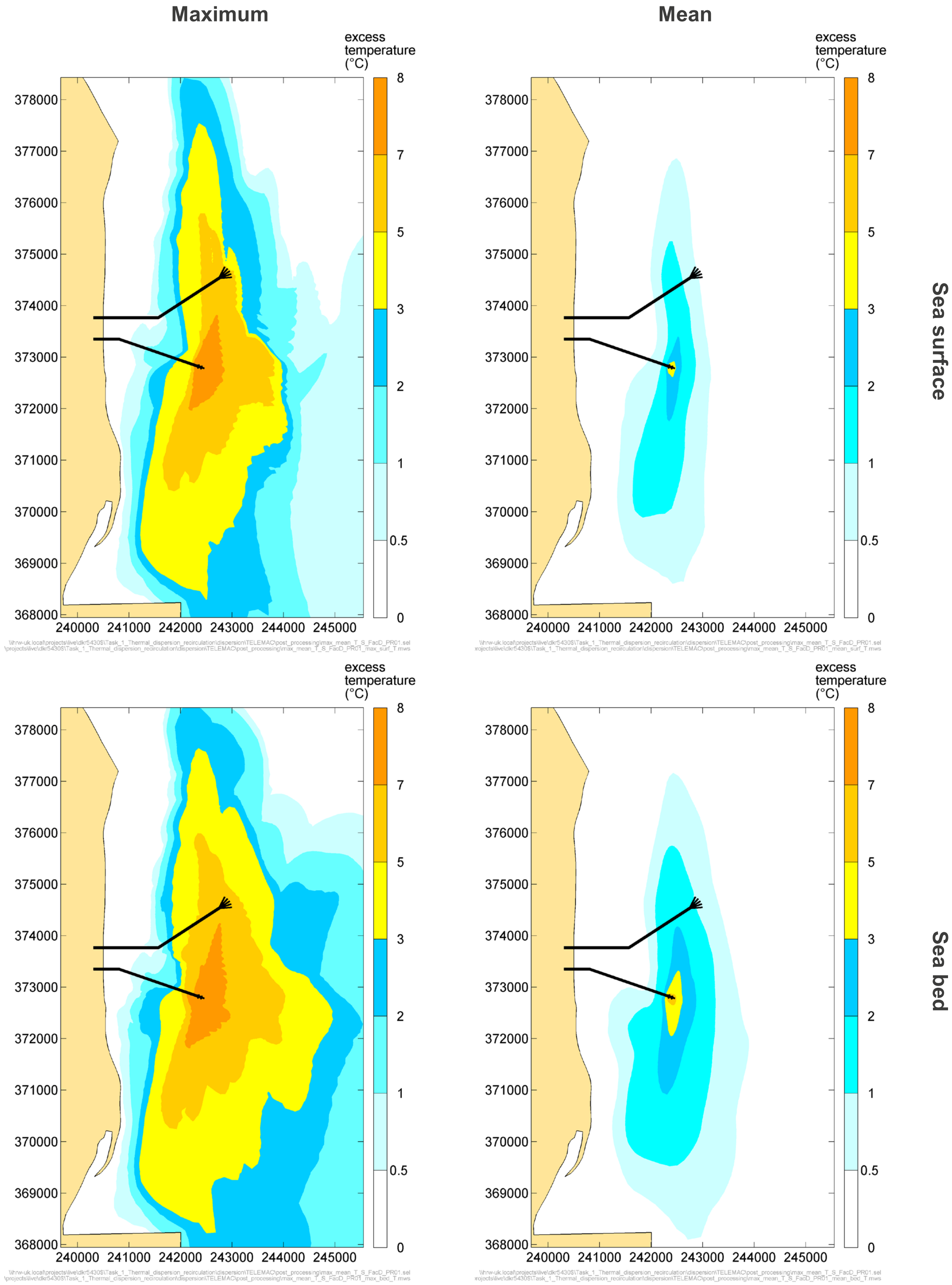

Figure 6.8: Maximum and mean sea surface and sea bed excess temperature, summer, calm, standard operation

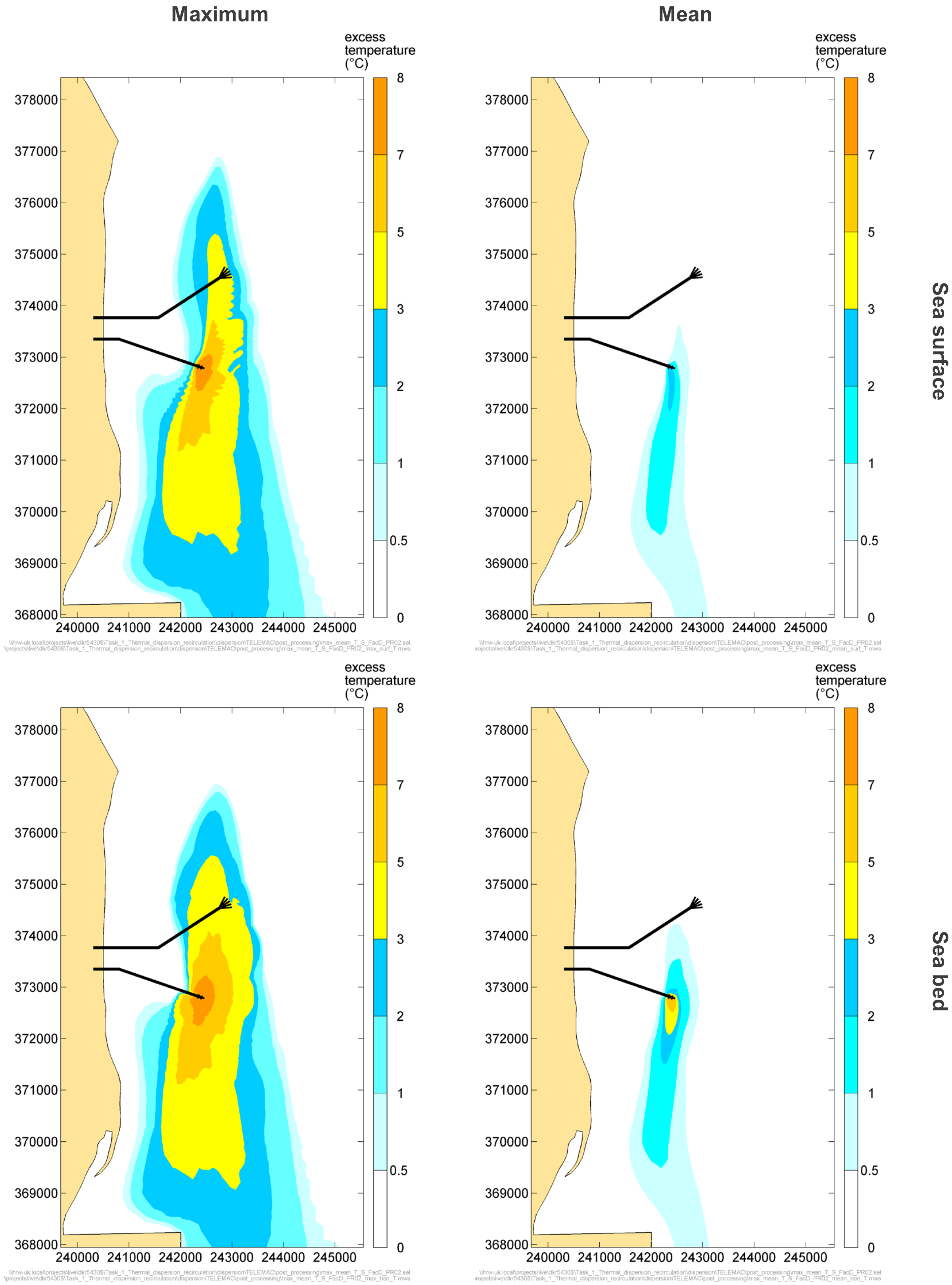

Figure 6.9: Maximum and mean sea surface and sea bed excess temperature, summer, north-west wind, standard operation

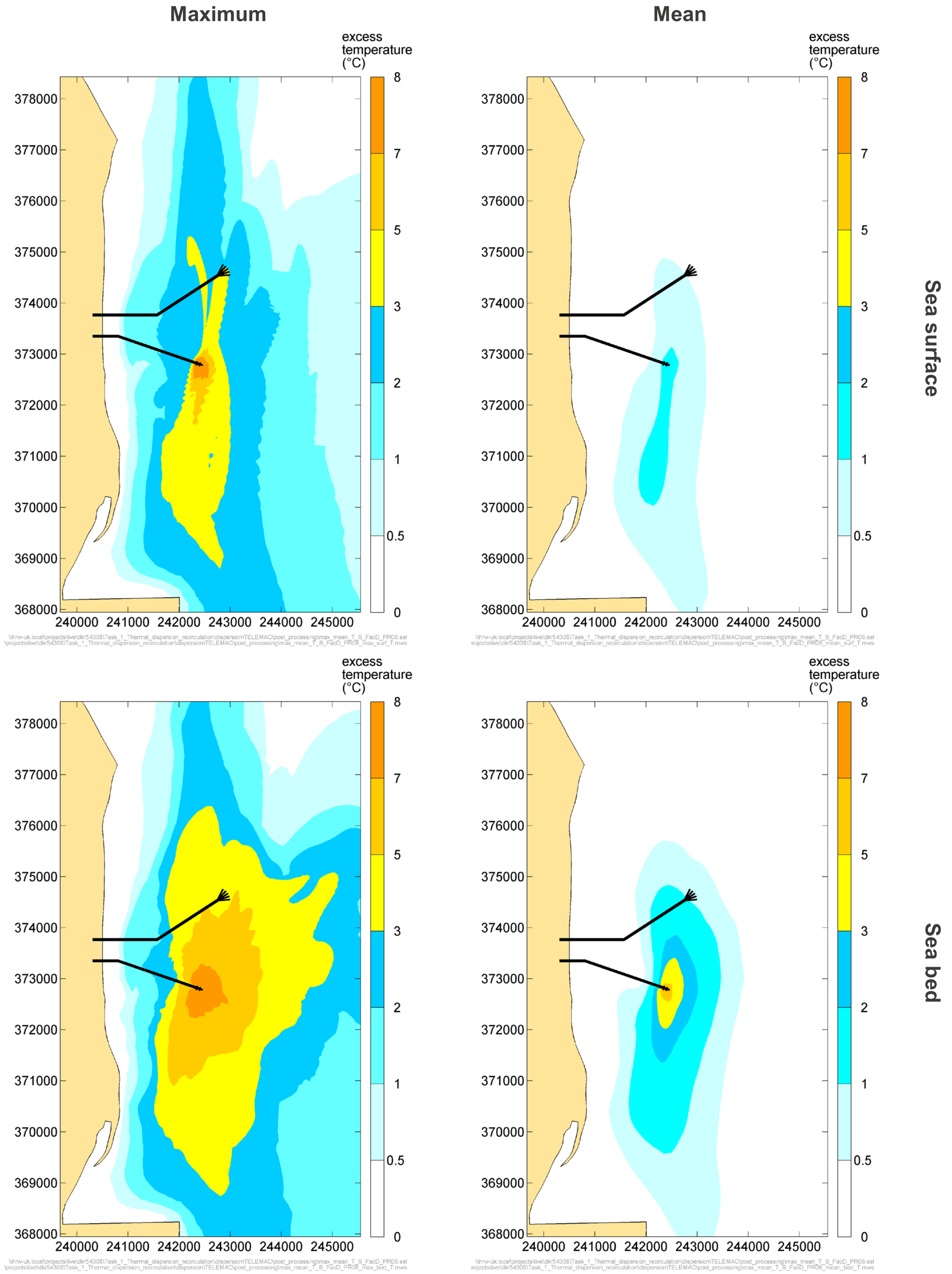

Figure 6.10: Maximum and mean sea surface and sea bed excess temperature, winter, observed wind, standard operation

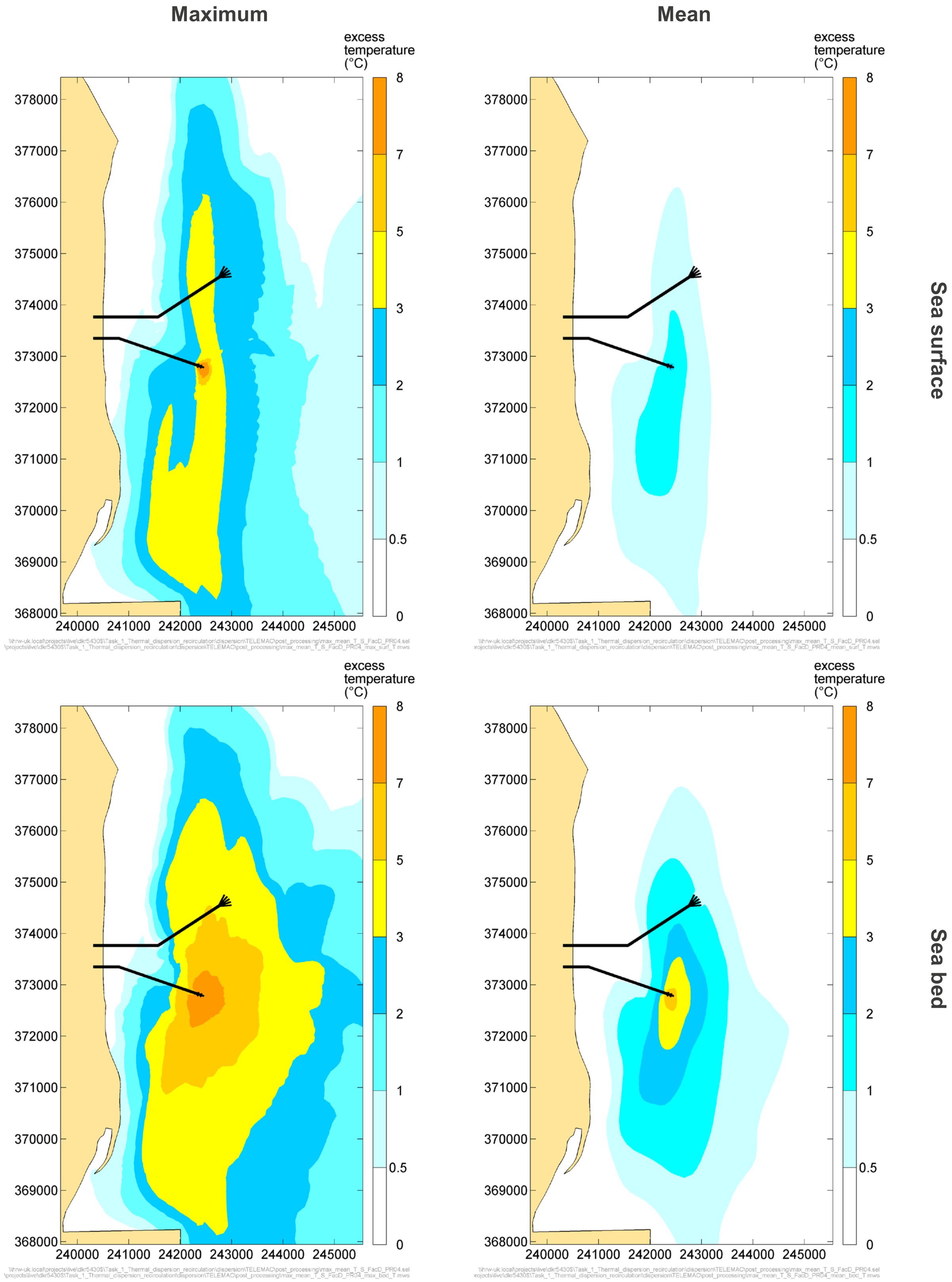

Figure 6.11: Maximum and mean sea surface and sea bed excess temperature, winter, calm, standard operation

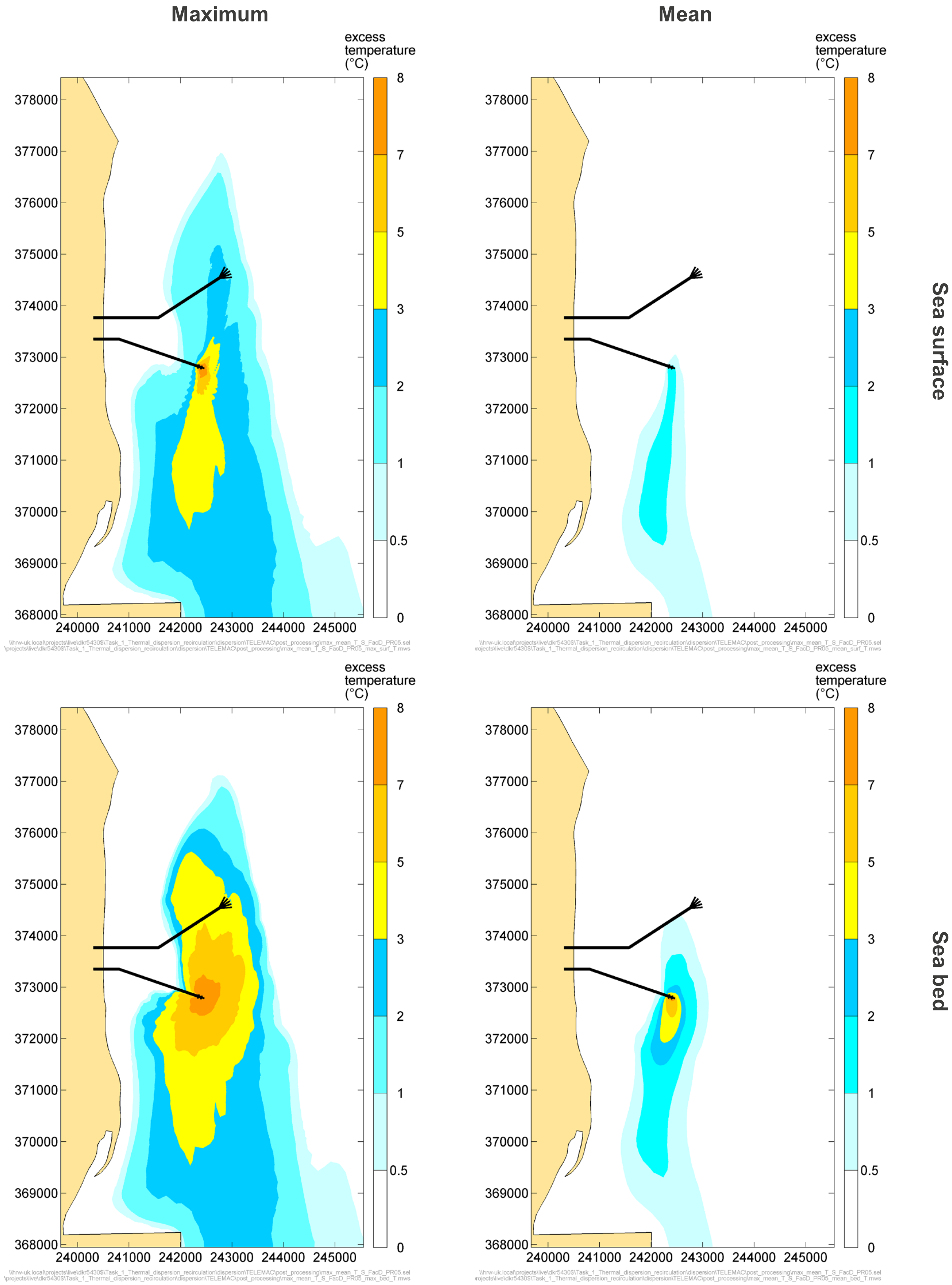

Figure 6.12: Maximum and mean sea surface and sea bed excess temperature, winter, north-west wind, standard operation

6.8.2. Early operation phase

Figure 6.13 to Figure 6.18 show contour plots of the maximum and mean sea surface and sea bed excess salinities for the early operation phase simulations. The extent of the 5 ppt mixing zone (approximately 10% of the background salinity) is marked by the boundary between the blue and the light green colours. The region where the sea bed excess salinity is above 5 ppt is around 1.5 km across. Contour plots of the excess temperatures for the early operation phase are given in Appendix B, as the excess temperature is less than environmental limit of 3°C at all times throughout the simulations.

The high density of the early operation phase discharge results in larger plume footprints at the sea bed than at the sea surface. Summer and winter ambient conditions give similar results in terms of plume extent. Results from the simulations with calm conditions and the observed wind condition are similar. This is due to the observed wind being mostly weak - around 3 m/s on average (see Figure 3.2). The stronger north-west wind has more effect on the plume dispersion and reduces marginally the overall plume footprint.

The areas where average excess salinity at the sea bed is more than 10% (4.6 ppt) above the background salinity have been calculated. The results are shown in in Table 6.6; the area is found to be around 0.1 km^2 in all simulations.

Table 6.6: Areas over which the time-averaged sea bed excess salinity exceeds 4.6 ppt during early operation phase

	Area (m^2)	Area (km^2)
Summer, observed wind	121942	0.12
Summer, calm	127823	0.13
Summer, north-west wind	60121	0.06
Winter, observed wind	122699	0.12
Winter, calm	128583	0.13
Winter, north-west wind	59508	0.06

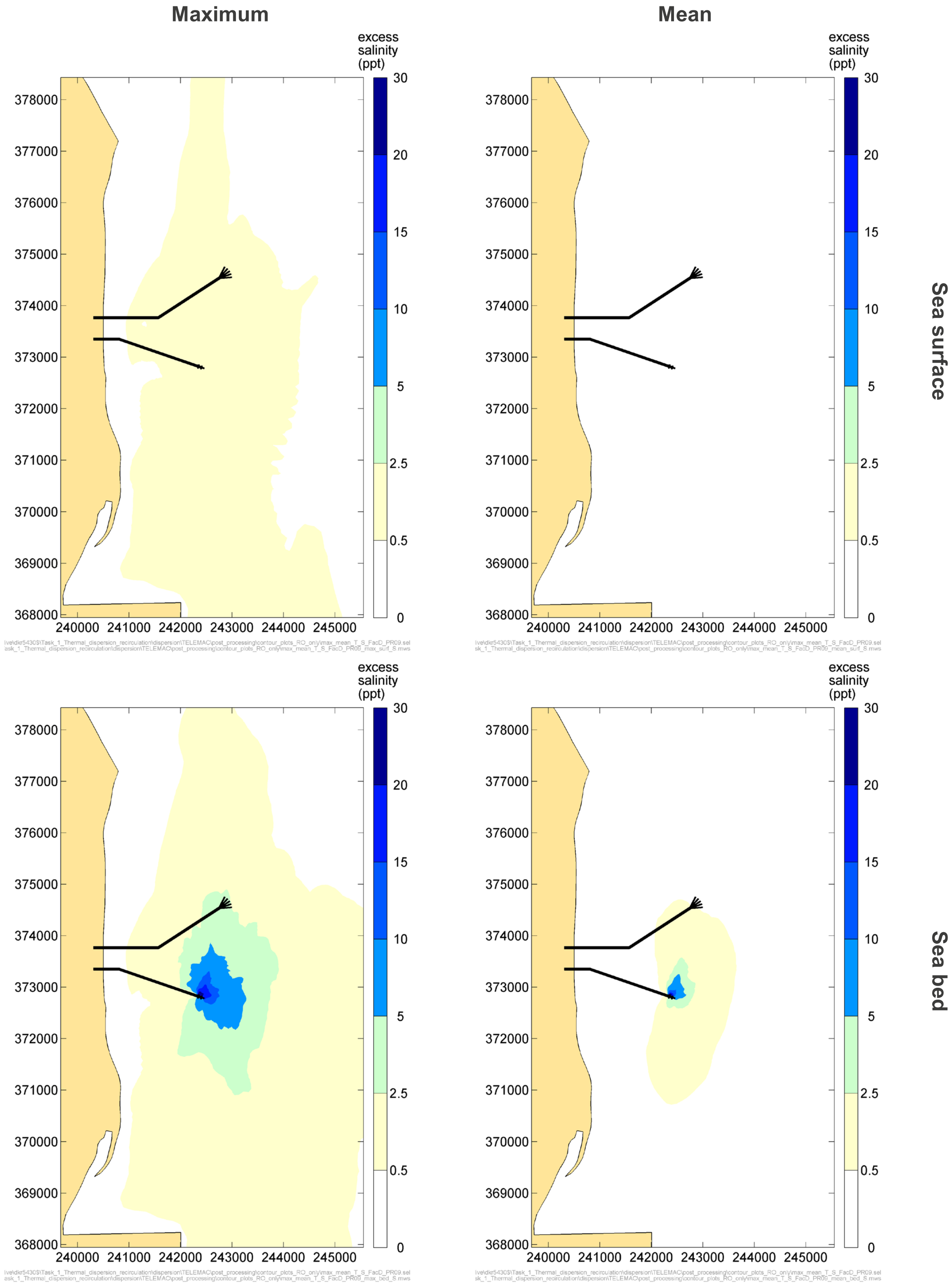

Figure 6.13: Maximum and mean sea surface and sea bed excess salinity, summer, observed wind, early operation

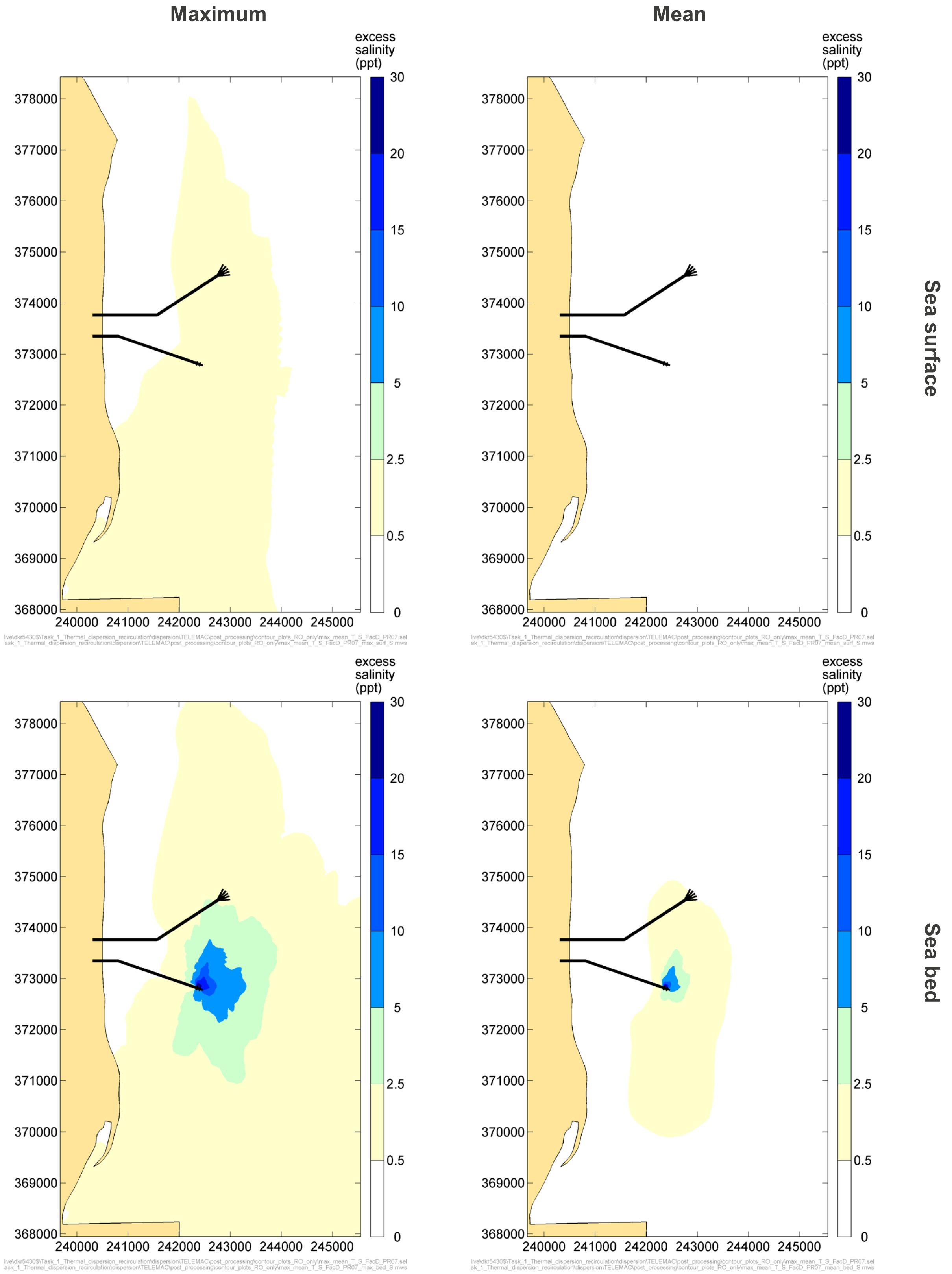

Figure 6.14: Maximum and mean sea surface and sea bed excess salinity, summer, calm, early operation

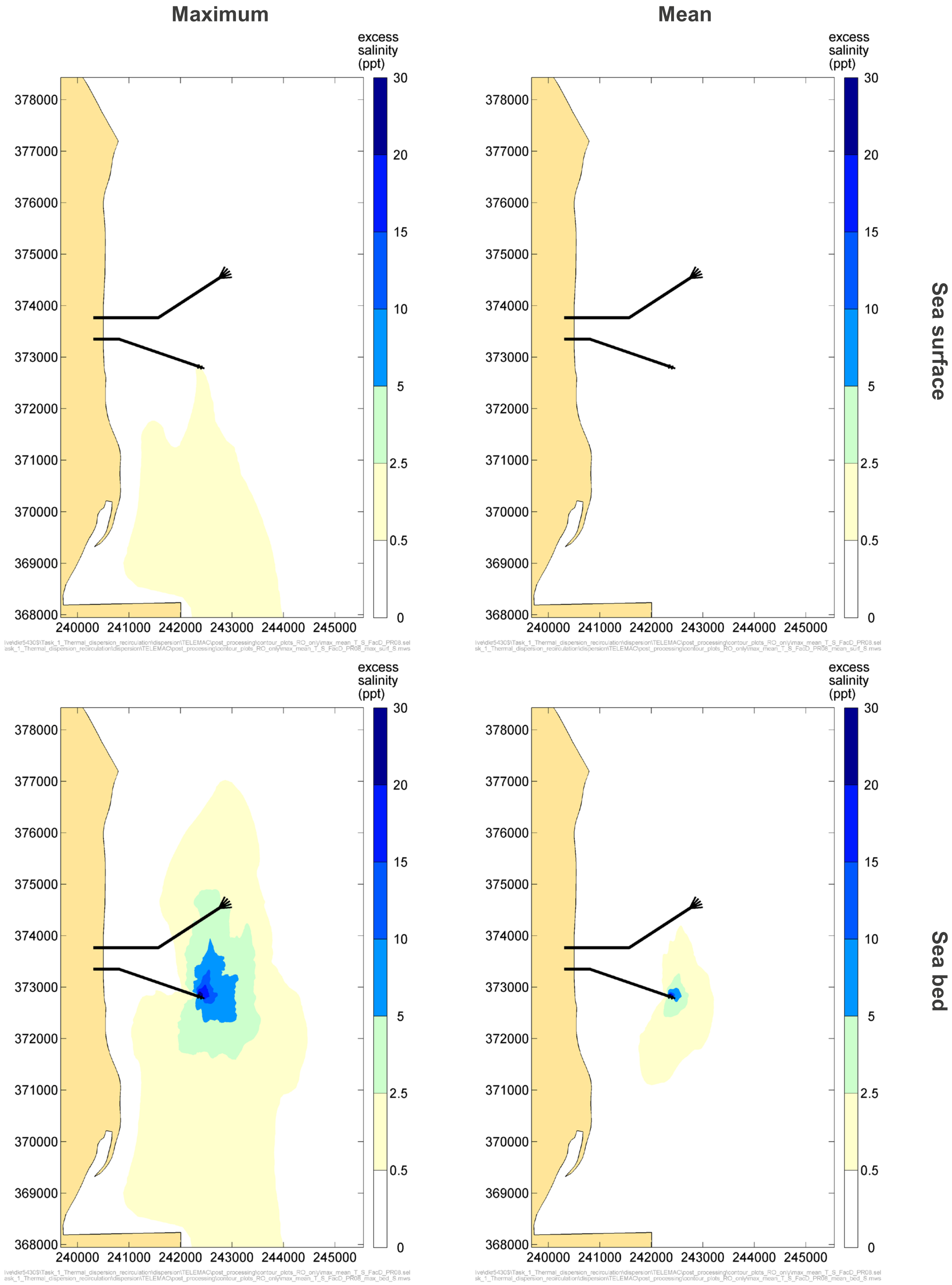

Figure 6.15: Maximum and mean sea surface and sea bed excess salinity, summer, north-west wind, early operation

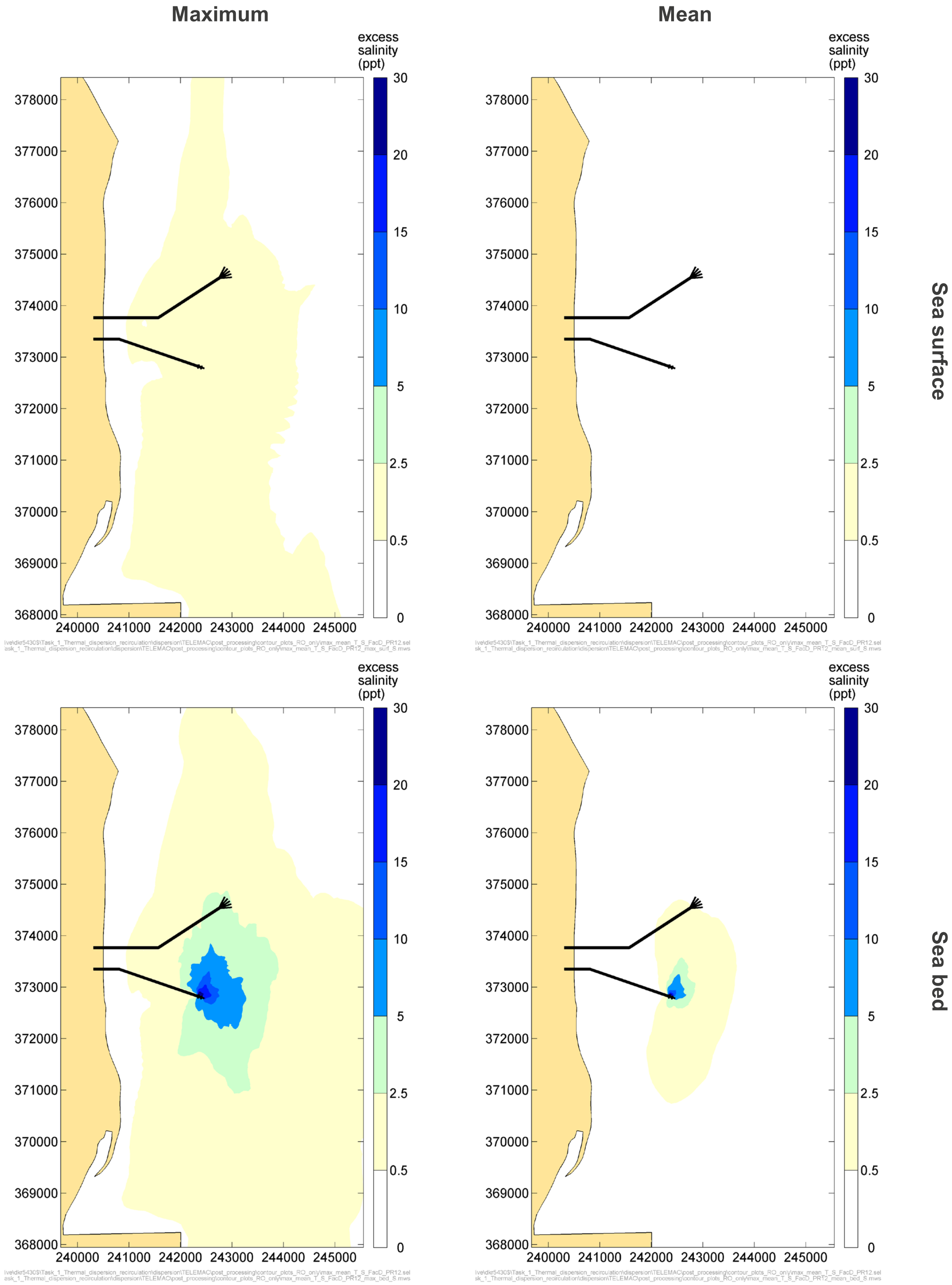

Figure 6.16: Maximum and mean sea surface and sea bed excess salinity, winter, observed wind, early operation

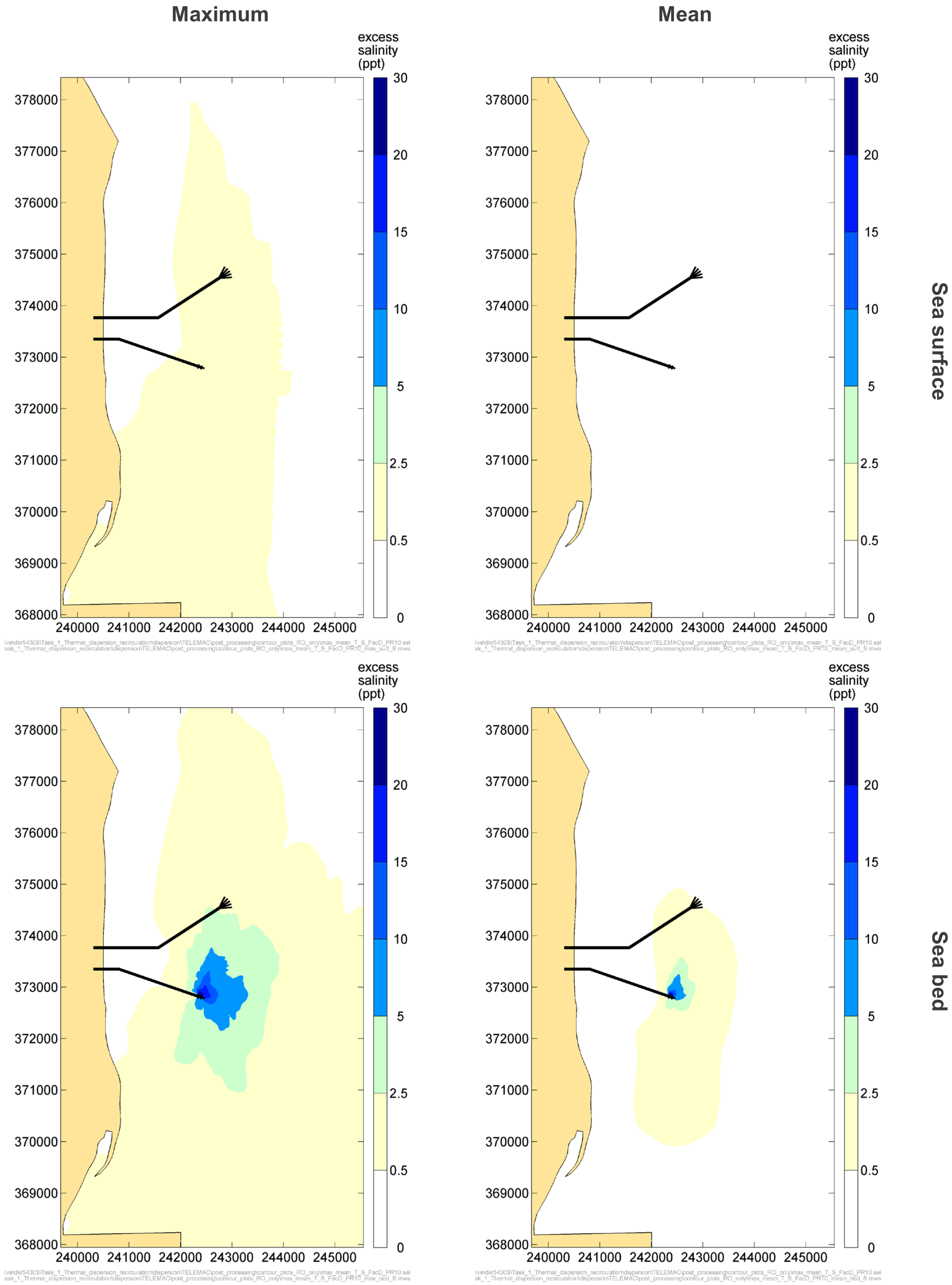

Figure 6.17: Maximum and mean sea surface and sea bed excess salinity, winter, calm, early operation

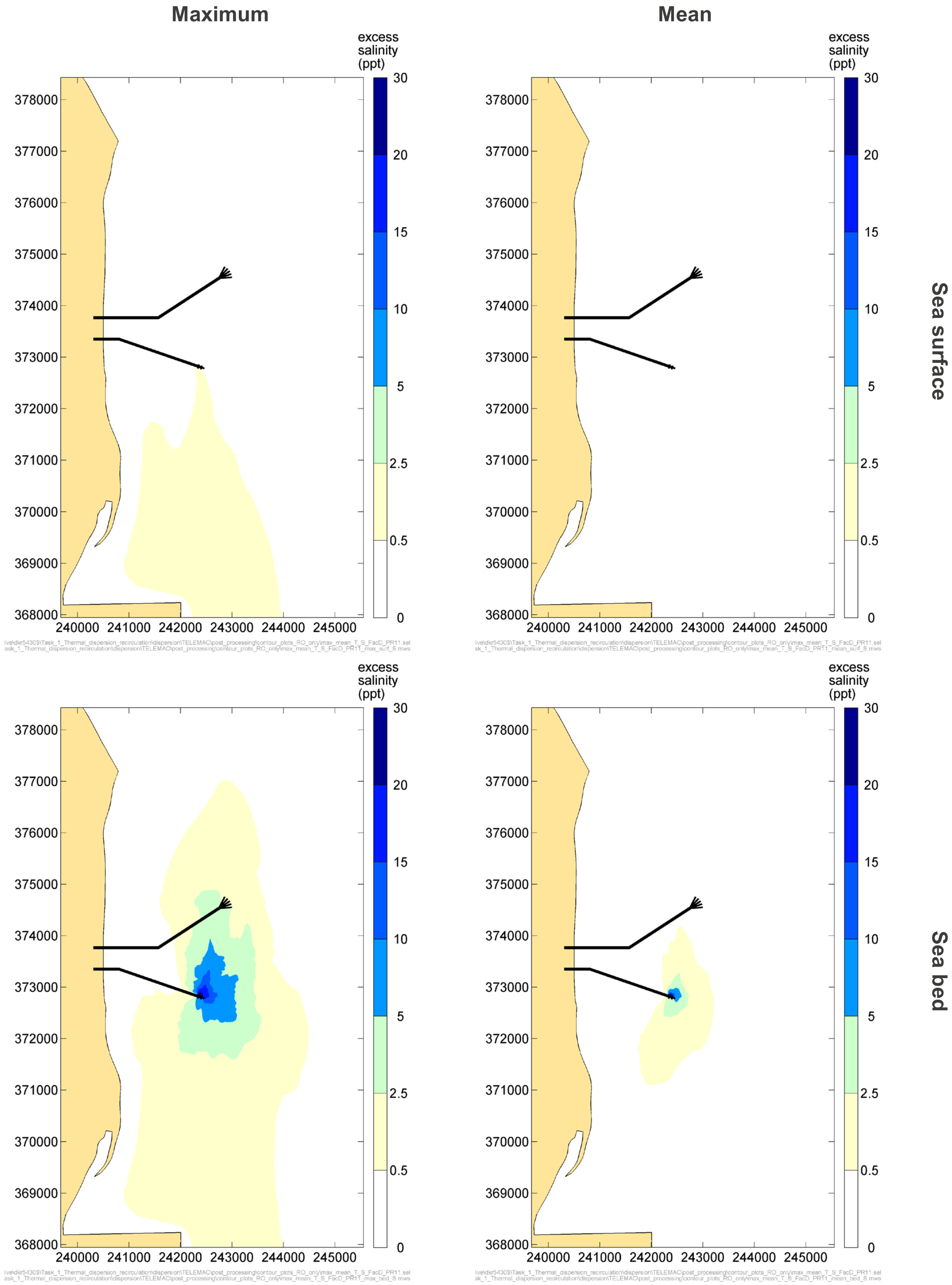

Figure 6.18: Maximum and mean sea surface and sea bed excess salinity, winter, north-west wind, early operation

6.8.3. Recirculation assessment

Time series of excess temperatures and excess salinities at the UHP intake are presented in Figure 6.19 to Figure 6.24 for the standard operation phase simulations. The time series for the observed wind and calm conditions are broadly similar with a sequence of peaks of around 8 to 10 hours duration generated during the north-going ebb phase of the tide. Recirculation is reduced by the north-west wind condition as the plume is transported further south away from the intake. Table 6.7 to Table 6.10 show the maximum and average excess temperatures and salinities at the intake. On average the excess temperature is predicted to be less than 1°C and the excess salinity is predicted to be less than 1 ppt throughout the water column. The depth-averaged maximum temperature under calm conditions is less than 3°C except during the periods of smallest tidal range when the peak value reaches up to 5.9°C. The highest peak temperature under the observed wind condition occurs when both the wind speed is relatively weak (< 3 m/s) and the tidal range is relatively small. Similarly peak excess salinities are generally less than 2 ppt, except when both the wind is weak and the tidal range is small.

Figure 6.25 to Figure 6.30 show the excess salinities at the intake for the early operation phase simulations. Similar to the standard operation simulations, the time series are dominated by peaks generated during the ebb phase of the tide. The excess salinities are again broadly similar under calm and observed wind conditions, and smaller for the north-west wind condition. Maximum and mean excess salinities at the intake are presented in Table 6.11 and Table 6.12. The average excess salinity is predicted to be less than 0.5 ppt throughout the water column. Excess temperatures at the intake for the early operation phase are predicted to be less than 0.3°C for all simulations.

Table 6.7: Maximum excess temperature at the intake, standard operation

	Maximum excess temperature (°C)					
	Summer			Winter		
	Observed wind	Calm	North-west wind	Observed wind	Calm	North-west wind
Depth-averaged	4.7	5.9	3.5	2.4	2.8	2.2
Near-surface	4.6	5.7	3.4	2.3	2.4	2.1
Mid-depth	4.7	5.9	3.5	2.4	2.9	2.1
Near-bed	4.8	6.1	3.6	3.9	4.0	3.3

Table 6.8: Average excess temperature at the intake, standard operation

	Mean excess temperature (°C)					
	Summer			Winter		
	Observed wind	Calm	North-west wind	Observed wind	Calm	North-west wind
Depth-averaged	0.5	0.6	0.2	0.5	0.6	0.2
Near-surface	0.5	0.5	0.1	0.4	0.5	0.1
Mid-depth	0.5	0.6	0.2	0.4	0.6	0.1
Near-bed	0.7	0.8	0.2	0.6	0.9	0.2

Table 6.9: Maximum excess salinity at the intake, standard operation

	Maximum excess salinity (ppt)					
	Summer			Winter		
	Observed wind	Calm	North-west wind	Observed wind	Calm	North-west wind
Depth-averaged	3.3	4.1	2.5	1.9	1.8	1.5
Near-surface	3.2	4.1	2.5	1.8	1.8	1.4
Mid-depth	3.3	4.1	2.5	1.9	1.9	1.4
Near-bed	3.5	4.2	2.6	2.4	2.5	2.0

Table 6.10: Average excess salinity at the intake, standard operation

	Mean excess salinity (ppt)					
	Summer			Winter		
	Observed wind	Calm	North-west wind	Observed wind	Calm	North-west wind
Depth-averaged	0.4	0.5	0.1	0.3	0.5	0.1
Near-surface	0.4	0.4	0.1	0.3	0.4	0.1
Mid-depth	0.4	0.5	0.1	0.3	0.4	0.1
Near-bed	0.5	0.7	0.1	0.4	0.6	0.1

Table 6.11: Maximum excess salinity at the intake, early operation

	Maximum excess salinity (ppt)					
	Summer			Winter		
	Observed wind	Calm	North-west wind	Observed wind	Calm	North-west wind
Depth-averaged	0.7	0.7	0.4	0.7	0.7	0.4
Near-surface	0.6	0.7	0.2	0.6	0.7	0.2
Mid-depth	0.7	0.7	0.2	0.6	0.7	0.2
Near-bed	1.8	1.9	1.5	1.8	1.9	1.5

Table 6.12: Average excess salinity at the intake, early operation

	Mean excess salinity (ppt)					
	Summer			Winter		
	Observed wind	Calm	North-west wind	Observed wind	Calm	North-west wind
Depth-averaged	0.2	0.2	<0.1	0.2	0.2	<0.1
Near-surface	0.1	0.1	<0.1	0.1	0.1	<0.1
Mid-depth	0.1	0.2	<0.1	0.1	0.2	<0.1
Near-bed	0.3	0.4	0.1	0.3	0.4	0.1

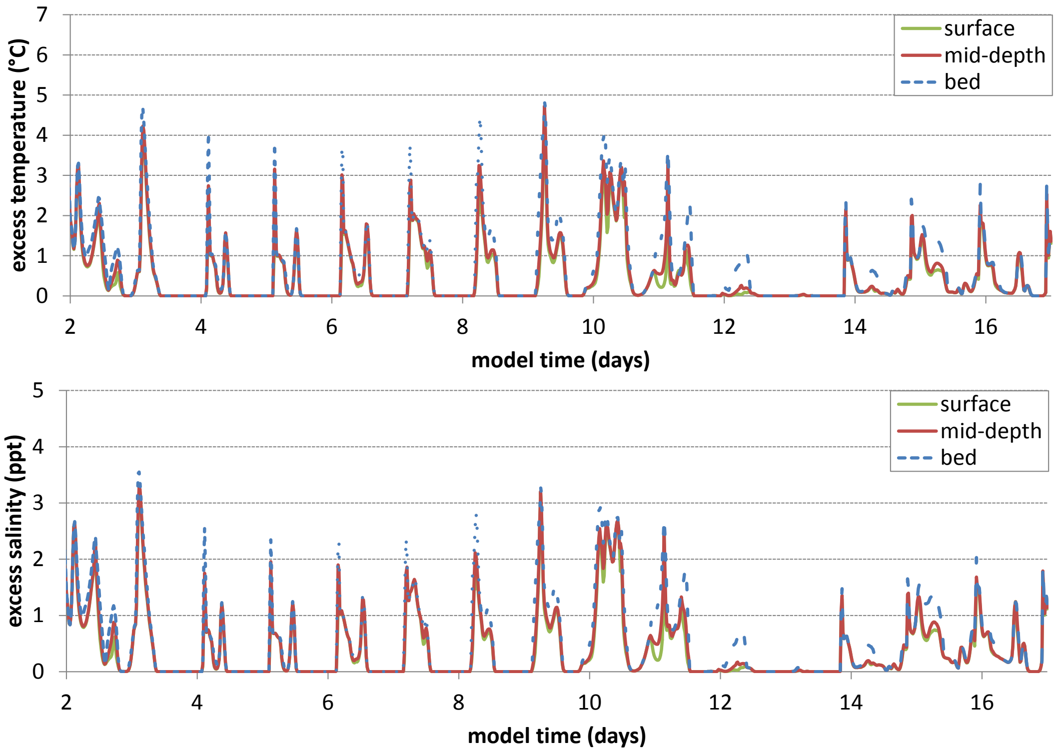

Figure 6.19: Excess temperature and salinity at the intake, summer, observed wind, standard operation

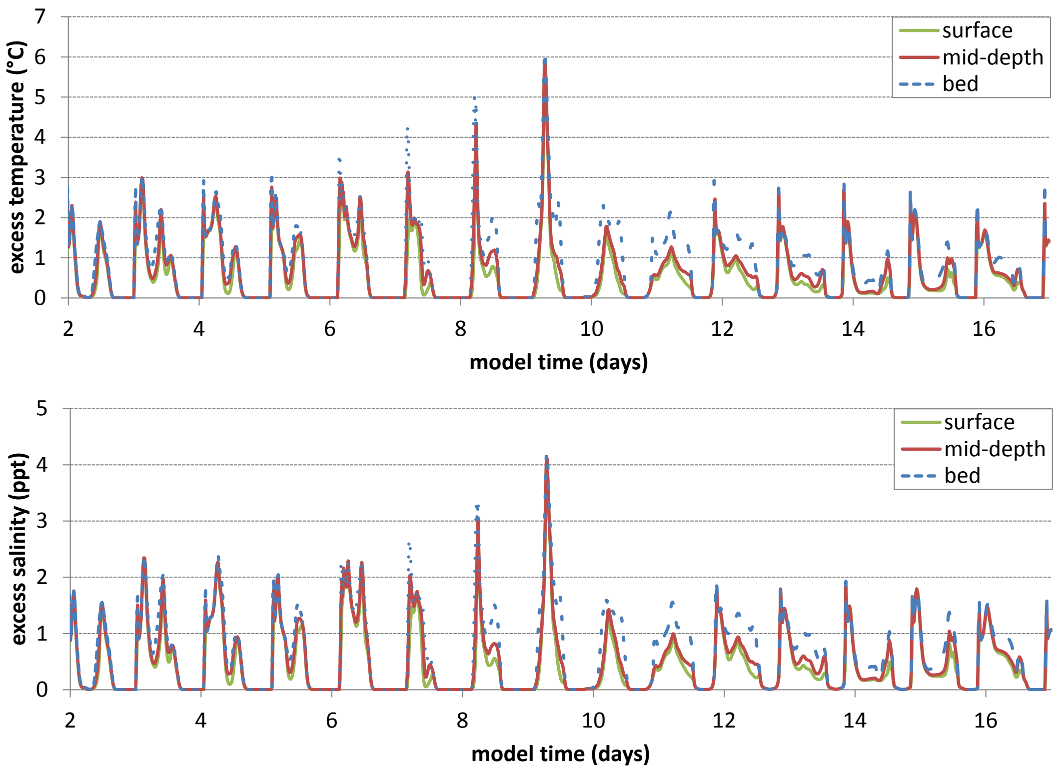

Figure 6.20: Excess temperature and salinity at the intake, summer, calm, standard operation

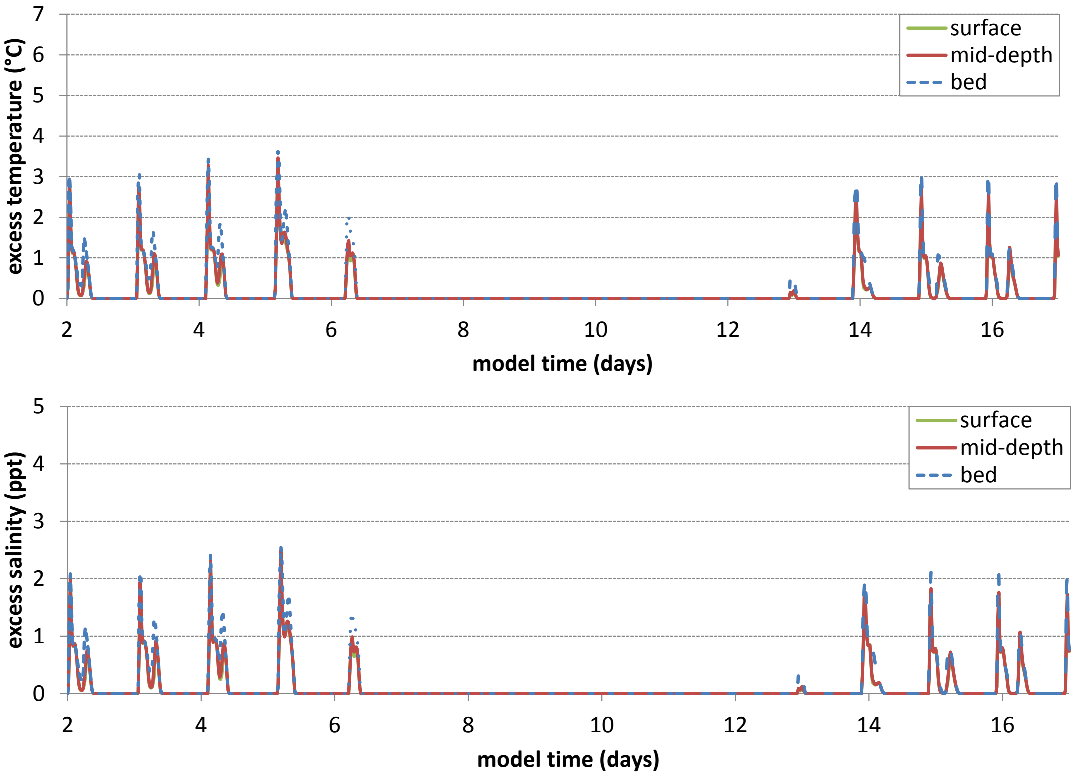

Figure 6.21: Excess temperature and salinity at the intake, summer, north-west wind, standard operation

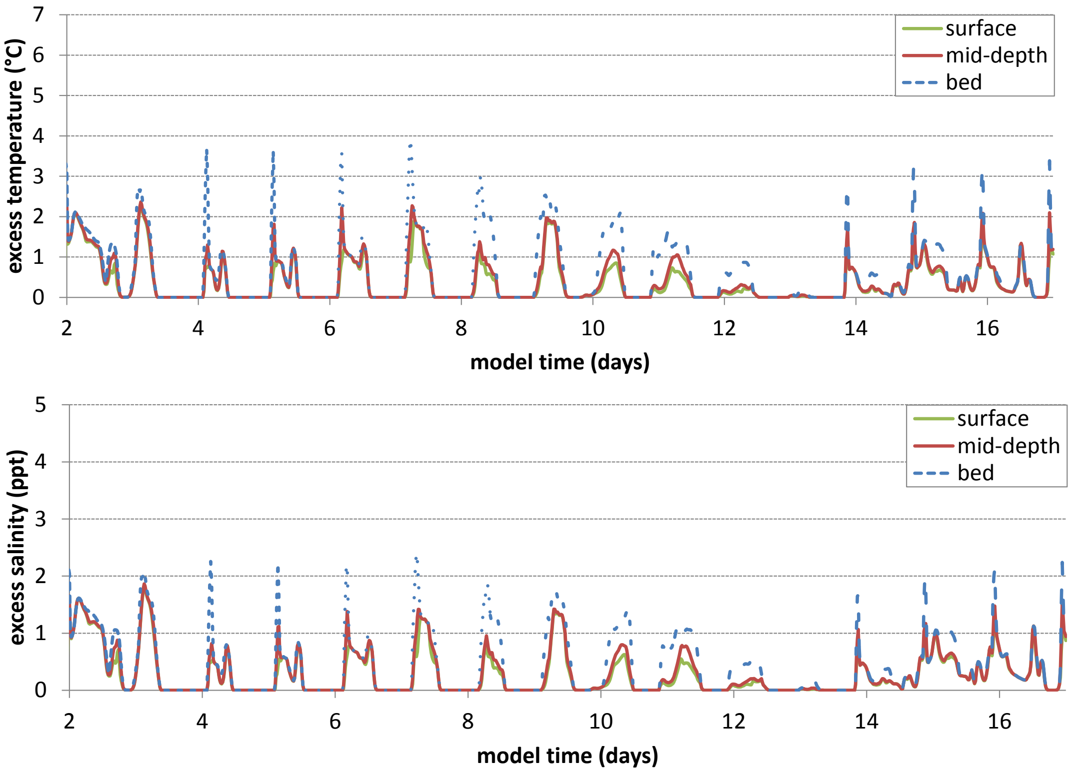

Figure 6.22: Excess temperature and salinity at the intake, winter, observed wind, standard operation

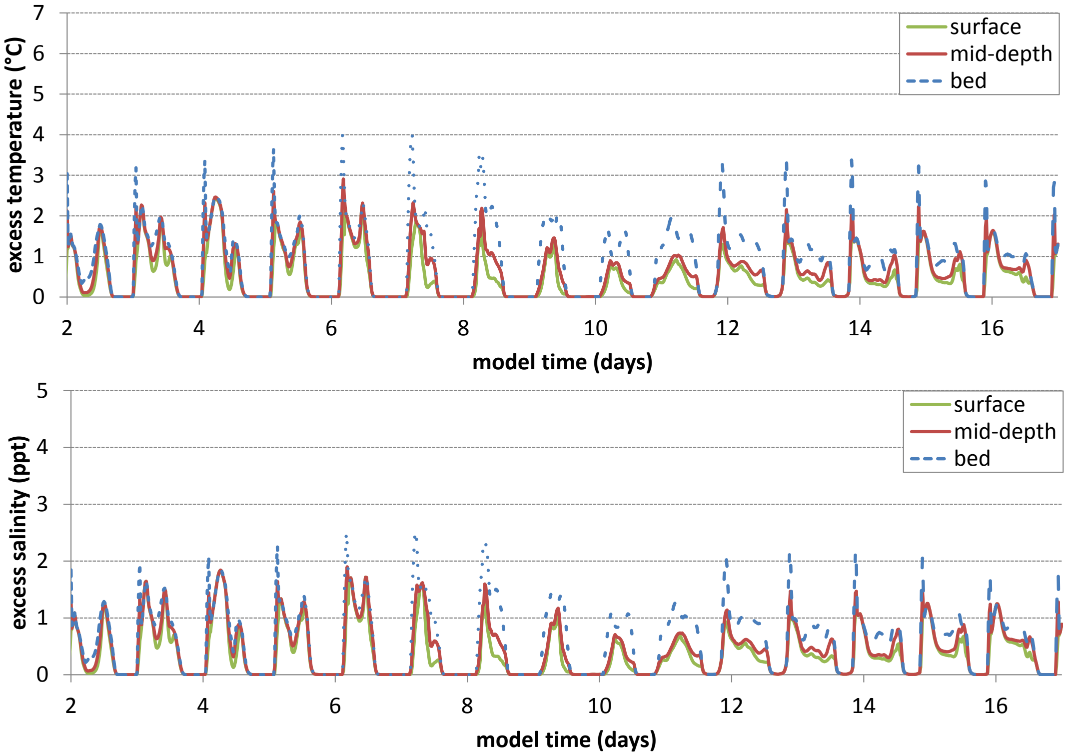

Figure 6.23: Excess temperature and salinity at the intake, winter, calm, standard operation

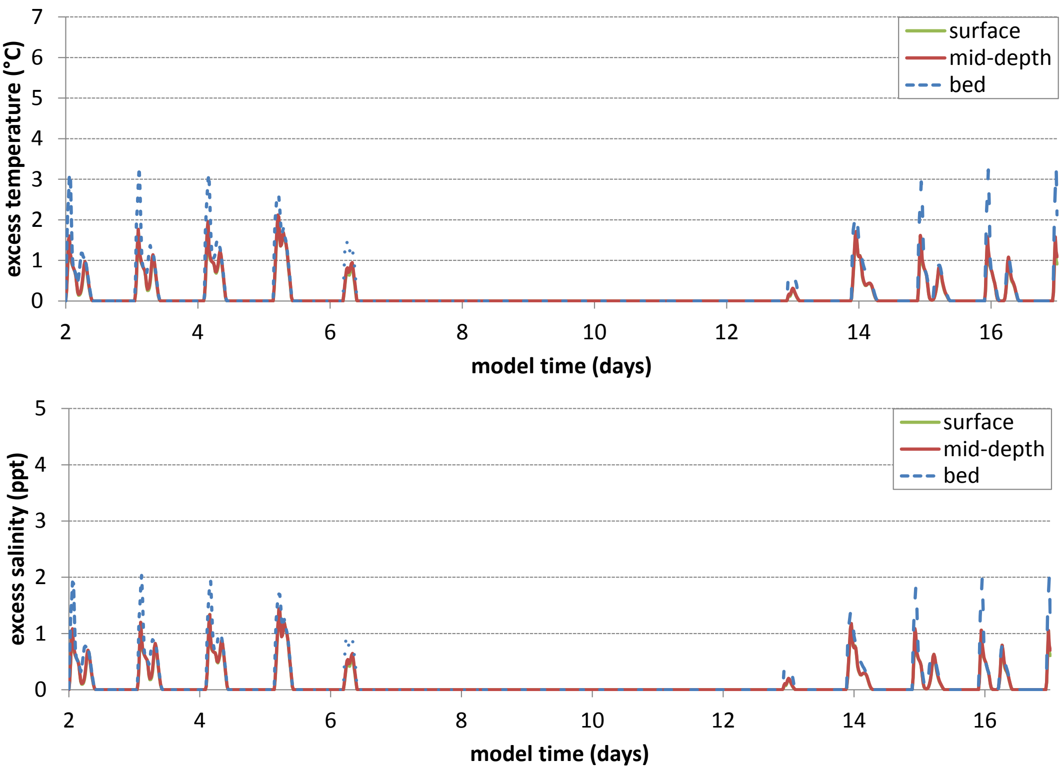

Figure 6.24: Excess temperature and salinity at the intake, winter, north-west wind, standard operation

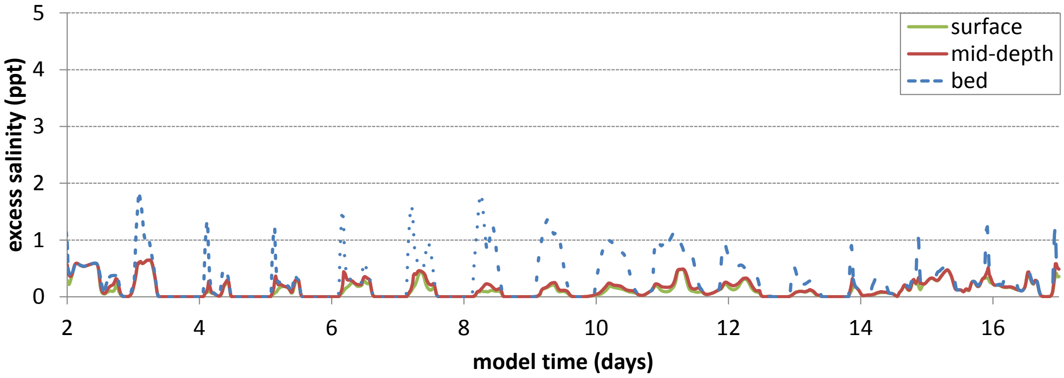

Figure 6.25: Excess salinity at the intake, summer, observed wind, early operation

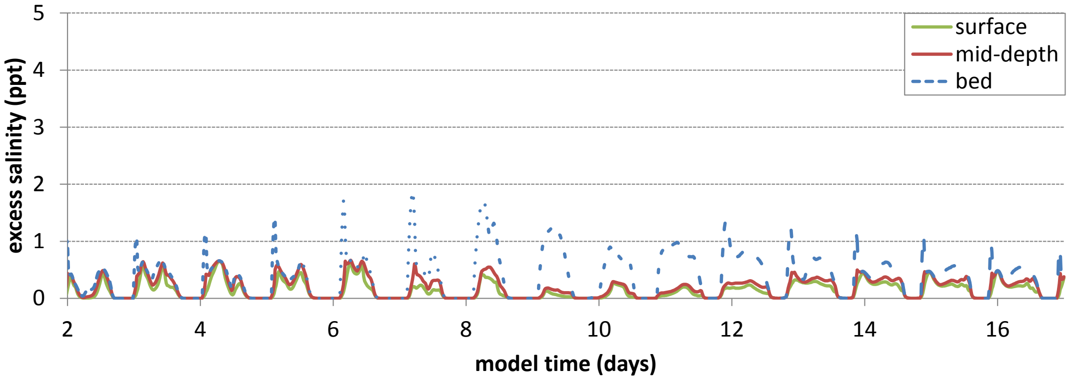

Figure 6.26: Excess salinity at the intake, summer, calm, early operation

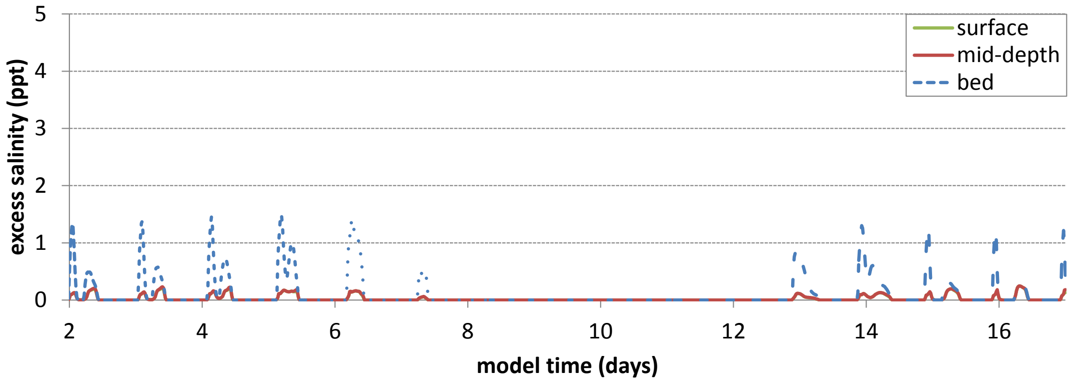

Figure 6.27: Excess salinity at the intake, summer, north-west wind, early operation

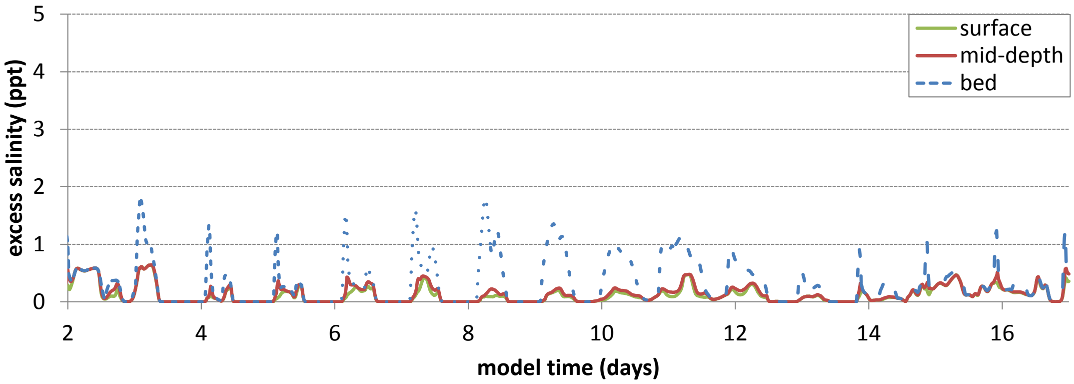

Figure 6.28: Excess salinity at the intake, winter, observed wind, early operation

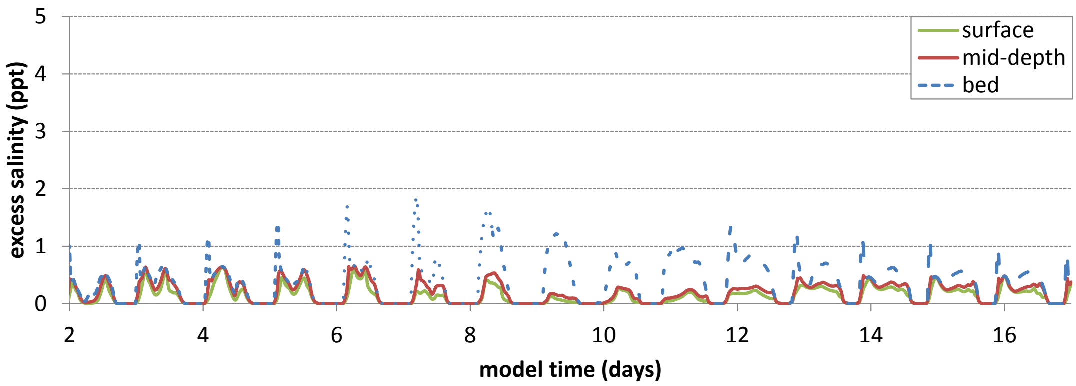

Figure 6.29: Excess salinity at the intake, winter, calm, early operation

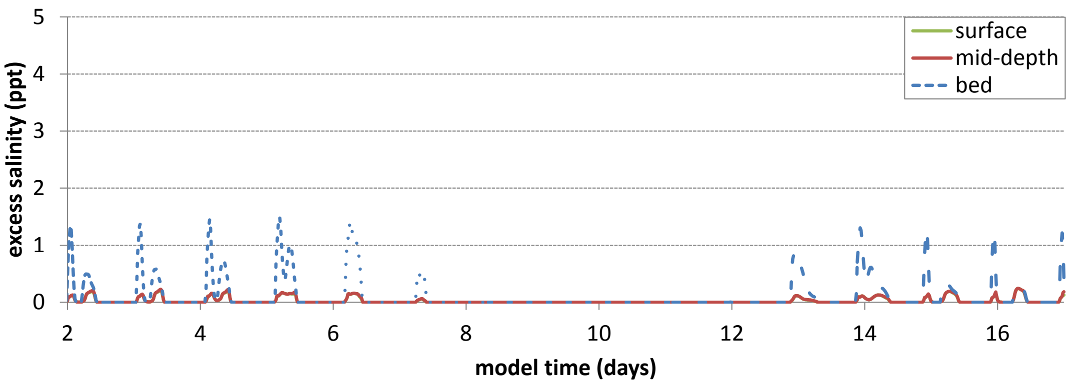

Figure 6.30: Excess salinity at the intake, winter, north-west wind, early operation

7. Impact of nearby discharges

The Ras Abu Fontas (RAF) power and desalination plants are located approximately 10 km north of UHP (Figure 7.1). These facilities discharge heated and saline effluent, and could potentially impact the behaviour of the UHP discharge plume and recirculation levels.

Figure 7.1: Site locations of UHP and RAF

7.1. Model configuration

The impact of the RAF discharges was assessed using the TELEMAC-3D model described in Chapter 6. The model was updated to include the RAF discharges using the outfall characteristics from HR Wallingford's previous study at the site (Table 7.1). The RAF intakes were not included in the model. The model mesh and bathymetry were slightly modified in the vicinity of RAF to ensure that the simulated far-field plume behaviour was consistent with the results from the previous studies at RAF.

Table 7.1: RAF outfall parameters

Outfall	Summer			Winter		
	Flow rate (m^3/s)	Excess temperature (°C)	Excess salinity (ppt)	Flow rate (m^3/s)	Excess temperature (°C)	Excess salinity (ppt)
A North	10.60	11.00	7.30	7.74	15.80	6.95
A South	21.11	9.00	8.71	8.90	17.50	10.12
A1	13.11	10.00	7.80	6.19	17.90	16.40
A2	10.68	8.80	7.69	6.24	12.50	13.03
B	25.97	8.00	4.00	9.10	13.30	4.58
B2	12.97	10.00	5.20	11.17	10.00	6.00

Source: HR Wallingford (2012)

Simulations were conducted for the standard operation phase of the UHP facility under summer and winter ambient conditions. The observed wind condition was applied to represent realistic wind conditions at the site. The boundary conditions developed during the hydrodynamic model calibration (Chapter 4) were applied at the offshore boundary and the model was run for 17 days.

7.2. Results

The maximum and mean excess salinities and temperatures at the sea surface and sea bed are shown in Figure 7.2 to Figure 7.5. These should be compared with the similar plots for UHP on its own (Figure 6.7, Figure 6.10, Figure 6.13 and Figure 6.16). The RAF effluent plumes do not appear to interact strongly with the UHP plumes, so the that original UHP dispersion patterns are still visible in the combined results. The RAF plumes increase both temperature and salinity around the UHP land site, inshore of the UHP plumes.

The mean excess temperature patterns in both simulations are largely unchanged by the addition of the RAF discharges. The maximum excess temperature plots indicate an area of higher temperature to the north of the UHP site near the shoreline. Similarly the maximum excess salinity plots contain a region of higher salinity near the shore which extends to the south of the UHP site. These patterns are produced by a short-lived event in the simulation, when persistent winds from the north transported the RAF plume to the south. The mean excess salinity in the vicinity of the UHP outfall and intake is not visibly affected by the RAF discharges. Near the shore the mean excess salinity is marginally increased.

Time series of the excess temperature and excess salinity at the intake are shown in Figure 7.6 and Figure 7.7. There is generally little difference between these time series and those for the simulations without the RAF discharges (Figure 6.19 and Figure 6.22) except around days 3 and 4 where the temperature and salinity are slightly elevated. These small increases occur during the period of persistent northerly wind.

Table 7.2 to Table 7.5 show the maximum and mean excess temperatures and salinities at the intake. The recirculation levels for the simulations without RAF have been included for comparison. The average excess temperature and excess salinity at the intake are increased by up to 0.1°C and 0.3 ppt. The maximum excess temperature and excess salinity are increased by up to 0.8°C and 0.8 ppt respectively. These variations may be comparable to natural variations in the ambient seawater characteristics.

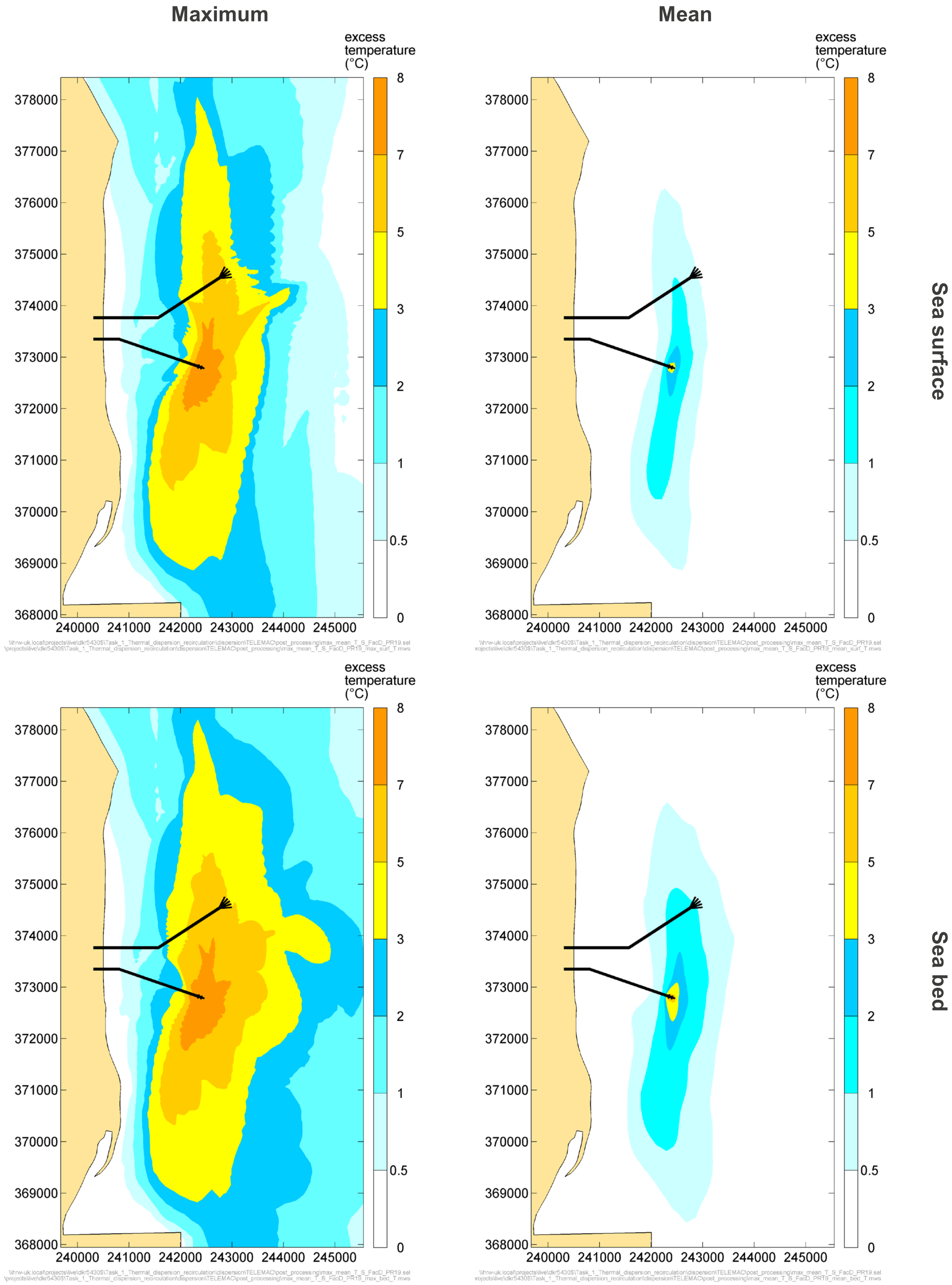

Figure 7.2: Maximum and mean sea surface and sea bed excess temperature, summer, observed wind, standard operation with RAF discharges

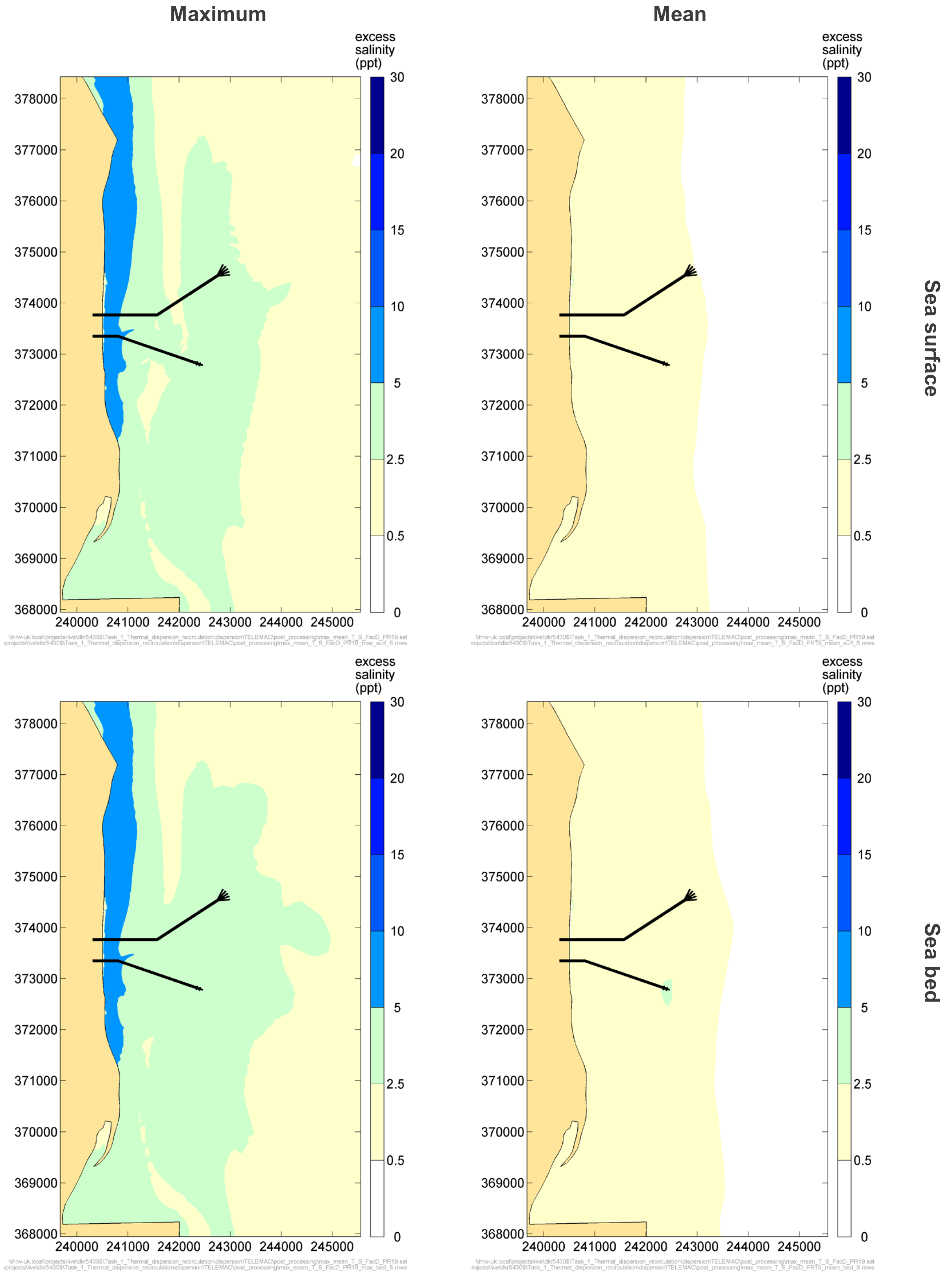

Figure 7.3: Maximum and mean sea surface and sea bed excess salinity, summer, observed wind, standard operation with RAF discharges

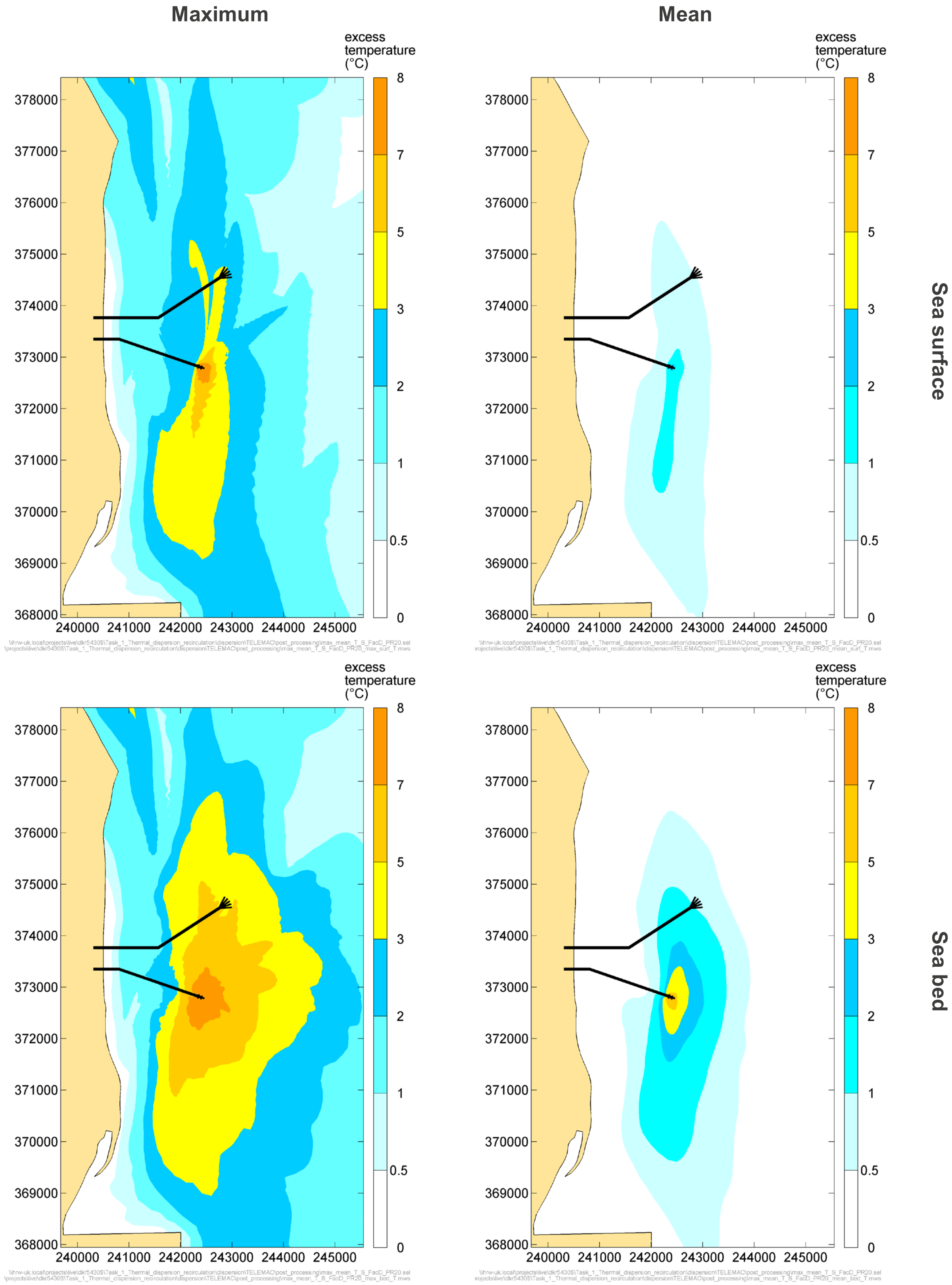

Figure 7.4: Maximum and mean sea surface and sea bed excess temperature, winter, observed wind, standard operation with RAF discharges

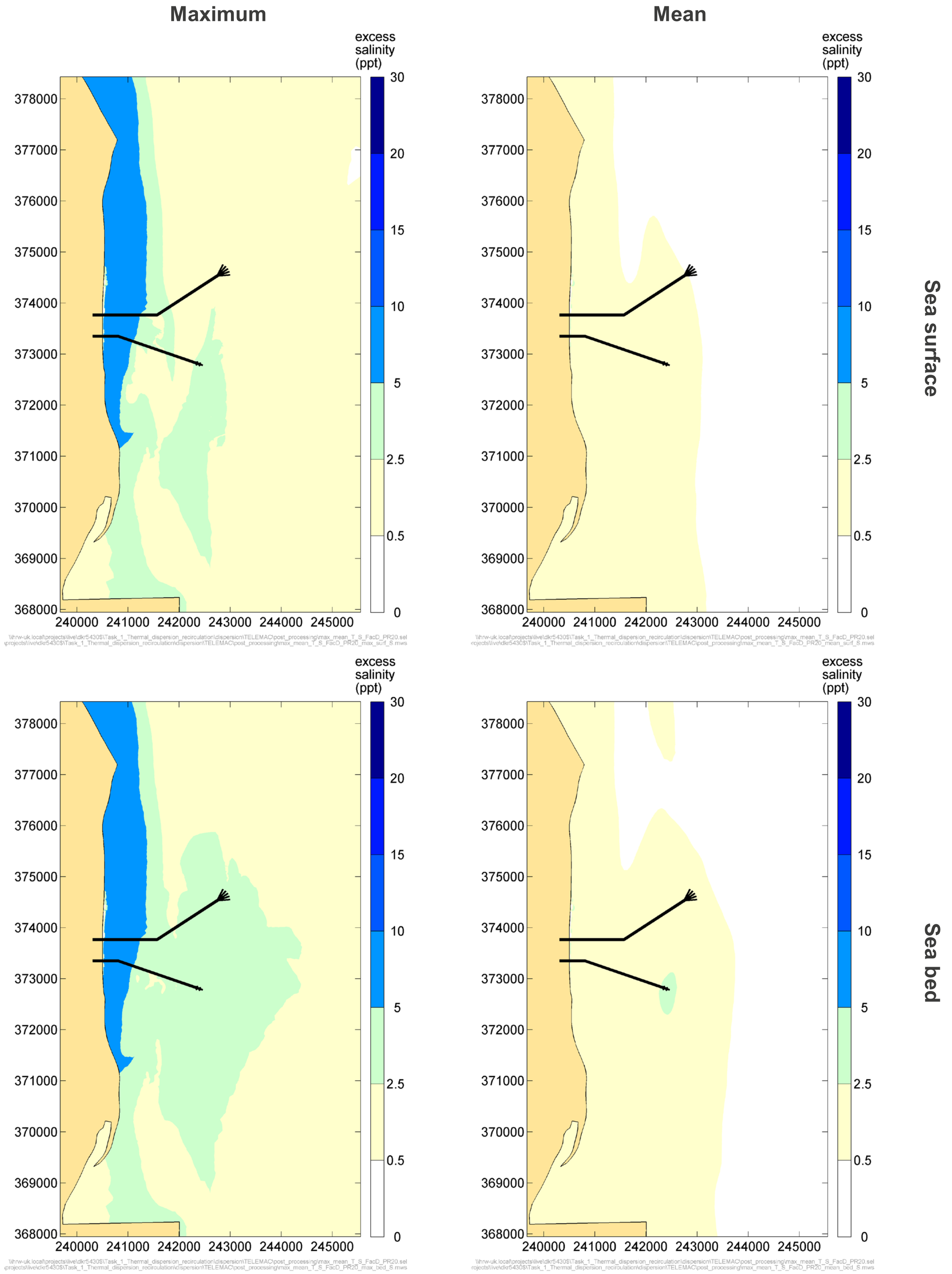

Figure 7.5: Maximum and mean sea surface and sea bed excess salinity, winter, observed wind, standard operation with RAF discharges

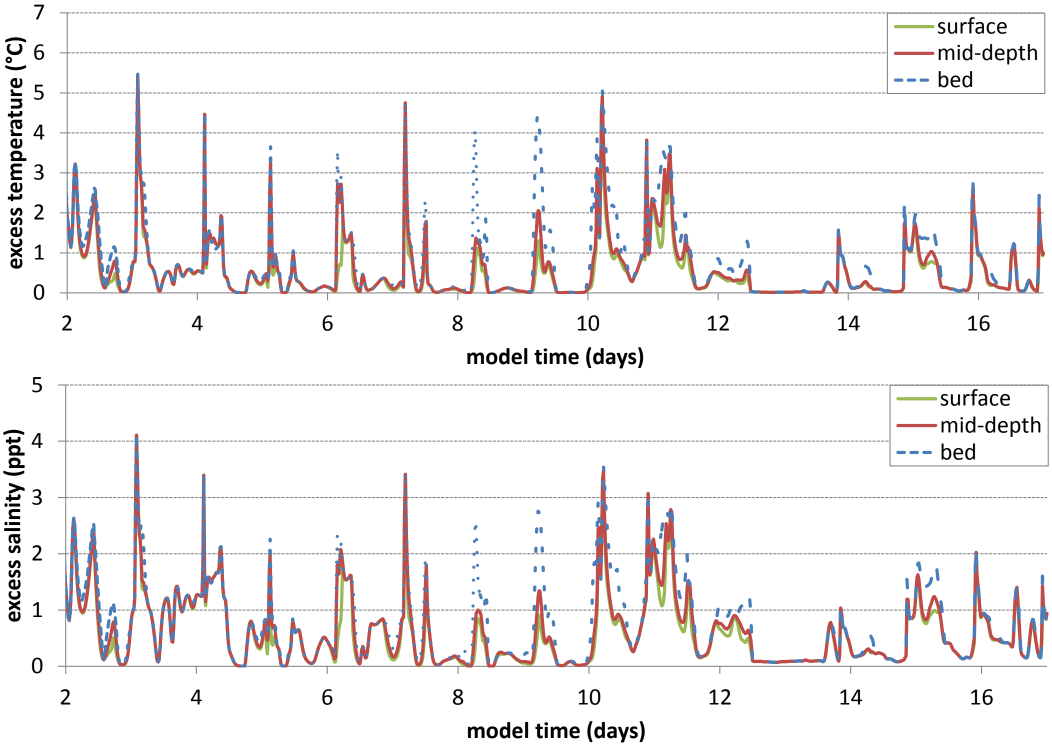

Figure 7.6: Excess temperature and salinity at the intake, summer, observed wind, standard operation with RAF discharges

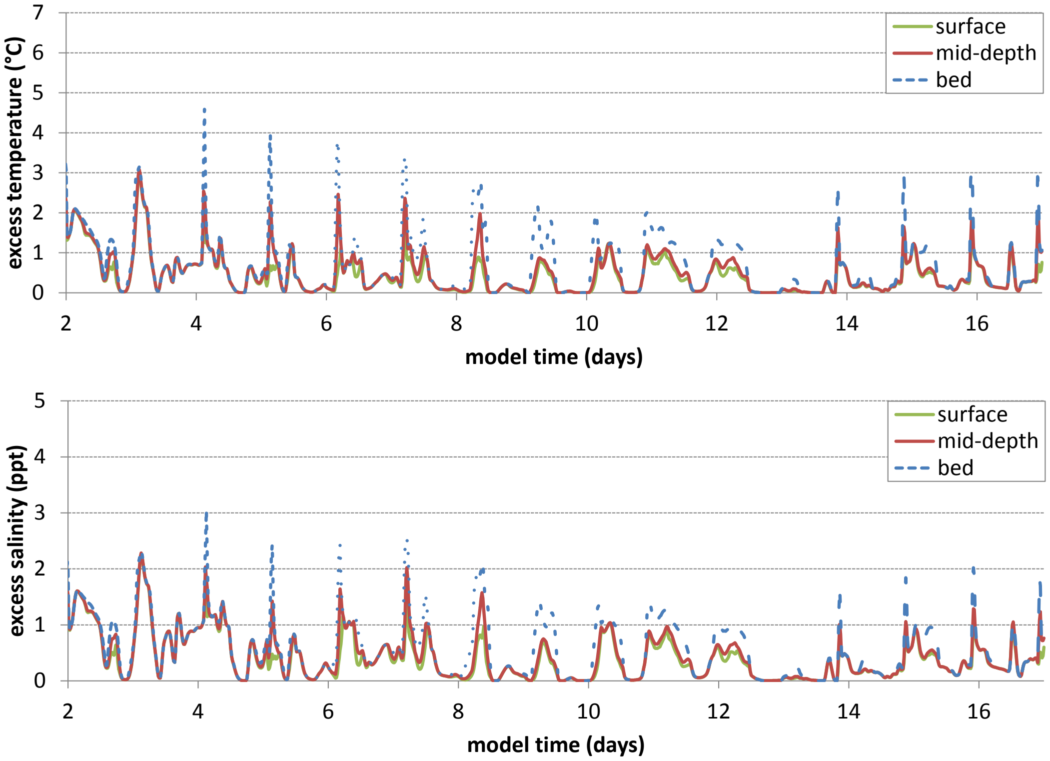

Figure 7.7: Excess temperature and salinity at the intake, winter, observed wind, standard operation with RAF discharges

Table 7.2: Maximum excess temperature at the UHP intake, standard operation, observed wind

	Maximum excess temperature (°C)			
	Summer		Winter	
	With RAF	Without RAF	With RAF	Without RAF
Depth-averaged	5.4	4.7	3.1	2.4
Near-surface	5.4	4.6	3.0	2.3
Mid-depth	5.4	4.7	3.1	2.4
Near-bed	5.5	4.8	4.6	3.9

Table 7.3: Average excess temperature at the UHP intake, standard operation, observed wind

	Mean excess temperature (°C)			
	Summer		Winter	
	With RAF	Without RAF	With RAF	Without RAF
Depth-averaged	0.6	0.5	0.5	0.5
Near-surface	0.5	0.5	0.4	0.4
Mid-depth	0.6	0.5	0.5	0.4
Near-bed	0.7	0.7	0.7	0.6

Table 7.4: Maximum excess salinity at the UHP intake, standard operation, observed wind

	Maximum excess salinity (ppt)			
	Summer		Winter	
	With RAF	Without RAF	With RAF	Without RAF
Depth-averaged	4.1	3.3	2.3	1.9
Near-surface	4.1	3.2	2.3	1.8
Mid-depth	4.1	3.3	2.3	1.9
Near-bed	4.1	3.5	3.0	2.4

Table 7.5: Average excess salinity at the UHP intake, standard operation, observed wind

	Mean excess salinity (ppt)			
	Summer		Winter	
	With RAF	Without RAF	With RAF	Without RAF
Depth-averaged	0.7	0.4	0.5	0.3
Near-surface	0.6	0.4	0.4	0.3
Mid-depth	0.6	0.4	0.5	0.3
Near-bed	0.8	0.5	0.6	0.4

8. Conclusions

Results from a hydrographic survey undertaken in April-May 2105 have been reviewed and used to calibrate HR Wallingford's hydrodynamic model of coastal waters around the Umm Al Houl Power (UHP) site. Thermal and saline dispersion from the proposed UHP have been predicted under normal and early operating conditions.

The survey observations indicated that currents at the UHP site flow predominantly north-south, approximately parallel to the coastline. In the region most likely to be occupied by the UHP effluent plume (around 2 km offshore), currents during the period of the survey were generally weak with depth-averaged speeds of less than 0.3 m/s.

A hydrodynamic 3D model of the waters near UHP has been developed as part of the recirculation and dispersion studies. The model has been calibrated and validated against the surveyed tidal elevations and current speeds measured at an ADCP located approximately 2.5 km offshore where the sea bed elevation is approximately -5 m QNHD and an Aquadopp located approximately 4 km offshore at a sea bed elevation of -10 m QNHD. The predicted average tidal range is within 0.08 m of the observations at both locations. For the same period, the average predicted peak current speed is within 0.04 m/s of the measured data at the ADCP location and within 0.08 m/s at the Aquadopp location. These values indicate a good level of agreement between the model predictions and the observed variations, and therefore the model has been accepted for use in the recirculation and dispersion assessment.

Thermal and saline dispersion have been assessed for the proposed UHP using the calibrated 3D model. Two operational phases of UHP were simulated for a range of environmental conditions. The key findings are:

- During the standard operational phase of the facility the area where average temperatures are predicted to be more than 3°C above the ambient is generally less than 0.1 km^2. The discharge salinity is sufficiently low that it does not require detailed assessment.
- During the early operation phase of the facility, the model predicts that a region of the sea bed approximately 0.1 km^2 in size may be exposed to average salinities more than 10% above the background salinity. The discharge temperature is sufficiently low that it does not require detailed assessment.
- The recirculation assessment indicates that (under the tide and wind conditions considered) average excess temperatures at the UHP intake will be less than 1°C and average excess salinities less than 1 ppt during the standard operation phase of the facility. Under calm or weak wind conditions during neap tides, excess temperatures at the intake may exceed 4°C.
- During the early operation phase of the facility the predicted average recirculation temperatures and salinities are less than 0.1°C and 0.5 ppt, respectively.
- The impacts of the discharges from the nearby Ras Abu Fontas power and desalination plants on the UHP have been assessed. The model predictions show that the UHP plume dispersion patterns are largely unchanged by the Ras Abu Fontas discharges, but the intake temperature and salinity are slightly increased. The average excess temperature at the UHP intake is increased by 0.1°C in the simulation with RAF, and the average excess salinity by 0.3 ppt, .

9. References

HR Wallingford (2012). Ras Abu Fontas A2 Plant. Dispersion modelling and recirculation assessment, HR Wallingford Report, EX 6839, Release 2.0, August 2012.

HR Wallingford (2014). Qatar Facility ‘D’ IWPP: Recirculation Study – Layout Case 3, HR Wallingford Report DER5229-RT003, Release 1.0, May 2014.

HR Wallingford (2015). Umm al Houl Power Project, Qatar: Modelling studies to support EIA, HR Wallingford Report DER5448-RT001, Release 3.0, July 2015.

El-Dessouky and Ettouny (2002). Fundamentals of Sea Water Desalination, Thermodynamic Properties, Appendix A. Elsevier.

QSCE (2003). Final SCE Standards. Qatar Supreme Council for the Environment & Natural Reserves. 9 June 2003.

United Kingdom Hydrographic Office (2014). Admiralty tide tables, 2015: Volume 3, Indian Ocean. Crown copyright.

Appendices

A. Intake and outfall layout

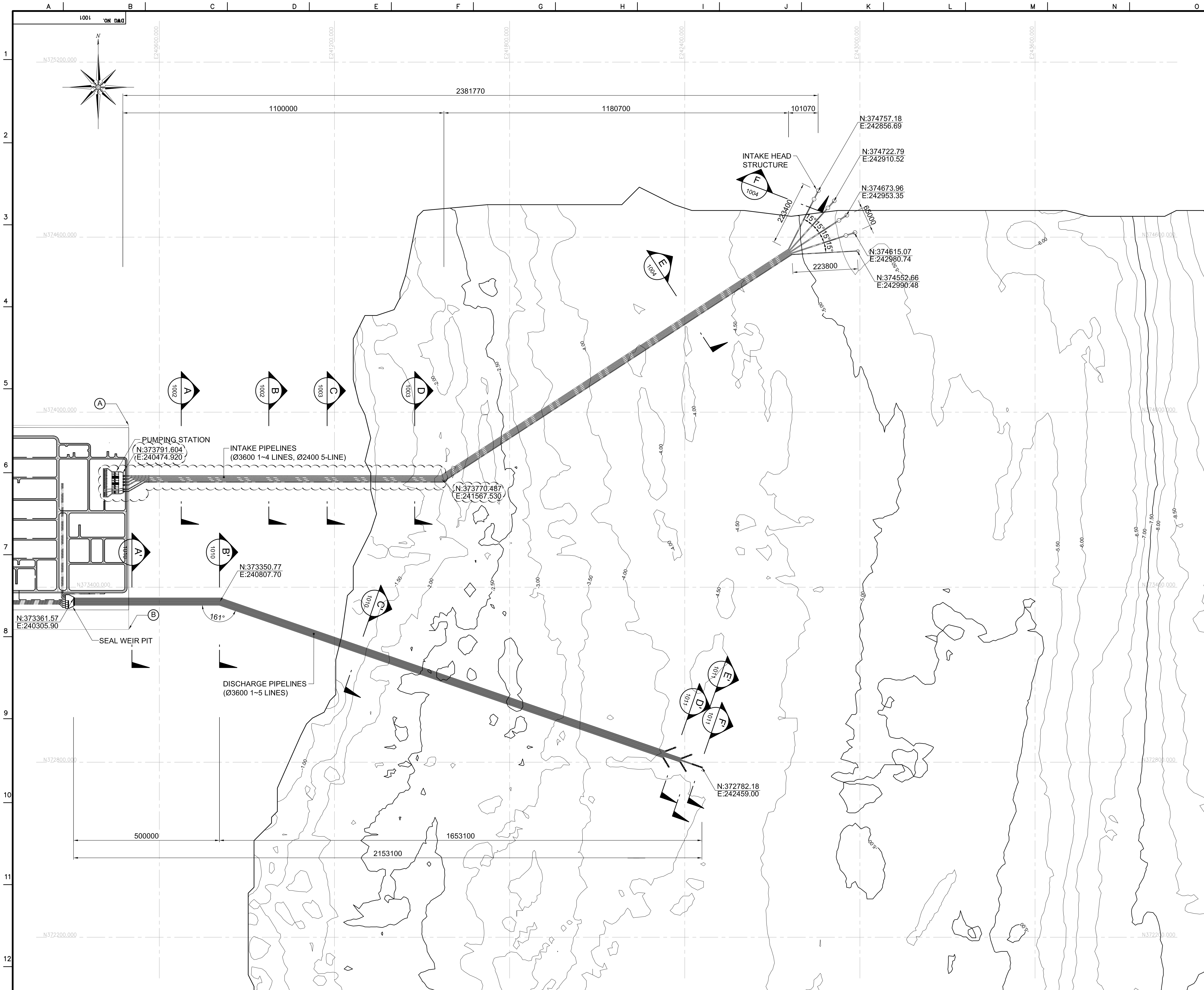

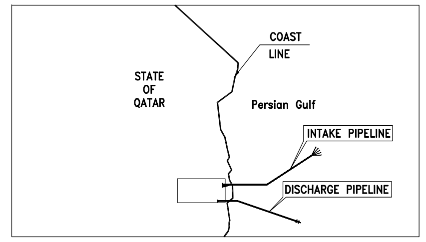

KEYPLAN

NOTES.

1. UNITS ARE SI UNITS.
2. ALL DIMENSIONS ARE IN MILLIMETERS UNLESS OTHERWISE NOTED.
3. ALL ELEVATIONS ARE IN METERS ABOVE QNHD (MSL) UNLESS SPECIFIED OTHERWISE.
4. ALL COORDINATES ARE IN METERS AND CORRESPOND TO QATAR NATIONAL GRID(QNG)
5. VERTICAL DATUM G.L. ±0.0 = +4.0m QNHD = +4.0 ABOVE MEAN SEA LEVEL
6. DESIGNATION OF AREA BOUNDARY
   - INDICATES PROPERTY BOUNDARY
   - INDICATES SECURITY FENCE BOUNDARY

COORDINATES

NO.	EASTING	NORTHING
A	24049500.00	37395500.00
B	24049500.00	37325500.00

REV.	DATE	DESCRIPTION	DWN	CHKD	APVD	AUTH

OWNER :

Umm Al Houl Power

OWNER's ENGINEER :

Mott MacDonald

PROJECT TITLE :

Umm Al Houl Power IWPP

CONSORTIUM MEMBER

SAMSUNG C & T

Hitachi Zosen

TITLE

INTAKE & DISCHARGE
OVERALL LAYOUT

SCALE	REF. NUMBER		REV:	SHEET NO.
1/6000	DRAWING NUMBER	1001	REV:	

A1(841x594m/m)

B. Additional dispersion modelling results

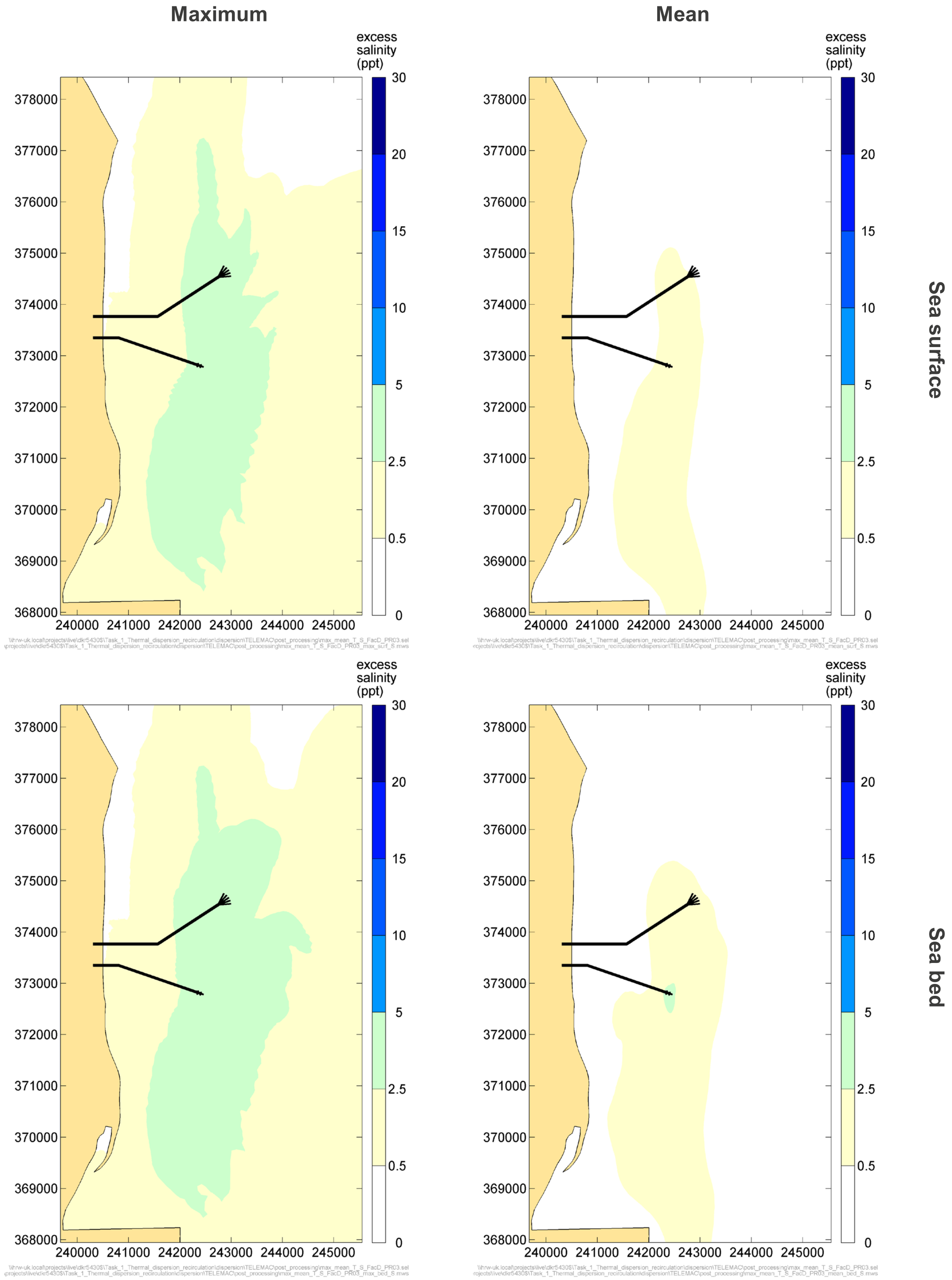

Figure B.1: Maximum and mean sea surface and sea bed excess salinity, summer, observed wind, standard operation

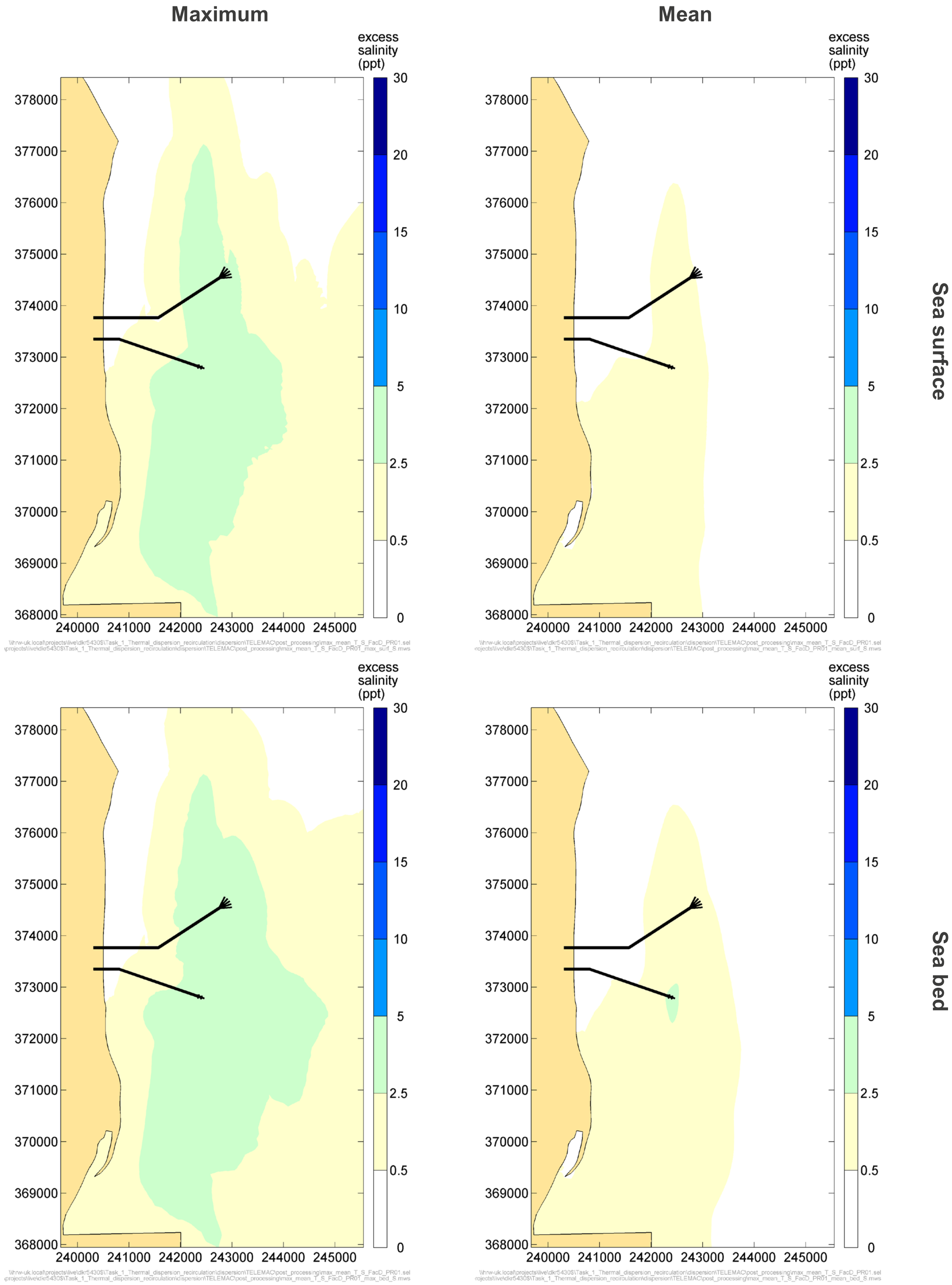

Figure B.2: Maximum and mean sea surface and sea bed excess salinity, summer, calm, standard operation

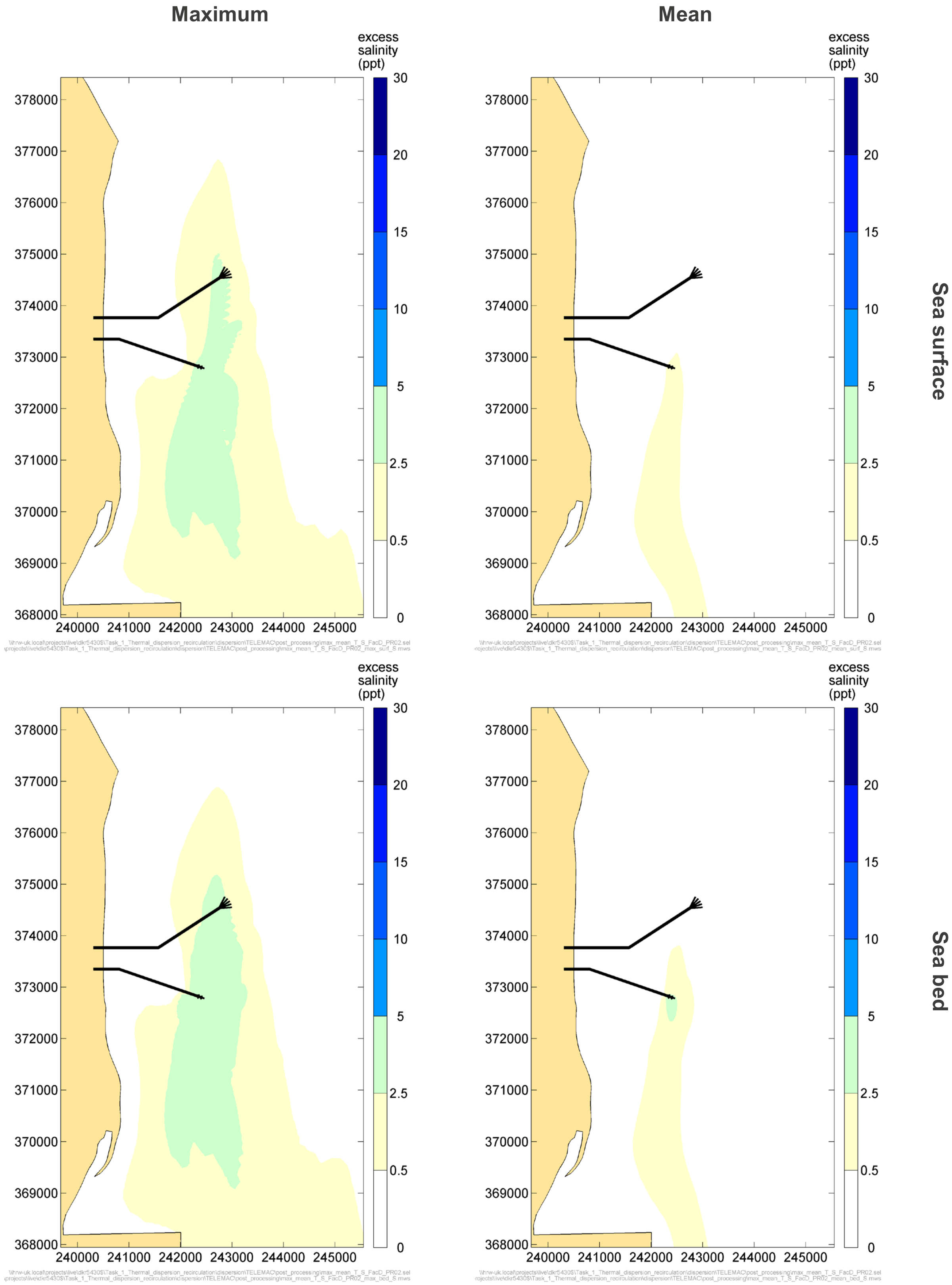

Figure B.3: Maximum and mean sea surface and sea bed excess salinity, summer, north-west wind, standard operation

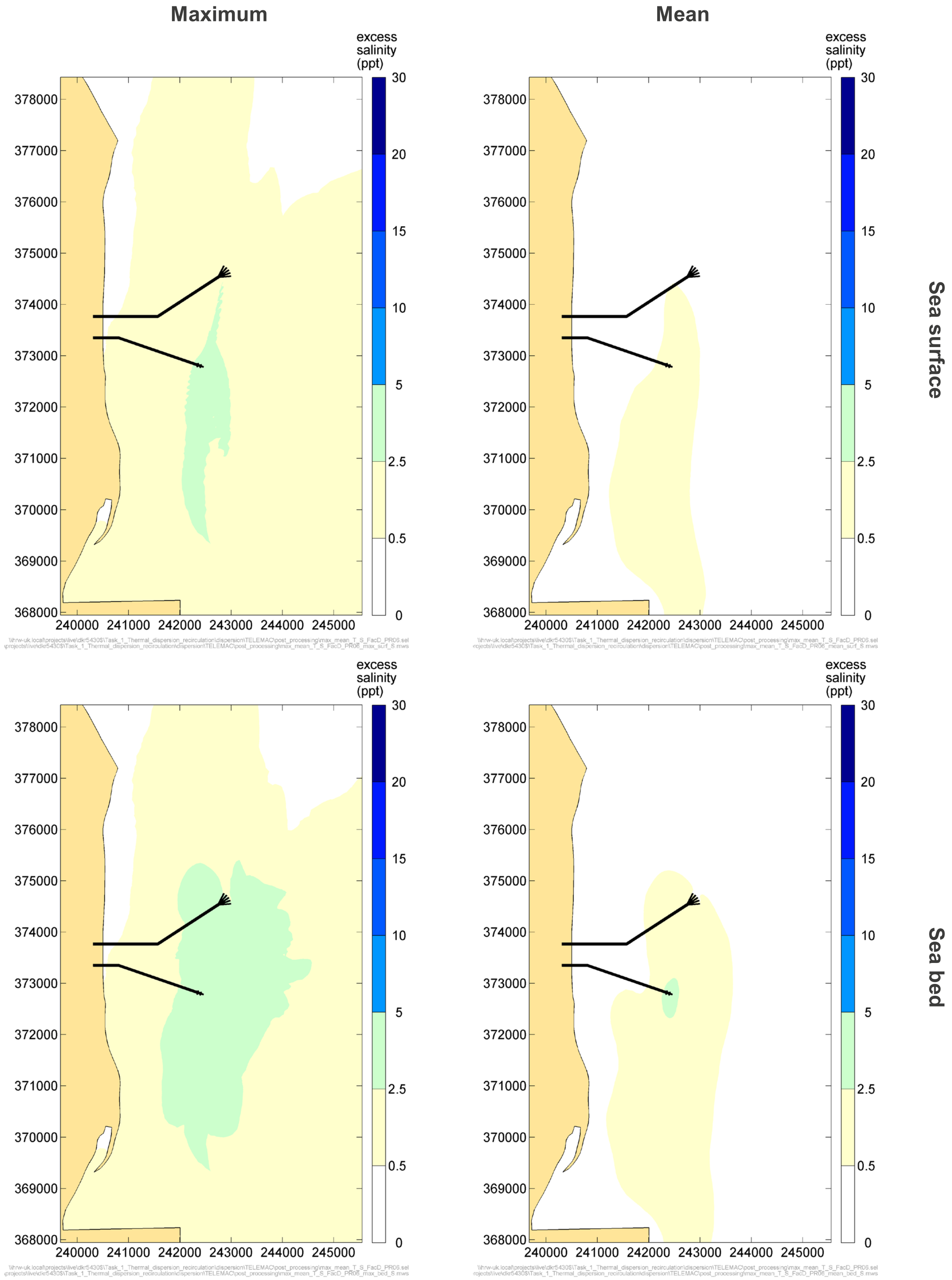

Figure B.4: Maximum and mean sea surface and sea bed excess salinity, winter, observed wind, standard operation

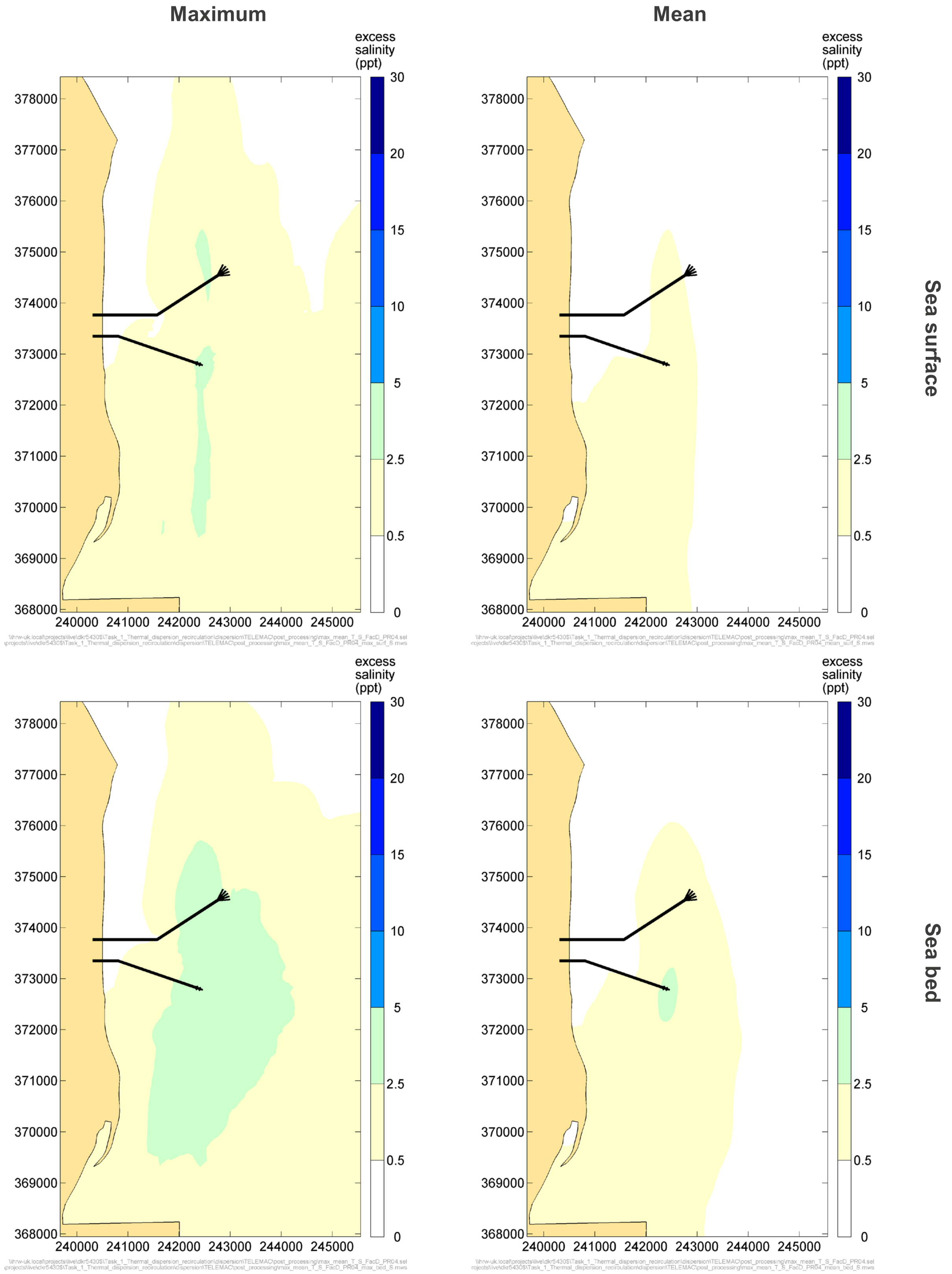

Figure B.5: Maximum and mean sea surface and sea bed excess salinity, winter, calm, standard operation

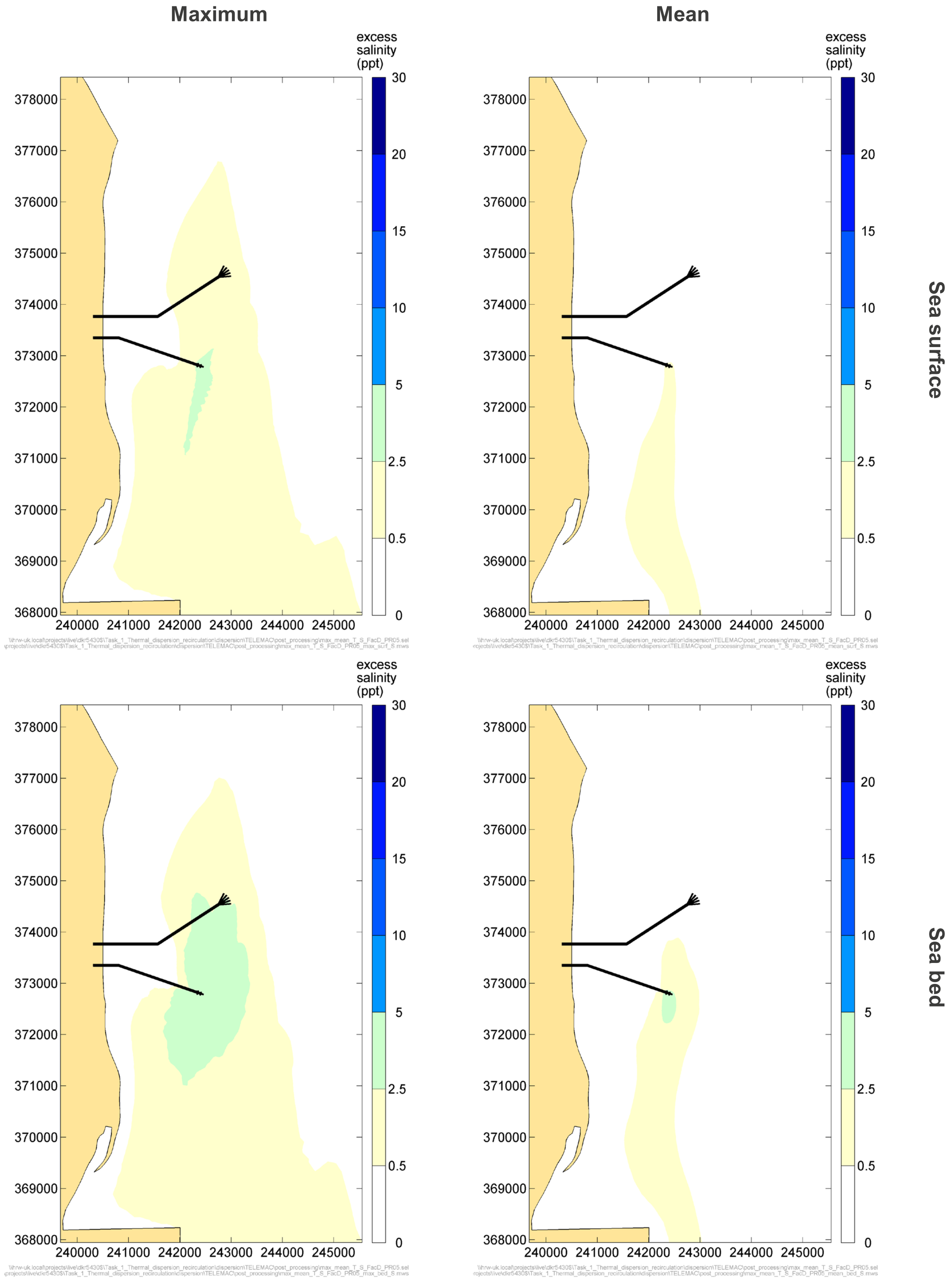

Figure B.6: Maximum and mean sea surface and sea bed excess salinity, winter, north-west wind, standard operation

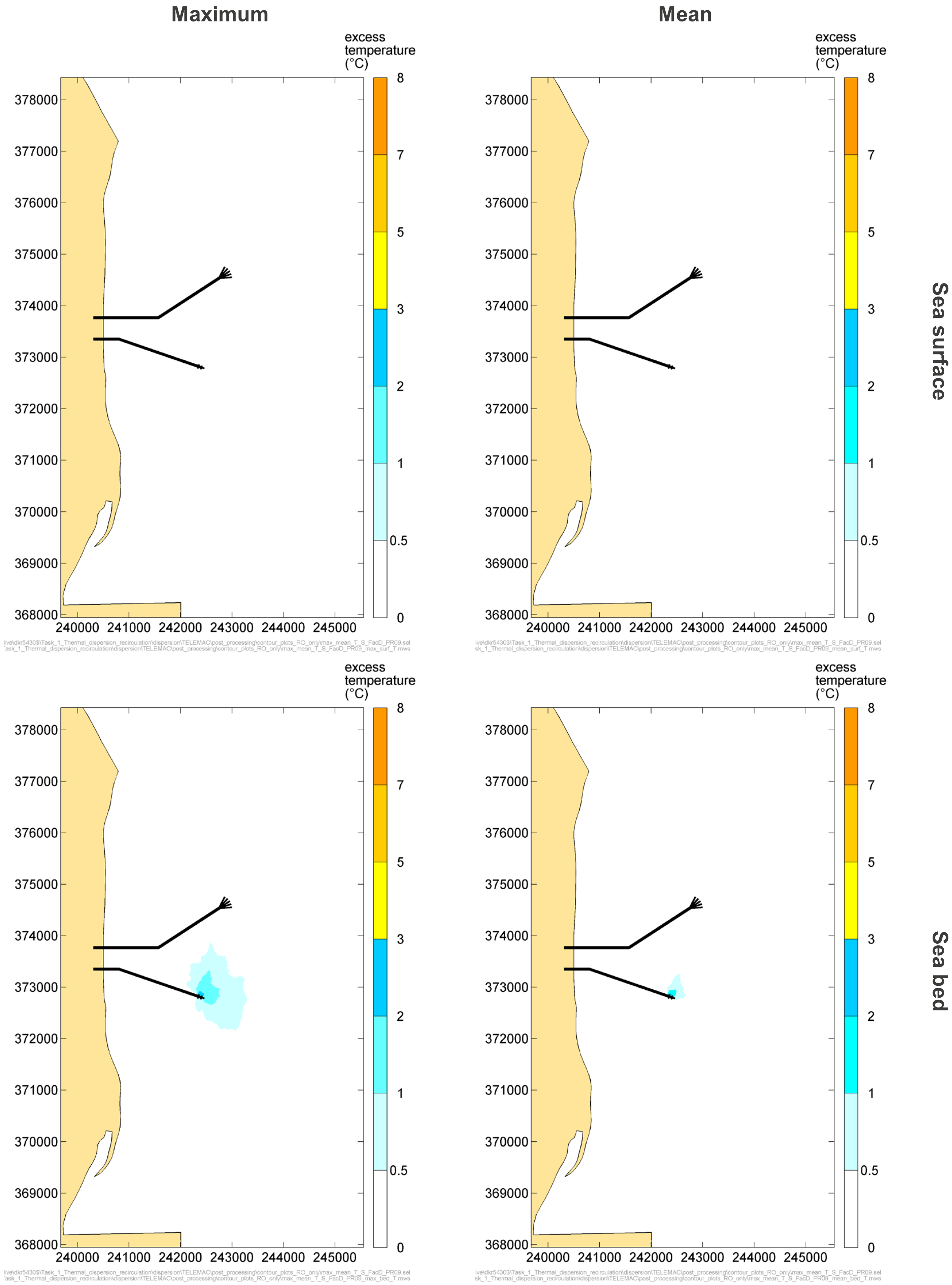

Figure B.7: Maximum and mean sea surface and sea bed excess temperature, summer, observed wind, early operation

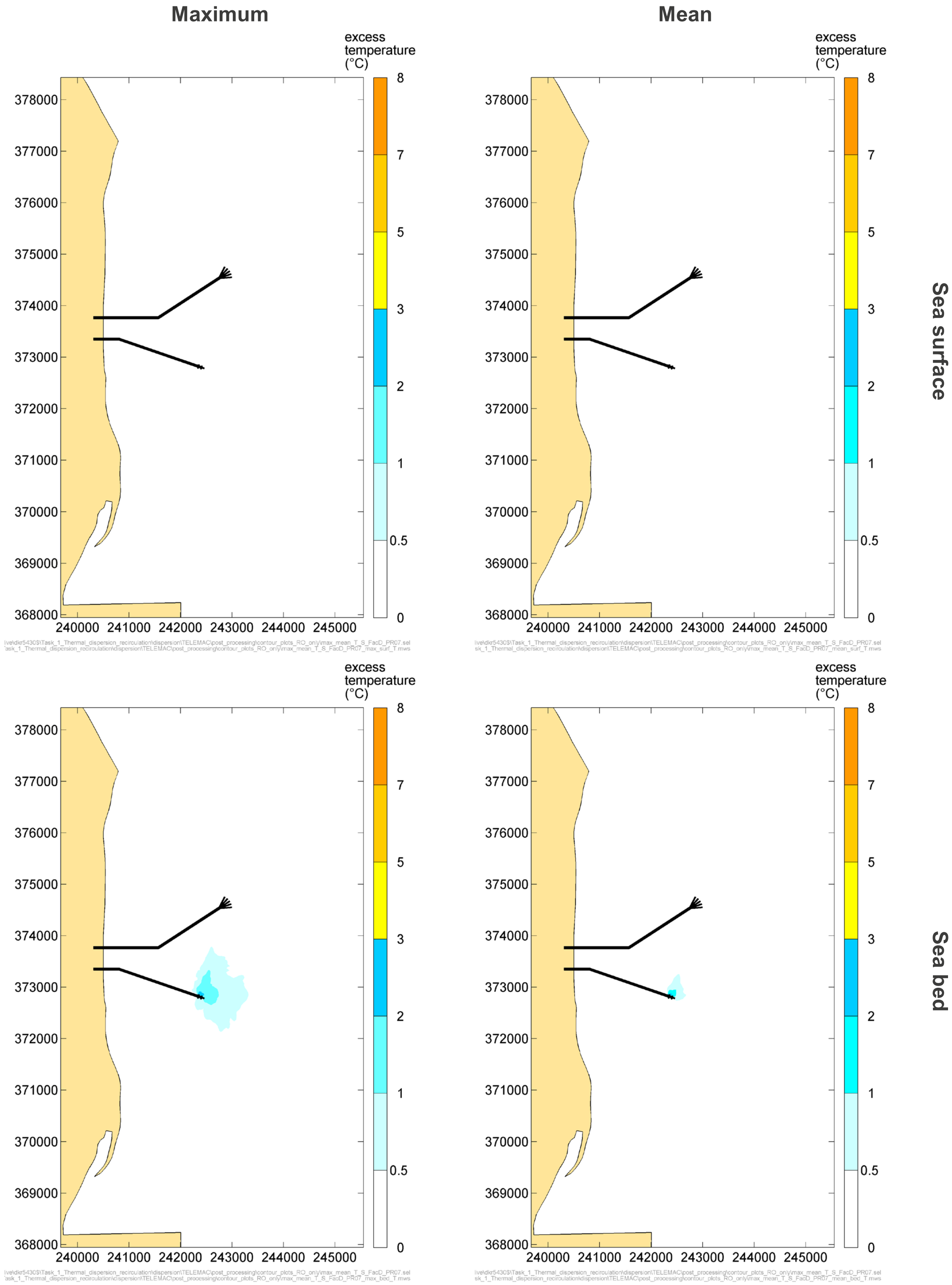

Figure B.8: Maximum and mean sea surface and sea bed excess temperature, summer, calm, early operation

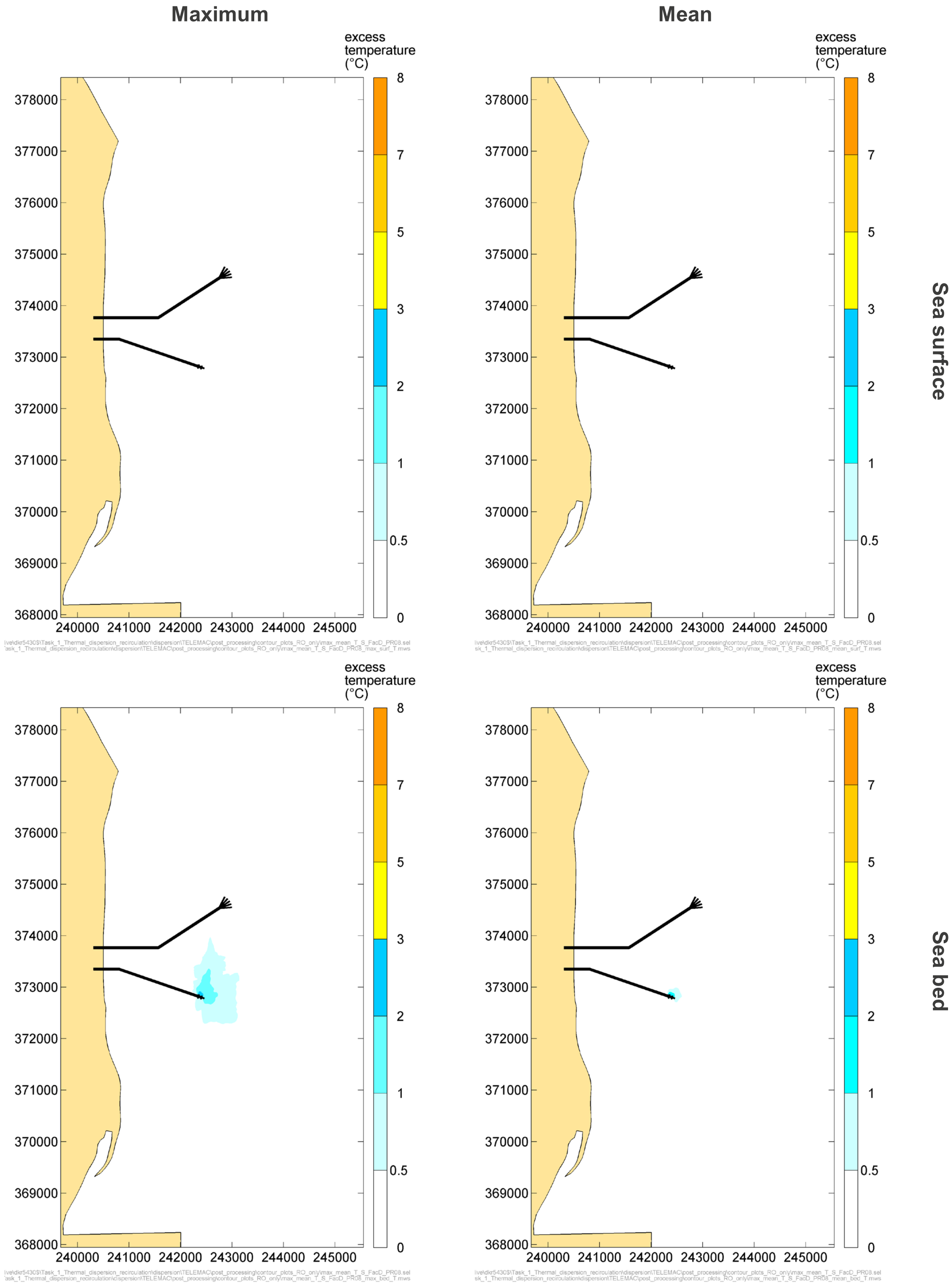

Figure B.9: Maximum and mean sea surface and sea bed excess temperature, summer, north-west wind, early operation

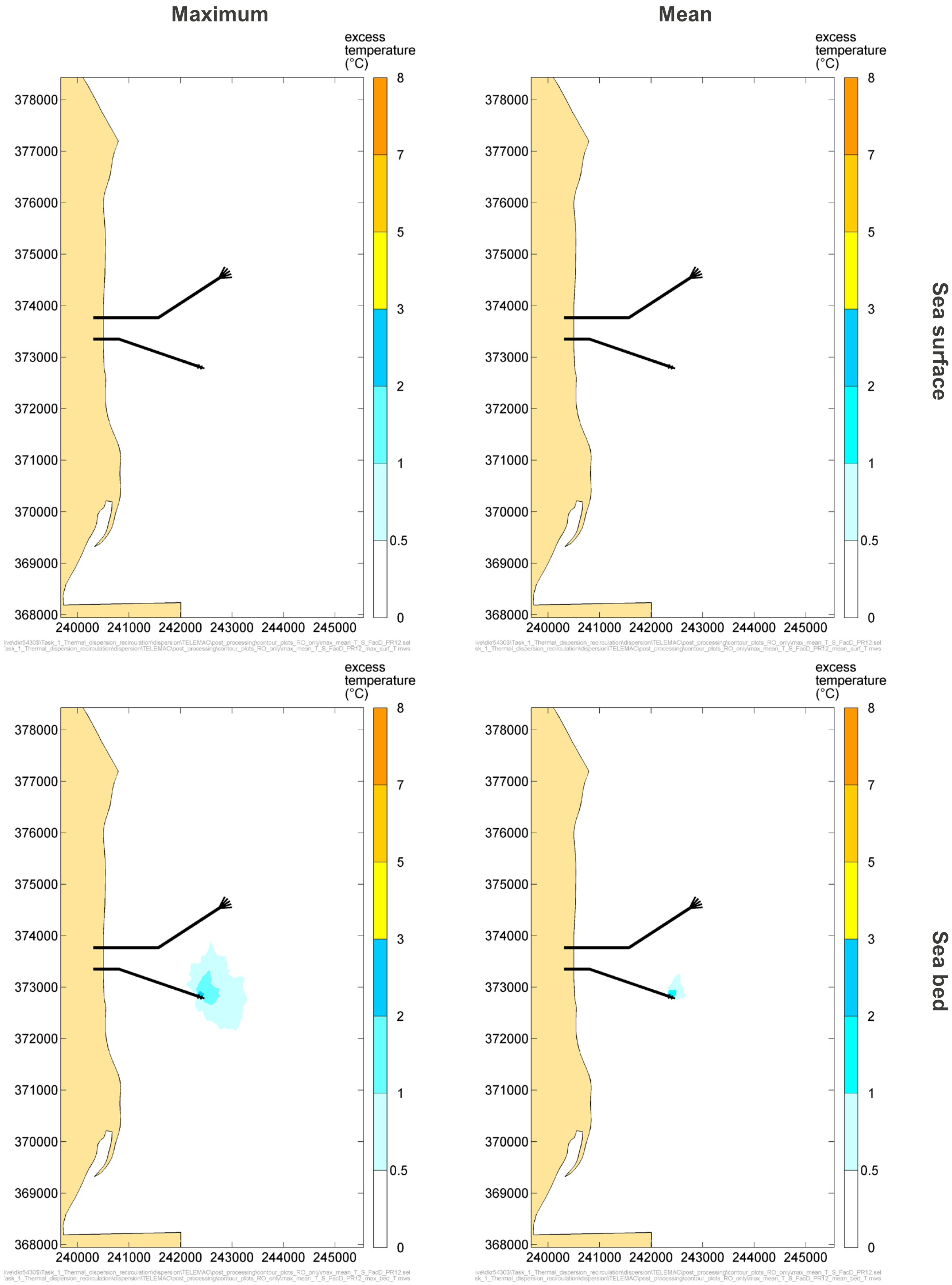

Figure B.10: Maximum and mean sea surface and sea bed excess temperature, winter, observed wind, early operation

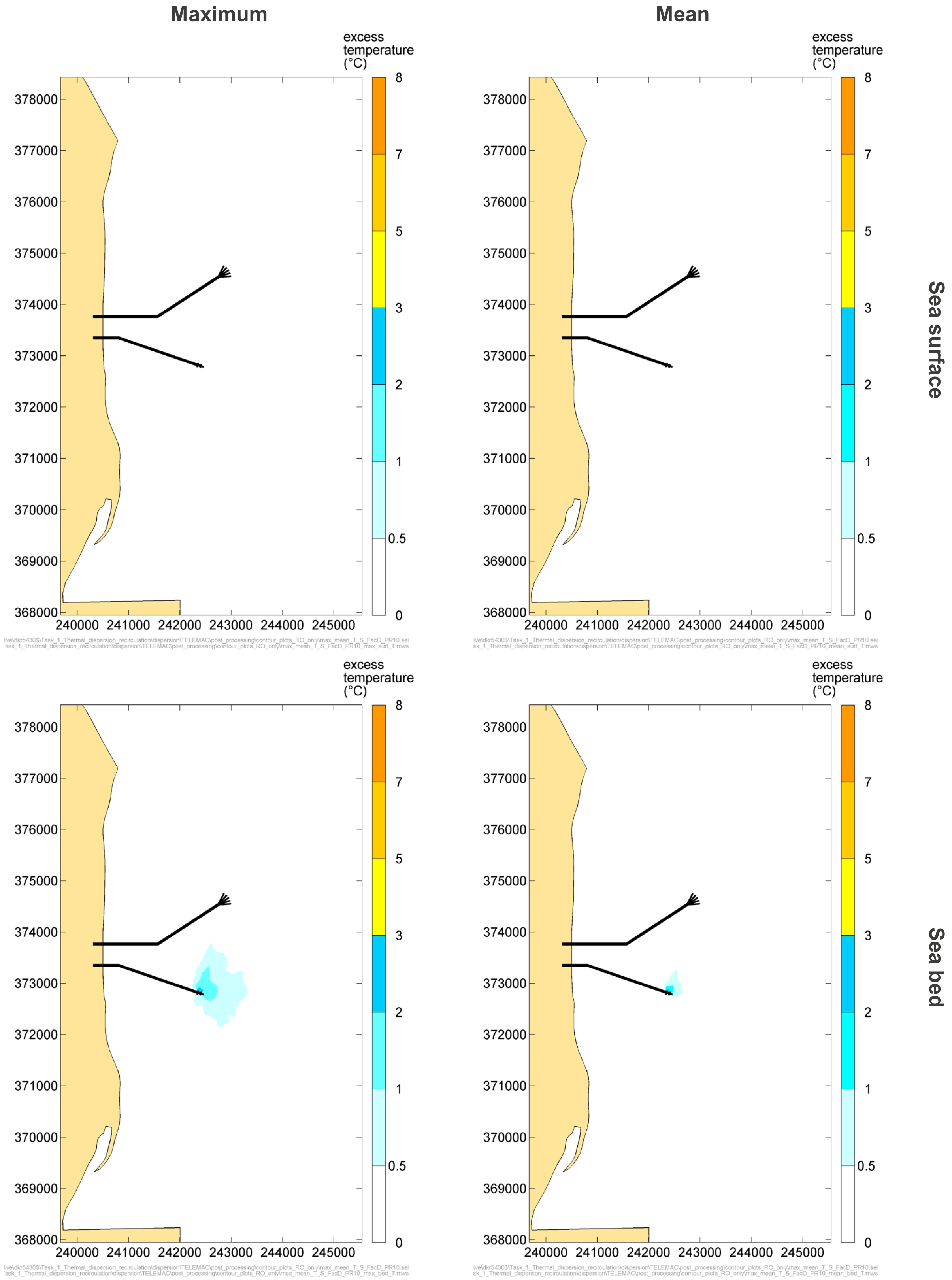

Figure B.11: Maximum and mean sea surface and sea bed excess temperature, winter, calm, early operation

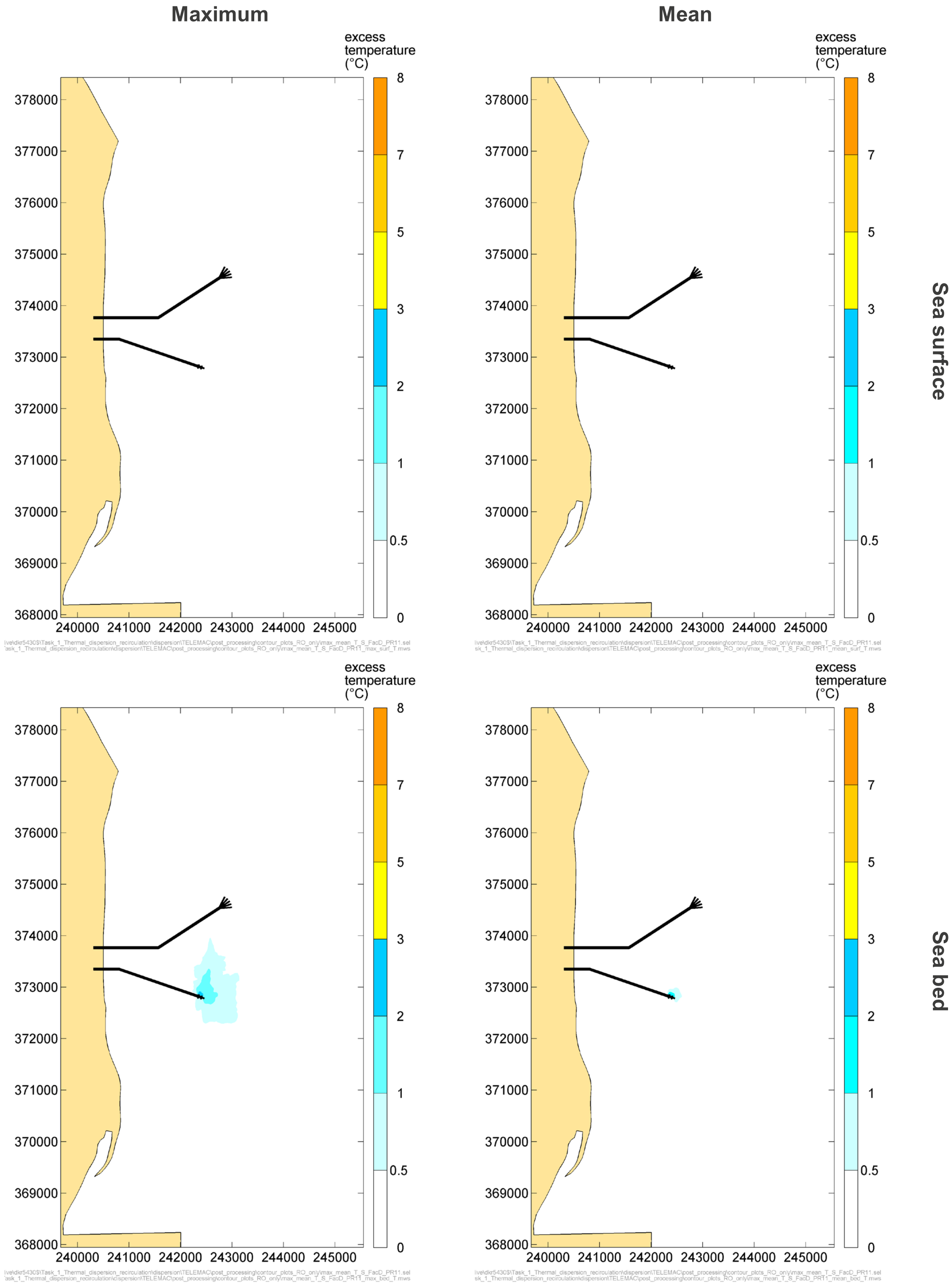

Figure B.12: Maximum and mean sea surface and sea bed excess temperature, winter, north-west wind, early operation

C. Additional analysis for EIA

Mott MacDonald is conducting the Environmental Impact Assessment (EIA) for the UHP project.
HR Wallingford has conducted preliminary thermal dispersion modelling to support the EIA (HR Wallingford (2015)). The results presented in the previous section will be used to update the EIA, along with the analysis of the impact on sensitive habitats presented here.

The marine habitat map of the site from the baseline environmental survey was provided by Mott MacDonald and is shown in Figure C.1. The layout considered in this study is indicated in black. The map shows areas of seagrass of varying density and areas of mixed oyster beds. These regions are likely to be most sensitive to changes in temperature and salinity caused by the discharge.

The increases in temperature and salinity in the various marine habitats near the outfall have been assessed using the results from the twelve simulations presented in the previous section. For the standard operation phase, the area with time-averaged and depth-averaged excess temperatures above 3°C is entirely located within the coarse sand region for all conditions. Therefore the sensitive habitats, such as seagrasses and oyster beds, are not predicted to be affected, within the mixing zone criteria stipulated by MoE. Similarly for the early operation phase, the area with average sea bed excess salinities greater than 10% of the background salinity is located entirely within the coarse sand habitat for all conditions.

Time series of temperature and salinity have been extracted at the locations A1, A2, A3 shown in Figure C.1. These locations have been selected as representing the nearest major sensitive habitats to the outfall. Point A1 is located within dense seagrasses and points A2 and A3 are located within the mixed oyster bed habitat.

The time series for the standard operation phase are presented in Figure C.2 to Figure C.19 with profiles shown at the sea bed, mid-depth and sea surface. At point A1 (dense seagrasses), excess temperatures and salinities are generally low with maximum values around 3°C and 3 ppt under calm conditions. At point A2, the time series are dominated by peaks corresponding to times when the currents are south-going. These peaks typically last around 12 hours and have maximum temperatures and salinities of up to 7°C and 4.5 ppt. Excess temperatures and salinities at point A3 are small during the constant wind condition, on average less than 0.2°C and 0.2 ppt. For the calm and observed wind conditions the time series at point A3 are comprised mainly of short period peaks (around 6 hours) with maximum values of 6°C and 4 ppt respectively.

Time series of excess salinities are also presented in Figure C.20 to Figure C.37 for the early operation phase. The excess salinity at point A1 is low, less than 1 ppt, in all simulations. At point A2 the time series are dominated by peaks of 12 hours in duration of up to around 3 ppt. These peaks correspond to times when the currents are south-going. The time series at point A3 show short period peaks of up to around 4.5 ppt at the sea bed. These are generated by the edges of the plume passing over this location.

The time series of temperature for the early operation phase are omitted as excess temperatures were found to be less than 0.5°C throughout the simulations at the three locations.

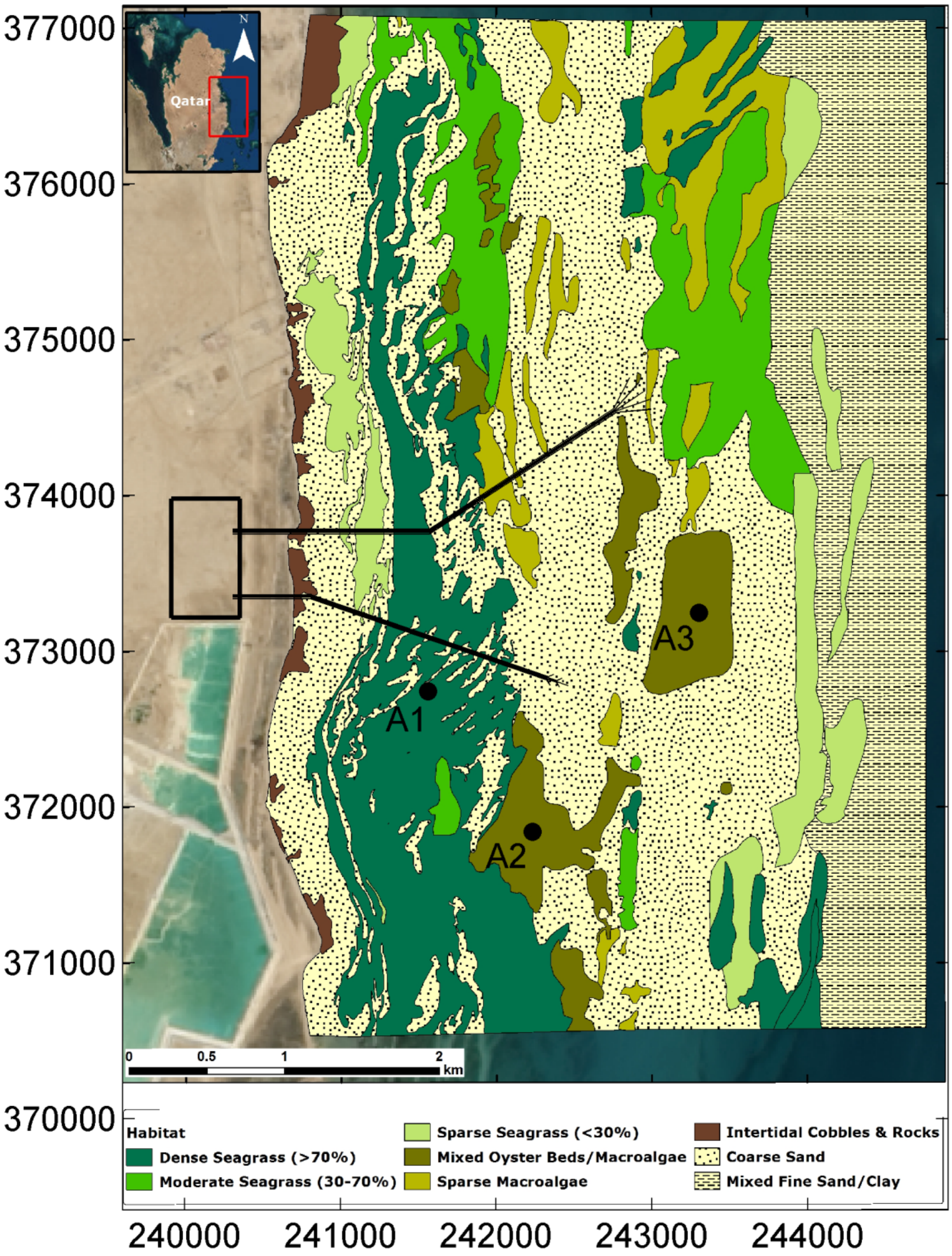

\\hrw-uk.local\projects\live\der5448$\model\janet\geom_FacilityD_DER5448_L2.sel
\\hrw-uk.local\projects\live\dkr5430$\Task_1_Thermal_dispersion_recirculation\report_figures\habitat_map_ts_locs.mws

Figure C.1: Marine habitat map and time series location points

Source: Mott MacDonald